Matter

CellPress

Article

Spontaneous Non-stoichiometry and Ordering in Degenerate but Gapped Transparent Conductors

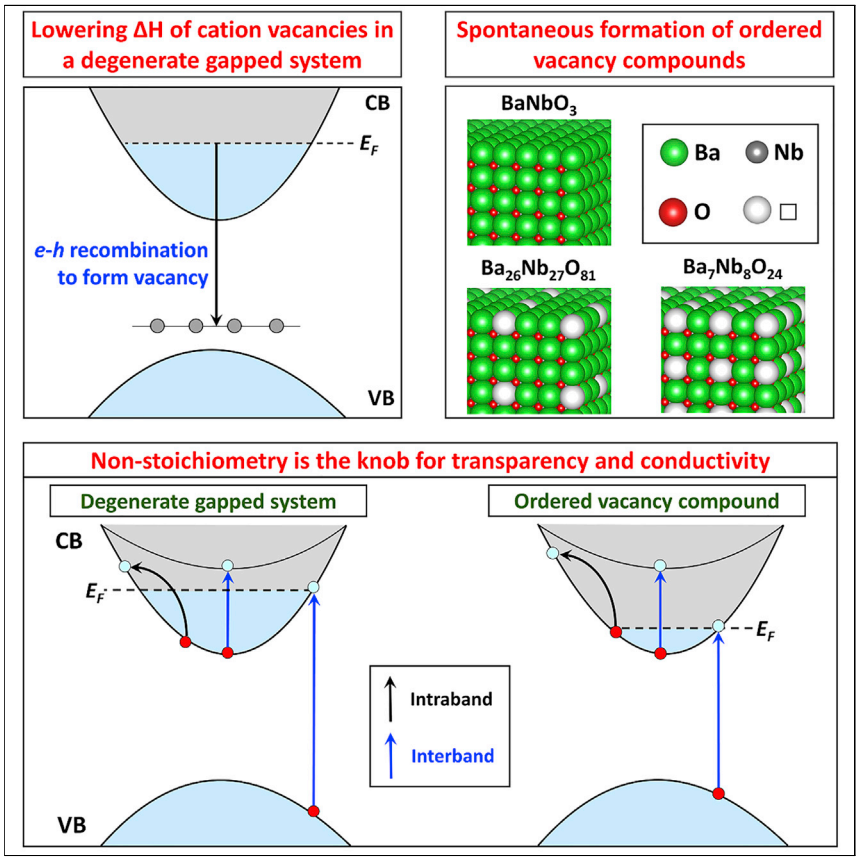

Formation of non-stoichiometric compounds is often thought to be a growth effect rather than a specific electronic instability. We demonstrate that degenerate gapped compounds with large internal gap and Fermi level in the conduction band can have spontaneous non-stoichiometry, even at low temperatures, due to decay of a fraction of the free electrons into the hole states formed by such vacancies. This unique material feature allows controllable non-stoichiometry to be used to archive target material stability and optoelectronic properties for transparent conductors and electrides.

Discovery
A new material or phenomena

Oleksandr I. Malyi, Michael T. Yeung, Kenneth R. Poeppelmeier, Clas Persson, Alex Zunger

oleksandrmalyi@gmail.com (O.I.M.)
alex.zunger@colorado.edu (A.Z.)

HIGHLIGHTS

Carriers in degenerate gapped compounds can cause spontaneous non-stoichiometry

Spontaneous non-stoichiometry can result in formation of ordered vacancy compounds

Different ordered vacancy compounds can be realized by controlling growth conditions

Controllable non-stoichiometry is the knob that tunes transparency and conductivity

Malyi et al., Matter *1*, 280–294
July 10, 2019
https://doi.org/10.1016/j.matt.2019.05.014

Matter

CellPress

Article

Spontaneous Non-stoichiometry and Ordering in Degenerate but Gapped Transparent Conductors

Oleksandr I. Malyi,[1,2,*] Michael T. Yeung,[3] Kenneth R. Poeppelmeier,[3] Clas Persson,[2] and Alex Zunger[1,4,*]

SUMMARY

We highlight a class of materials representing an exception to the Daltonian view that compounds maintain integer stoichiometry at low temperatures and use this behavior to select ordered vacancy compounds (OVCs) striking a wanted compromise between carrier concentration, transparency, and phase stability, crucial for transparent conductors (TCs). We show that carriers in the conduction band (CB) of degenerate gapped $BaNbO_3$, $Ca_6Al_7O_{16}$, and $Ag_3Al_{22}O_{34}$ compounds can cause a self-regulating instability, whereby cation vacancies form exothermically because a fraction of the CB electrons decays into the hole states formed by such vacancies, and this electron-hole recombination offsets the positive energy associated with vacancy bond breaking. This Fermi level-induced spontaneous non-stoichiometry can lead to the formation of OVCs with different optoelectronic properties and stable in different ranges of chemical potentials. Thus, we demonstrate how a window of opportunity can be determined between opposing tendencies of transparency, conductivity, and stability to design TCs.

INTRODUCTION

Spontaneous Non-stoichiometry as a Fermi Level Instability

The fact that compounds manifest integer ratios between component elements (the law of definite proportions[1]) has been the cornerstone of our understanding of formal oxidation states (taking up integer values) and defect physics (showing that violation of integer ratios by formation of defects costs energy and is thus unlikely at low temperatures). This thinking of the Daltonides school (the paradigm of stoichiometry) stood in stark contrast with the non-stoichiometric Berthollides[2] school, who argued that compounds could possess a range of compositions entirely dependent on the starting synthetic conditions. We point out an interesting class of exceptions to the Daltonide universal understanding, whereby a degenerate but gapped compound with Fermi energy (E_F) inside the conduction band (CB) and a large internal band gap (E_g^{int}) between the valence band maximum (VBM) and conduction band minimum (CBM) (as shown in Figure 1A) could form a significant concentration of low-energy vacancies, violating the rule of integer stoichiometry.

This understanding has an important implication on transparent conductors (TCs),[3] those rare compounds in which the generally mutually exclusive properties of optical transparency (usually common only in electrical insulators) and conductivity (usually common only in opaque metals) coexist. This internal contradiction has been the reason why finding good TCs has proven to be so difficult. The old class of TCs was developed by starting with an insulator (such as In_2O_3 or ZnO, schematically shown

Progress and Potential

Degenerate gapped compounds, those with their Fermi levels inside the conduction band and sufficiently large "internal band gaps" below this Fermi level, are shown here to have negative formation enthalpy for cation vacancies, leading to spontaneous non-stoichiometry and formation of characteristic ordered vacancy compounds (OVCs), even at low temperature, in defiance of Daltonian stoichiometry. Selection during the growth of a specific OVC can be used to mitigate the notoriously difficult conflict between transparency and conductivity, with potential interests beyond of transparent conductors, including electrides and photocatalysts. This surprising prediction is validated with two key experimental findings: silver beta-alumina $Ag_3Al_{22}O_{34.5}$ leeches out silver atoms upon any attempt to introduce electron carriers, whereas a number of different OVC structures stabilized by effective reconstructions are observed during the synthesis of the tetragonal tungsten bronze $Ba_3Nb_5O_{15}$.

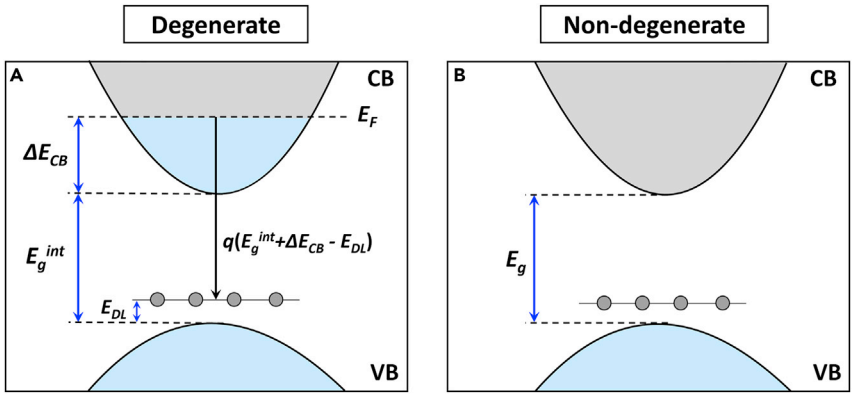

Figure 1. Mechanism for Lowering Formation Energy of an Acceptor in Degenerate Gapped Material
Schematic illustration of defect formation in (A) degenerate gapped compounds and (B) non-degenerate gapped insulators, showing lowering defect formation energy governed by removing an electron from the conduction band. Blue (gray) areas represent occupied (empty) states. Here, ΔE_{CB} is the occupied part of the conduction band; E_g^{int} is the internal band gap, and E_{DL} is the electron-trap defect level produced by, e.g., cation vacancies.

in Figure 1B) and then attempting heavy doping (by Sn or Al, respectively), making it conductive. This has faced severe "doping bottlenecks,"[4] whereby intended doping by electrons creates "electron killers" in the form of intrinsic acceptors. An alternative strategy[5] is to start from a metal (Figure 1A) and attempt to make it transparent, avoiding doping bottlenecks. The deeper understanding of spontaneous non-stoichiometry discussed here clarifies that the latter approach can present an unusual window of opportunity, whereby (1) transparency, (2) conductivity, and (3) phase stability can coexist and be selected by zooming in on specific growth conditions (chemical potentials). Specifically, a compound that has the Fermi level inside the CB (a nominal band conductor with free electrons) could become opaque because too many electrons create a strong plasma absorption in the visible range. But if this compound also has a sufficiently large internal band gap below the Fermi energy (i.e., being degenerate but gapped, Figure 1A), it will create spontaneous defects (here, cation vacancies that are hole-producing acceptors) that, while violating Daltonian stoichiometry, also regulate the carrier concentration by compensating the native electrons via the spontaneously produced holes. It is the exothermic electron-hole compensation reaction that drives non-stoichiometry. Unlike the case of the limited formation of dilute vacancies in ordinary insulators (Figure 1B), if there is an internal gap (Figure 1A), then, at the concentrated limit, such vacancies can condense into ordered crystallographic arrays (Figures 2A and 2B), thus explaining the hitherto peculiar occurrence[6] of macroscopically observed sequences of ground state ordered vacancy compounds (OVCs),[7–10] such as $Ba_lNb_mO_n$, with l:m:n ratios of 1:2:6, 3:5:15, 5:4:15, 7:6:21, 7:8:24, 9:10:30, and 26:27:81. We highlight cases in which the vacancy ordering is clearly visible (Figure 2B) versus cases in which, following vacancy ordering, further total energy relaxation yielded structural changes (reconstruction) that make it difficult to visualize the original vacancy ordering. These otherwise peculiar integer ratios emerge as stable, T = 0 K ground state structures obtained via a first-principles total energy search. It turns out that such cation vacancy compounds occur as a sequence of discrete phases, each with its own vacancy concentration (e.g., 7:8:24, 9:10:30, and 26:27:81, with 12.5%, 10%, and 3.7% of Ba vacancies, respectively) and each is stabilized at specific reactant chemical potentials (colored domains in Figure 2A). Because of the discrete vacancy ratios, each phase, as illustrated below, has its characteristic residual (post-compensation) electron

[1]Renewable and Sustainable Energy Institute, University of Colorado, Boulder, CO 80309, USA

[2]Centre for Materials Science and Nanotechnology, Department of Physics, University of Oslo, PO Box 1048 Blindern, 0316 Oslo, Norway

[3]Department of Chemistry, Northwestern University, Evanston, IL 60208, USA

[4]Lead Contact

*Correspondence: oleksandrmalyi@gmail.com (O.I.M.), alex.zunger@colorado.edu (A.Z.)

https://doi.org/10.1016/j.matt.2019.05.014

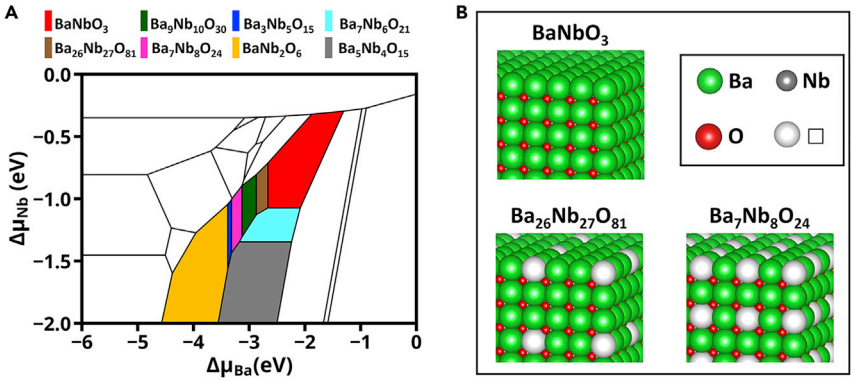

Figure 2. Formation of Stable OVCs in the Ba-Nb-O System

(A) Chemical potential diagram for the Ba-Nb-O system, showing stability chemical potential zones for $BaNbO_3$ and each stable OVC phase.

(B) Crystal structures of $BaNbO_3$ and its unreconstructed OVCs demonstrating long-range ordering of Ba vacancies.

concentration and optical response. Such phases (Figure 2A) could then, in principle, be selected during growth by targeting the requisite cation chemical potential, so that the desired optoelectronic properties can be achieved. This work demonstrates that controlled deviation from Daltonian stoichiometry can be used as a knob to regulate transparent conductivity. We validate our theory with two key experimental findings: silver β-alumina $Ag_3Al_{22}O_{34.5}$ leeches out silver atoms forming Ag vacancies upon any attempt to introduce electron carriers, and tetragonal tungsten bronze $Ba_3Nb_5O_{15}$, in which the cation vacancy formation favors the formation of secondary phases. Our paper is the first attempt to understand and unravel the intrinsic complex connection between stoichiometry and properties, creating a roadmap for the future. This work has broad implications, as degenerate gapped compounds have been generating increasing interest in many fields beyond that of TCs, including the colored metallic photocatalysts as seen in the substoichiometric $Sr_{1-x}NbO_3$,[11] the electron-donating promotors for catalysts[12] to low work function compliance layers.[13] Furthermore, our work explains why many of these degenerate gapped compounds require exotic synthesis conditions to be prepared stoichiometrically.

RESULTS AND DISCUSSION

Dilute Metal Vacancies Can Form Readily in Degenerate Gapped Compounds

The formation of vacancies in ordinary insulators (Figure 1B) involves breaking of stable chemical bonds without restoring any of the spent energy, so a significant concentration of such defects can exist only at increased temperatures. The situation can be different in degenerate gapped compounds (with E_F located at an energy ΔE_{CB} above the CBM, as in $BaNbO_3$, $Ca_6Al_7O_{16}$, and $Ag_3Al_{22}O_{34}$ discussed below) with an internal band gap E_g^{int} between the CBM and VBM (Figure 1A). Here, the formation of dilute concentration of metal vacancies can create electron acceptor states near the valence band (at energy E_{DL}), resulting in the opportunity for decay of q CB electrons into these electron acceptor states, thereby regaining the energy $q(E_g^{int} + \Delta E_{CB} - E_{DL})$, which reduces the vacancy formation energy accordingly (see Figure 1A). When this energy exceeds the bond-breaking energy, one expects spontaneous non-stoichiometry. This defines an electronic Fermi level mechanism for Berthollides[2] non-stoichiometry.

To validate this concept, Figures 3A, 3C, and 3E show the results of density functional calculated formation energies of the Ba vacancy in $BaNbO_3$, the Ca vacancy

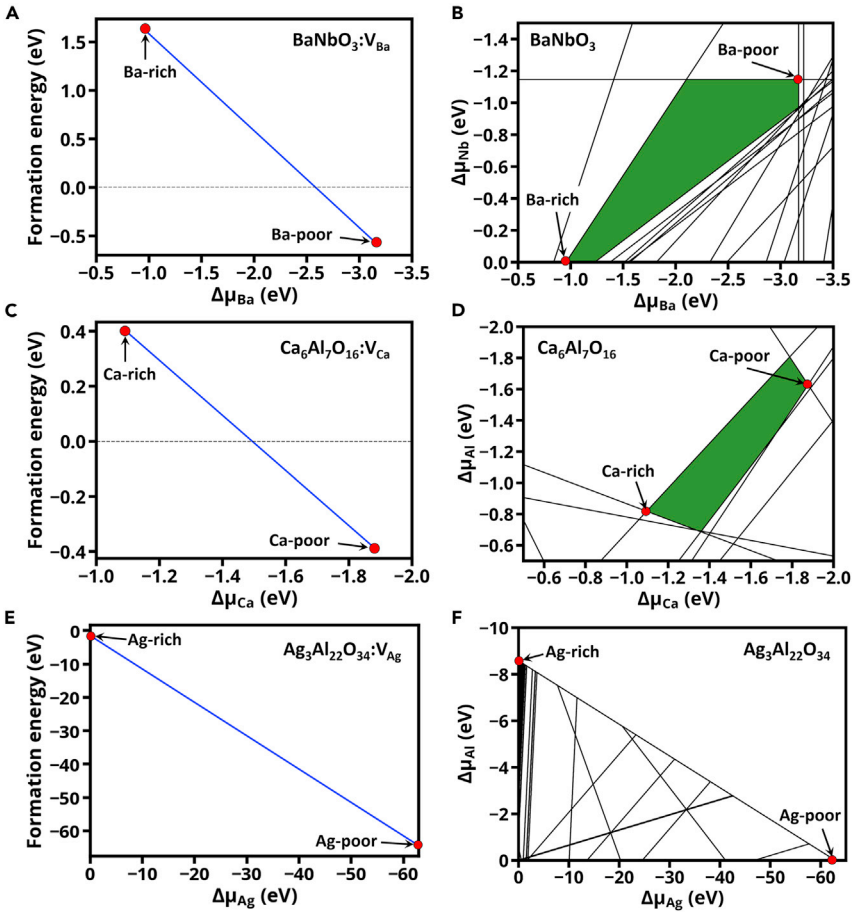

Figure 3. Spontaneous Vacancy Formation in Degenerate Gapped Insulators

Metal vacancy formation energy (left-hand panels) and region of chemical potentials (green zone) where the degenerate gapped insulator is stable (right-hand panels) for (A and B) $BaNbO_3$, (C and D) $Ca_6Al_7O_{16}$, and (E and F) $Ag_3Al_{22}O_{34}$. For $Ag_3Al_{22}O_{34}$, no green zone exists where the compound is stable. Only experimentally observed stoichiometric phases are used to calculate the ranges of chemical potentials under which the compounds are stable.

in $Ca_6Al_7O_{16}$, and the Ag vacancy in $Ag_3Al_{22}O_{34}$, as a function of the metal chemical potential (see Experimental Procedures). The allowed stable chemical potential regions (constructed by considering possible competing phases, see Experimental Procedures) of the respective bulk compounds are shown in Figures 3B, 3D, and 3F. We see that for the degenerate gapped compounds under cation-deficient chemical potential conditions, vacancy formation energies can be extremely low (in fact, negative). Whereas $BaNbO_3$ and $Ca_6Al_7O_{16}$ have stable chemical potential (green) zones at the respective stoichiometries indicated, $Ag_3Al_{22}O_{34}$ does not. In fact, in the latter case, the Ag vacancy formation energy (Figure 3E) is so strongly negative under all chemical potential conditions, that the CB is empty and the parent degenerate $Ag_3Al_{22}O_{34}$ phase is not stable (i.e., no green zone in Figure 3F).

Dilute Vacancies Can Condense into Stable OVCs Forming Homological Sequences

The negative formation energies of dilute vacancies open the possibility of vacancy condensation and long-range ordering (Figure 2B). To examine this possibility, we have calculated the T = 0 K stable phases ("ground state diagram" or "convex

Composition	Synthesis	Characterization	Possible OVC	RT Properties
Ba-Nb-O				
$BaNbO_3$[15,16]	Evacuated quartz tube, 1117 °C	pXRD	No	-
$Ba_{0.95}NbO_3$[17]	Flux growth, vacuum furnace	SC-XRD	Yes	-
$Ba_{0.97}NbO_3$[18]	Evacuated quartz tube, 1200 °C	pXRD	Yes	Metallic
$Ba_3Nb_5O_{15}$[19]	Flux growth, vacuum furnace	SC-XRD	Reconstructed	Semiconductor
$Ba_6Nb_{10}O_{30}$[20]	Evacuated quartz tube, 1100 °C	pXRD	Reconstructed	Semiconductor
$Ba_6Nb_{10}O_{30}$[21]	Evacuated quartz tube, 1200 °C	EDS, pXRD	Reconstructed	Semiconductor
$Ba_6Nb_{10}O_{30}$[22,23]	Low P_{O_2} sintering, 1360 °C	pXRD	Reconstructed	Metallic
$Ba_6Nb_{10}O_{30}$[24,25]	Low P_{O_2} sintering, 1300 °C	pXRD, TEM, EDS	Reconstructed	Semiconductor
$BaNb_2O_6$[26]	Flux growth, 1450 °C	SC-XRD	Reconstructed	Semiconductor
$Ba_5Nb_4O_{15}$[27]	Sintering, 1150 °C	pXRD	Reconstructed	Semiconductor
Ca-Al-O				
$Ca_{12}Al_{14}O_{32}$[28,29]	Floating zone, followed by Ca reduction	pXRD	No	Metallic
$Ca_{11.3}Al_{14}O_{32.3}$[30]	Zone melting	Neutron powder diffraction	Yes	Semiconductor

Figure 4. Summary for Experimental Results on Stable OVCs in Ba-Nb-O and Ca-Al-O Systems Reported in the Literature

Characterization techniques are labeled as powder X-ray diffraction (pXRD), single crystal X-ray diffraction (SC-XRD), energy-dispersive X-ray spectroscopy (EDS), and transmission electron microscopy (TEM). If the structure does not have a clearly defined vacancy site, it is labeled as reconstructed. Room temperature (RT) properties stand for the metallic or semiconductor nature of the compound based on the reported temperature dependence of the electronic conductivity. The synthesis field highlights key conditions for experimental realization of the specific material.

hull") of such ternary structures. This entails searching for configuration versus composition that lies on the energy convex hull,[14] which defines the phases with energy lower than a linear combination of any competing phases at the corresponding compositions. We create candidate configurations by considering a base compound ($BaNbO_3$, $Ba_3Nb_5O_{15}$, $Ca_6Al_7O_{16}$, or $Ag_3Al_{22}O_{34}$), then create a replica of N such units of the base compound and add successively p metal vacancies, i.e., OVC = $N \times$ (base) + pV_m, searching via total energy minimization for stable and metastable configurations. We also include experimentally known reconstructed OVCs, the compounds that satisfy the OVC expression but do not have clearly defined vacancy sites (e.g., $Ba_3Nb_5O_{15}$, $BaNb_2O_6$, and $Ba_5Nb_4O_6$).

Available information on the experimental literature[15–30] is provided in Figure 4, and the theoretical results of this work are summarized in Figure 5. The key point to notice is that there is a sequence of stable OVC phases, each having a specific concentration of electrons per formula unit (*e*/f.u.) in the CB (including possibly zero). This is illustrated in Figures 6A and 7A showing the ground state diagrams for Ba-Nb-O and Ca-Al-O systems and chemical potential stability diagrams (Figures 2A

OVC generator	Resulting OVC	N_e (*e/f.u*)	ΔE_{CB} (eV)	E_g^{int} (eV)	Material type	Symmetry
Ba-Nb-O						
1:1:3 (Base)	$BaNbO_3$	1	1.11	2.26	I	1:1:3
27×(1:1:3)+V_{Ba}	$Ba_{26}Nb_{27}O_{81}$	25/27	1.04	2.22	I	1:1:3-like
10×(1:1:3)+V_{Ba}	$Ba_9Nb_{10}O_{30}$	8/10	0.90	2.19	I	1:1:3-like
8×(1:1:3)+V_{Ba}	$Ba_7Nb_8O_{24}$	6/8	0.88	2.17	I	1:1:3-like
7×(1:1:3)+V_{Nb}	**$Ba_7Nb_6O_{21}$**	**2/7**	**0.40**	**2.20**	**II**	**Reconstructed**
5×(1:1:3)+2V_{Ba}	**$Ba_3Nb_5O_{15}$**	**1/5**	**0.46**	**1.87**	**II**	**Reconstructed**
2×(1:1:3)+V_{Ba}	$BaNb_2O_6$	0	0	2.72	III	Reconstructed
5×(1:1:3)+V_{Nb}	$Ba_5Nb_4O_{15}$	0	0	2.65	III	Reconstructed
Ca-Al-O						
6:7:16 (Base)	$Ca_6Al_7O_{16}$	1	0.96	3.49	I	6:7:16
4×(6:7:16)+V_{Ca}	**$Ca_{23}Al_{28}O_{64}$**	**2/4**	**0.67**	**3.10**	**II**	**6:7:16-like**
2×(6:7:16)+V_{Ca}	$Ca_{11}Al_{14}O_{32}$	0	0	3.40	III	6:7:16-like

Figure 5. Summary of the Computational Results on Stable OVCs in Ba-Nb-O and Ca-Al-O Systems

The OVCs are generated by creating supercells of a base cell as OVC = N × (base) + pV_m, where N and p are integer numbers. Number of electrons (N_e) in the conduction band is given per formula unit (f.u.) of the base compound (i.e., $BaNbO_3$ or $Ca_6Al_7O_{16}$). In general, the number of electrons in the conduction band for the degenerate gapped Ca-Al-O and Ba-Nb-O compounds can be predicted from the sum of composition-weighted formal oxidation states assuming Ba^{2+}, Ca^{2+}, Al^{3+}, Nb^{5+}, and O^{2-} for each material. ΔE_{CB} is the occupied energy range of conduction band and E_g^{int} is the internal gap between CBM and VBM (Figure 1A) estimated from the density of states. Types of materials I, II, and III stand for non-transparent metals, potentially TCs (shown in red), and insulators, respectively. If the OVC in the lowest energy state does not have clearly defined vacancy sites, it is labeled as reconstructed.

and 7B) demonstrating the phases that are stabilized as the chemical potentials of the atoms being removed are continuously changed between their allowed values. Finally, we show how a window of opportunity can be determined computationally between opposing tendencies of (1) stability (Figures 2A and 7B), (2) conductivity (Figures 6B–6D and 7C), and (3) transparency (Figure 8) to design new TCs.

Stable Phases and OVCs for the Ba-Nb-O System

Computationally, we find 25 binary and ternary ground state compounds (described in Data S1) of which $Ba_7Nb_6O_{21}$, $Ba_5Nb_4O_{15}$, $Ba_3Nb_5O_{15}$, $Ba_7Nb_8O_{24}$, $Ba_9Nb_{10}O_{30}$, $Ba_{26}Nb_{27}O_{81}$, and $BaNb_2O_6$ are OVCs (Figure 5). Here, 7:8:24, 9:10:30, and 26:27:82 phases have clearly defined vacancy sites, and 1:2:6, 3:5:15, and 5:4:15 OVCs are reconstructed compounds observed experimentally before.[19,26,27,31,32] It should be noted that for the perovskite $BaNbO_3$ (Figure 4), there has been a focused effort to quantify the occupancy of the A site via diffraction, and authors have noted that there are possible vacancies, as "…slight departures of the stoichiometry below the detection limits of the neutron powder diffraction technique cannot be

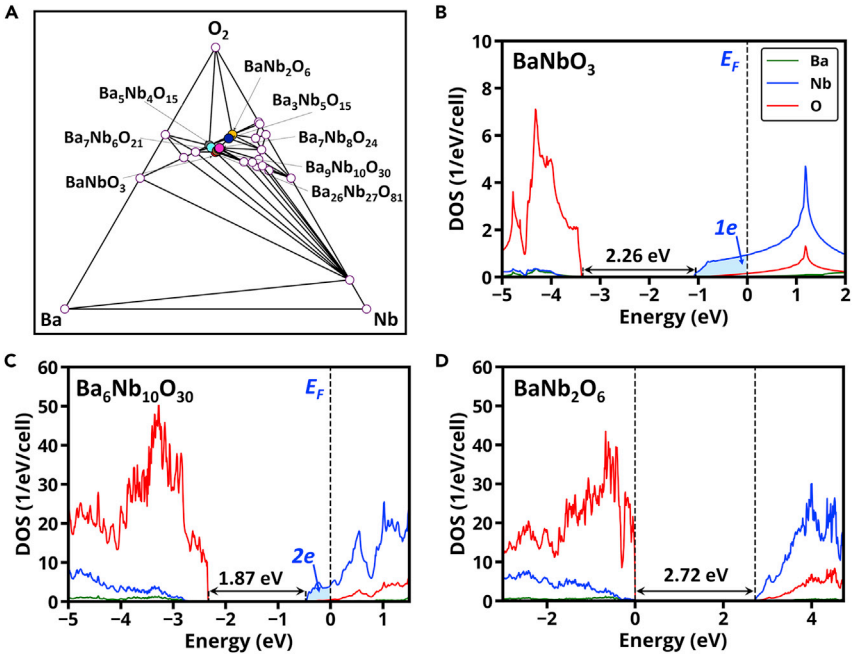

Figure 6. Stability and Electronic Structures of $BaNbO_3$ and Its OVCs

(A) Convex hull for the Ba-Nb-O system indicating the OVCs in color. In Figure 3B, the OVCs were not included in the calculations of the stability green zone of $BaNbO_3$, but they are included in (A) and Figure 2A. This redefines the chemical potential stability zone under which the base compound can exist, and consequently the formation energy of Ba vacancy in $BaNbO_3$ is about 0 eV under the redefined cation-poor conditions.

Density of states for (B) $BaNbO_3$, (C) $Ba_6Nb_{10}O_{30}$, and (D) $BaNb_2O_6$, indicating the number of electrons in the conduction band per formula unit.

excluded."[18] Indeed, several potential experimental compositions (i.e., $Ba_{0.95}NbO_3$ and $Ba_{0.97}NbO_3$) nearly match predicted phases ($Ba_{26}Nb_{27}O_{81} \approx Ba_{0.963}NbO_3$), whereas other predicted compositions (i.e., $Ba_7Nb_8O_{24}$ and $Ba_9Nb_{10}O_{30}$) exceed the observed vacancy concentration.

Stable Phases and OVCs for the Ca-Al-O System

We identify computationally a total of ten binary and ternary ground state compounds (described in Data S2) of which $Ca_{11}Al_{14}O_{32}$ and $Ca_{23}Al_{28}O_{64}$ are OVCs (Figure 5). Here, both OVCs have clearly defined vacancy sites with the long-range ordering of Ca vacancies. Despite the limited information on the formation of non-stoichiometric $Ca_{6-x}Al_7O_{16}$ systems (Figure 4), $Ca_{11.3}Al_{14}O_{32.3}$ compound with $Ca_6Al_7O_{16}$-like structure and partial occupancy of Ca sites has been reported experimentally,[30] which indirectly support our theoretical predictions.

Stable Phases and No OVCs for the Ag-Al-O System

We find computationally a total of four binary and ternary ground state compounds (described in Data S3): Al_2O_3, Ag_2O, AgAl, and $AgAlO_2$. None of them are OVCs. In fact, the $Ag_3Al_{22}O_{34}$ and its $Ag_2Al_{22}O_{34}$ OVC lie energetically above the convex hull by 0.034 and 0.01 eV/atom, respectively. Specifically, $Ag_3Al_{22}O_{34}$ decomposes to $AlAgO_2$, Ag, and Al_2O_3 phases, while $Ag_2Al_{22}O_{34}$ decomposes to $AgAlO_2$ and Al_2O_3. In other words, the formation of Ag vacancy is highly effective and drains all electrons from the CB; thus, $Ag_2Al_{22}O_{34}$ is an insulator. This vacancy formation increases the system stability (the energy above the convex hull is smaller for $Ag_2Al_{22}O_{34}$ than that for $Ag_3Al_{22}O_{34}$), but both $Ag_3Al_{22}O_{34}$ and $Ag_2Al_{22}O_{34}$ are

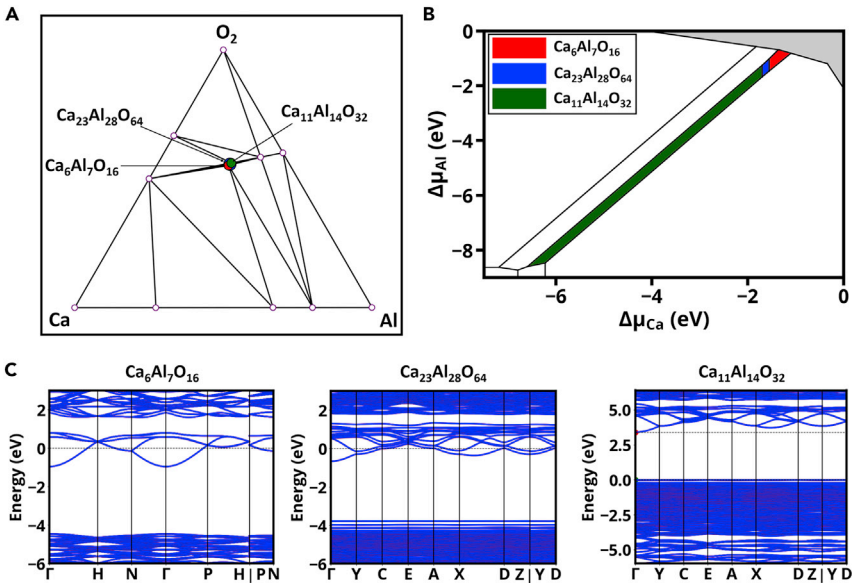

Figure 7. Stability and Electronic Structures of $Ca_6Al_7O_{16}$ and Its OVCs

(A) Convex hull for the Ca-Al-O system indicating the OVCs in color.

(B) Chemical potential diagram for the Ca-Al-O system, showing the stability chemical potential zone for each stable OVC phase in colors corresponding to the ground states in (A). The gray zone corresponds to the prohibitive chemical potential stability zone of binary Ca-Al systems. In Figure 3D, the OVCs were not included in the calculations of the stability green zone of $Ca_6Al_7O_{16}$, but they are included (A and B). This redefines the chemical potential stability zone under which the base compound can exist, and consequently the formation energy of Ca vacancy in $Ca_6Al_7O_{16}$ is about 0 eV under the redefined cation-poor conditions.

(C) Band structures for $Ca_6Al_7O_{16}$ and its OVCs.

unstable with respect to competing phases. Our experimental attempts to reduce synthesized $Ag_3Al_{22}O_{34.5}$ to $Ag_3Al_{22}O_{34}$ via heating the compound to 700°C to liberate oxygen results in the formation of free metallic silver and $Ag_{2.5}Al_{22}O_{34.25}$ (Note S1). These results suggest that despite the fact that $Ag_3Al_{22}O_{34}$ might be attractive as an intrinsic TC[5] if Ag vacancy formation can be partially inhibited, the system is not likely to be realized experimentally under normal conditions.

Different OVCs Have Different Number of Free Carriers, Absorption, and Conductivity

Trends in the Number of Electrons in the CB of Intrinsic TCs and the Metal-Insulator Transition

For the Ba-Nb-O system (Figure 5), among the ground state structures, the phases 1:1:3, 7:6:21, 26:27:81, 9:10:30, 7:8:24, and 3:5:15 have electrons in the CB and wide internal band gaps. From the sequences of OVCs, we find that both Ba and Nb vacancies act as acceptors, removing 2*e* and 5*e* per vacancy from the CB (Figures 6B–6D). The electronic properties of Ba-Nb-O systems were studied experimentally by various groups (Figure 4). Specifically, it has been shown that the 1:1:3 compound is a metal,[18] whereas the 1:2:6 and 5:4:15 OVCs are insulators.[26,27,33,34] At the same time, despite a few experimental works reporting low resistivity for the 3:5:15 compound, the temperature dependence of the resistivity (metal versus semiconductor nature) is different for different studies.[19–22,25] These results are not surprising considering the tiny range of chemical potentials under which the 3:5:15 OVC exists (Figure 2A), low defect formation energy in degenerate gapped compounds, and

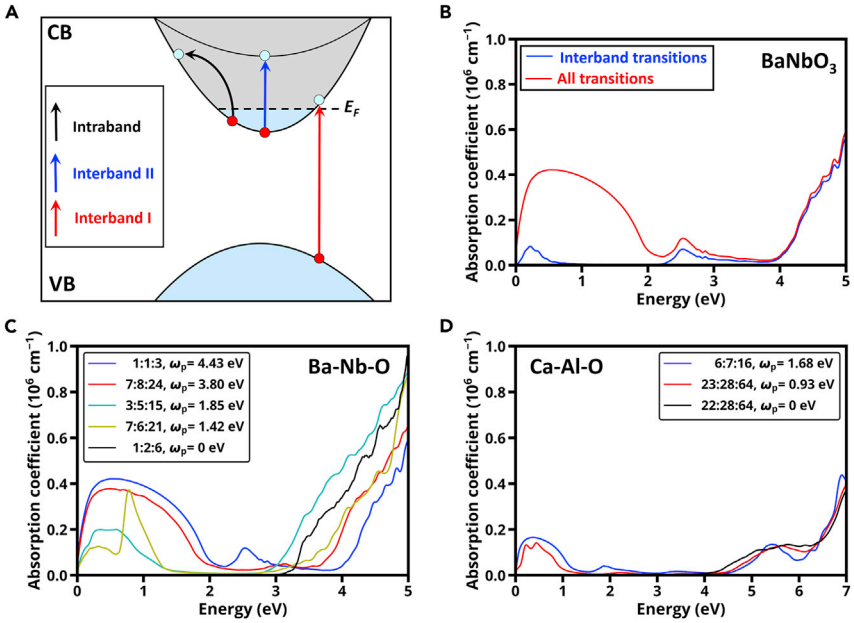

Figure 8. Effect of Non-stoichiometry on Optoelectronic Properties

(A) Schematic illustration of different contributions to optical properties in degenerate gapped compounds.

(B) Absorption spectra for $BaNbO_3$ considering only interband transitions and superposition of interband and intraband transitions.

(C) Effect of non-stoichiometry on the average absorption spectra of degenerate gapped compounds in the Ba-Nb-O system.

(D) Effect of non-stoichiometry on the average absorption spectra of degenerate gapped compounds in the Ca-Al-O system. The averaged plasma frequency over the three Cartesian directions is given for each system.

complexity of material synthesis. In our own work on 3:5:15 OVC, we see the preferential formation of the secondary reconstructed 1:2:6 and 5:4:15 OVCs over the targeted compound (Note S2). This reflects the narrow stability region of the 3:5:15 phase versus the reconstructed OVCs. Hence, the sensitivity of sample preparation conditions reignites the need for high-quality single crystals to quantify potential vacancy concentration and to understand the potential structural/electronic impact of vacancy formation.

For the Ca-Al-O system (Figure 5), from the analysis of electronic structures of the ground state compounds, we identify the phases 6:7:16 and 23:28:64 as degenerate gapped compounds with 1*e*/f.u. and 2*e*/f.u. in the CB, respectively. At the same time, the 11:14:32 OVC has no CB electrons, i.e., it is an insulator with a wide band gap. The results for electronic structures of OVCs suggest that Ca vacancy in 6:7:16-based degenerate gapped compounds acts as acceptor removing 2*e* from the CB. However, in contrast to the OVCs in the Ba-Nb-O system, the formation of Ca vacancy produces in-gap occupied defect states that reduce both the internal band gap energy and the energy range of occupied states (Figure 7C). The high electronic conductivity of 6:7:16 is known from experimental studies (Figure 4),[28,29] but the insulating and conducting properties of 11:14:32 and 23:28:64 OVCs are yet to be confirmed. It should also be noted that 6:7:24 and its 23:28:64 OVC have clearly defined 0-dimensional charge carrier density localization, which implies that both compounds are not only degenerate gapped compounds but also stable inorganic electrides (Note S3).

Spontaneously Formed Vacancies Enhance Transparency while Reducing Conductivity

The optical properties of a degenerate gapped compound are determined by superposition of interband and intraband transitions (Figure 8A). Owing to the occupied CB, the band-to-band transitions can be divided into (I) interband transitions from the occupied valence to unoccupied conduction bands and (II) interband transition from occupied conduction to higher energy unoccupied bands. In the simplified model used here, the intraband transitions can be predicted within the Drude model[35] describing free-electron absorption.

The contribution of the aforementioned different types of transitions to the absorption spectra is illustrated in Figure 8B for $BaNbO_3$. Specifically, the interband transitions (I) contribute to the absorption spectra at energies slightly above $E_g^{int} + \Delta E_{CB}$ due to the curvatures of the valence and conduction bands. The interband transitions (II) contribute noticeably at energies below those for interband transitions (I) and determine the absorption spectra in the range from 2 to 4 eV. Finally, the intraband contribution determines the low-energy region of absorption spectra. This analysis defines the design principles for good intrinsic TCs that require (1) metals with large internal gaps between the valence and conduction bands to minimize the interband absorption in visible range and (2) a high enough carrier density (n_e) in the CB to provide conductivity, while having (3) a low enough carrier density, limiting the interband transition in the CB and plasma frequency ($\omega_p \sim \sqrt{n_e/m}$, where m is an effective carrier mass), so that free-electron absorption does not impede the needed optical transparency. Furthermore, (4) the free carriers in the CB above the internal band gap should not destabilize the compound by spontaneously creating Fermi level-induced defects that defeat conductivity.

For the Ba-Nb-O system, the 1:1:3 degenerate gapped compound has the highest plasma frequency (ω_p = 4.43 eV) among the considered materials which results in strong Drude contribution in the visible light range. Hence, despite high carrier concentration ($n_e = 1.38 \times 10^{22}$ cm^{-3}) and stability, the 1:1:3 compound is not TC due to low transparency. Indeed, the 1:1:3 samples have clearly distinct color in experimental studies.[18] At the low vacancy concentration, the effect of the defects on carrier density and optical properties is negligible. However, the increase in Ba or Nb vacancy concentration and formation of OVCs noticeably change the optoelectronic properties via reducing plasma frequency contribution and modifying the material band structure. Although 26:27:81, 9:10:30, and 7:8:24 OVCs have smaller carrier concentrations compared with 1:1:3 compound, the free-electron absorption is still a limiting factor as shown in the example of 7:8:24 OVC (Figure 8C). Among the stable degenerate Ba-Nb-O gapped compounds, 3:5:15 and 7:6:21 compounds have the smallest average absorption coefficients in the visible range (highest transparency).

For the Ca-Al-O system, the optical properties of degenerate gapped materials in the visible range in large part are determined by the interband transition from occupied conduction to unoccupied bands. Specifically, for the 6:7:16 compound, the carrier concentration of 2.26×10^{21} cm^{-3} results in the averaged plasma frequency of 1.68 eV, which does not induce noticeable free-electron absorption in the visible range. The interband transitions from the valence to the conduction bands are well separated in energy and contribute only above $E_g^{int} + \Delta E_{CB}$, which is over 4.4 eV (Figure 7C). Because of this, the absorption in the visible light range is mainly determined by interband transitions in the CB finally resulting in colored material. The Ca vacancy formation removing 2*e* from the CB per defect not only reduces the plasma

frequency but also changes the interband transition, which is illustrated in the absorption spectra of 6:7:16 and its OVCs (see Figure 8D). In particular, 23:28:64 OVC has the lowest absorption in the visible light range among the considered degenerate gapped compounds.

Stability of OVCs during Growth Is the Knob that Controls Vacancy Concentration and Hence Transparency and Conductivity

We have seen above that different OVCs have a different number of free carriers, absorption, and conductivity. What makes this a useful feature is that each such OVC can be realized in a unique and specific range of atomic chemical potentials that can, in principle, be controlled during growth. This is illustrated in Figure 2A for the Ba-Nb-O system and in Figure 7B for the Ca-Al-O system, whereas $Ag_3Al_{22}O_{34}$ offers no control as the Ag vacancy forms readily for any chemical potential. Significantly, the results in Figures 2A and 7B suggest that it is possible to stabilize different $Ba_lNb_mO_n$ and $Ca_lAl_mO_n$ OVCs by tuning Ba/Nb and Ca chemical potentials, respectively. As an illustration, considering the chemical potential stability zone for $BaNbO_3$ (Figure 2A), we find that the reduction of the Ba chemical potential results in stabilization of the 26:27:81, 9:10:30, 7:8:24, 3:5:15, and 1:2:6 OVCs, while 7:6:21 and 5:4:15 OVCs are stable under Nb-poor conditions. Formation of non-stoichiometric structures for Ba-Nb-O materials family has also been reported experimentally (Figure 4); our results extend the knowledge on non-stoichiometric structures, showing how non-stoichiometry often seen in the system is an electronic effect—a high Fermi energy induces the formation of electron-killer cation vacancies. This effect is argued to be rather widespread, not an exotic curiosity, as there are many compounds with large internal gaps and Fermi level in the CB. For instance, fairly recently, $Sr_{1-x}NbO_3$ (a $BaNbO_3$-like metal whose Fermi level sits above a ~1.8 eV gap) was found to be rare, colored, metallic photocatalyst[11] whose coloring and electronic conductivity can be controlled by synthesis conditions. Our results also provide insights into the stability of the transparent conductive states while pointing out that controllable formation of non-stoichiometric degenerate gapped compounds can be used to design next-generation TCs. Specifically, among the stable OVCs, $Ba_3Nb_5O_{15}$, $Ba_7Nb_6O_{21}$, and $Ca_{23}Al_{28}O_{64}$ OVCs are potential TCs. However, $Ba_3Nb_5O_{15}$ exists only under an extremely tiny range of chemical potentials (see Figure 2A). Because of this and low defect formation energy in degenerate gapped compounds, the further research is required to quantify the sensitivity of sample preparation conditions on the structural/electronic properties of the material. $Ba_7Nb_6O_{21}$ and $Ca_{23}Al_{28}O_{64}$ OVCs are first predicted to be stable ground state compounds and constitute opportunities for novel synthesis. Here, $Ca_{23}Al_{28}O_{64}$ OVC has the highest transparency among all considered systems, but due to the small stability zone, a precise control of chemical potentials is needed to realize the compound. $Ba_7Nb_6O_{21}$ exists in the widest range of chemical potentials among the potential TCs, which implies a simpler control of synthesis conditions to realize the material.

Conclusions

The existence of non-stoichiometry in oxides is often thought to be a growth effect rather than a specific electronic instability. However, we demonstrate via first-principles calculations that a degenerate gapped compound with sufficiently large internal gap and Fermi level in the CB can have a characteristically negative cation vacancy formation enthalpy; in other words, spontaneous non-stoichiometry occurs even at low temperatures, intrinsic to the compound (not due to extrinsic effects). At the concentrated limit, such vacancies condense into OVCs. We show that this is a generic behavior as cation vacancy formation results in the decay of CB electrons into electron

acceptor states. As a result, the negative electron-hole recombination energy offsets the positive energy associated with vacancy bond breaking. Our results thus explain and clarify how non-stoichiometry often seen in oxides is an electronic effect—a high Fermi energy induces the formation of electron-killer acceptors. This effect is argued to be rather widespread, not an exotic curiosity, as there are many compounds with such electronic structures. We demonstrate by the chemical potential phase diagrams the growth regimes where a particular *l*:*m*:*n* OVC with a fixed level of transparency and conductivity is stable. For example, whereas in $Ag_3Al_{22}O_{34}$, the Ag vacancies form readily (so the CB is completely depleted of carriers), in the Ca-Al-O and Ba-Nb-O systems there are well-defined chemical potential domains, where OVCs with an optimal number of carriers persist. Since each *l*:*m*:*n* OVC depletes the CB of electrons by a different amount, the controllable formation of OVCs can be used to modify interband absorption, enhance materials stability, reduce plasma absorption, and design next-generation TCs. Specifically, we identify $Ba_3Nb_5O_{15}$, $Ba_7Nb_6O_{21}$, and $Ca_{23}Al_{28}O_{64}$ OVCs as attractive candidatures for TC application. This work has broad implications as degenerate gapped compounds have been attracting much interest in many fields beyond that of TCs.

EXPERIMENTAL PROCEDURES

Density Functional Calculations

All spin-polarized calculations were carried out using Perdew-Burke-Ernzerhof functional[36] with DFT+U correction for Nb (U = 1.5 eV) and Ag (U = 5 eV) d-like orbitals as implemented by Dudarev et al.[37] and available in Vienna Ab Initio Simulation Package.[38] Although the DFT+U approach is a simplified self-interaction correction, it appears to describe correctly both reduced ligand states ("trapped holes") as well as ligands with conventional formal oxidation states, as demonstrated in tests described in literature.[39,40] It should be noted that the utilization of DFT+U with a larger U value (i.e., U = 3 eV) for Nb d-like orbitals results in incorrect insulating nature of the $BaNbO_3$ system. The cutoff energies for plane-wave basis were set to 500 and 600 eV for the final static and volume relaxation calculations, respectively. Γ-centered Monkhorst-Pack k-grids[41] were used in the Brillouin-zone integrations with grid densities of approximately 2,500 and 10,000 per reciprocal atom for volume relaxation and final static calculations. For each system, random atomic displacements within 0.1 Å were applied to avoid trap at a local minimum. The full optimization of lattice vectors and atomic positions was allowed. The results were analyzed using VESTA[42] and pymatgen.[43]

Calculations of Chemical Potential Domains

To calculate stability zones for $BaNbO_3$, $Ca_6Al_7O_{16}$, and $Ag_3Al_{22}O_{34}$ compounds presented in Figure 3, we used only experimentally known stoichiometric crystal structures available in the Inorganic Crystal Structure Database (ICSD)[6] and SpringerMaterial.[44] To predict convex hulls and chemical potential diagrams for Ca-Al-O and Ag-Al-O systems, in addition to the known experimental structures, we included generated OVCs and structures available in the Materials Project[45] database. For the Ba-Nb-O system (Figures 2A and 6A), we also considered stoichiometries inspired by II-V-O phase diagrams. The O_2 molecule was used as a reference state for the O_2 phase. The ground state compounds found in this work are given in Data S1–S3. We implemented fitted elemental-phase reference energy corrections[46] to correct chemical potentials for elemental reference states.

Optical Spectra

The optical properties (Figure 8) were computed within independent particle approximation.[47] To calculate plasma frequencies and interband transition spectra,

40 × 40 × 40, 20 × 20 × 20, 20 × 20 × 20, 8 × 24 × 8, 16 × 12 × 8, 20 × 20 × 20, 8 × 8 × 8, and 8 × 8 × 8 Γ-centered k-point grids were used for $BaNbO_3$, $Ba_7Nb_8O_{24}$, $Ba_7Nb_6O_{21}$, $Ba_3Nb_5O_{15}$, $BaNb_2O_6$, $Ca_6Al_7O_{16}$, $Ca_{23}Al_{28}O_{64}$, and $Ca_{11}Al_{14}O_{32}$, respectively. The Drude contribution to optical properties was included by utilizing kram code[48] with plasma frequencies calculated from first-principles calculations and the damping coefficient of 0.2 eV, which is analogous to traditional TCs.[49]

Defect Calculations

Supercells with 116, 135, and 236 atoms were used to calculate defect energetics in $Ca_6Al_7O_{16}$, $BaNbO_3$, and $Ag_3Al_{22}O_{34}$ systems, respectively. The defect formation energies (Figures 3A, 3C, and 3E) and finite size corrections were computed within the framework described by Lany and Zunger[50,51] and implemented in the pyladadefects code.[52] For the defect calculations, the ranges of chemical potentials were determined using only experimentally known stoichiometric crystal structures as described above. It should be noted that unlike conventional insulators where the Fermi energy can span the full range of the gap (Figure 1B), thus controlling the balance between different charges, if the Fermi energy resides inside a continuum band, as is the case in Figure 1A, it represents the energy to add or remove an electron from the host system, not from point defects in the gap. Thus, the conventional calculation of charged defects versus E_F is not meaningful in degenerate gapped materials.

DATA AND SOFTWARE AVAILABILITY

All data needed to evaluate the conclusions in the paper are present in the paper and the Supplemental Information. Additional data related to this paper may be requested from the authors.

SUPPLEMENTAL INFORMATION

Supplemental Information can be found online at https://doi.org/10.1016/j.matt.2019.05.014.

ACKNOWLEDGMENTS

The work of A.Z. and O.I.M. at University of Colorado Boulder, and of K.R.P. and M.T.Y. at Northwestern University, was supported by the NSF-DMR EPM program under grants DMR-1806939 and DMR-1806912, respectively. M.T.Y. would like to thank the Department of Energy (DOE) Office of Energy Efficiency and Renewable Energy (EERE) Postdoctoral Research Award under the EERE Solar Energy Technologies Office administered by the Oak Ridge Institute for Science and Education (ORISE) for the DOE. The ORISE is managed by Oak Ridge Associated Universities (ORAU) under DOE contract number DE-SC00014664. All opinions expressed in this paper are the authors' and do not necessarily reflect the policies and views of DOE, ORAU, or ORISE. O.I.M. and C.P. acknowledge support from the Research Council of Norway (contract no. 251131), and the Norwegian Metacenter for Computational Science (NOTUR) for providing access to supercomputer resources. We would like to thank Zachary Mansley for help with transmission electron microscopy.

AUTHOR CONTRIBUTIONS

O.I.M. carried out the theoretical calculations. M.T.Y. fabricated the samples and carried out structure analysis by X-ray powder diffraction. A.Z. directed the design of the research, analysis of the results, and writing of the paper. O.I.M. contributed most to writing of the paper, with contributions from all co-authors. K.R.P. supervised the experimental work. C.P. and A.Z. supervised all theoretical studies.

DECLARATION OF INTERESTS

The authors declare no competing interests.

Received: January 1, 2019
Revised: April 9, 2019
Accepted: May 13, 2019
Published: July 10, 2019

REFERENCES

1. Dalton, J. (1808). A New System of Chemical Philosophy, *Vol. 1* (W. Dawson).
2. Berthollet, C.-L. (1803). Essai de statique chimique, *Vol. 2* (F. Didot).
3. D.S. Ginley, H. Hosono, and D.C. Paine, eds. (2010). Handbook of Transparent Conductors (Springer Science & Business Media).
4. Zhang, S.B., Wei, S.H., and Zunger, A. (1999). Overcoming doping bottlenecks in semiconductors and wide-gap materials. Phys. B Condens. Matter *273-274*, 976–980.
5. Zhang, X., Zhang, L., Perkins, J.D., and Zunger, A. (2015). Intrinsic transparent conductors without doping. Phys. Rev. Lett. *115*, 176602.
6. Belsky, A., Hellenbrandt, M., Karen, V.L., and Luksch, P. (2002). New developments in the inorganic crystal structure database (ICSD): accessibility in support of materials research and design. Acta Crystallogr. B *58*, 364–369.
7. Hart, G.L.W., and Zunger, A. (2001). Origins of nonstoichiometry and vacancy ordering in $Sc_{1-x}\square_xS$. Phys. Rev. Lett. *87*, 275508.
8. Zhang, S.B., Wei, S.-H., and Zunger, A. (1997). Stabilization of ternary compounds via ordered arrays of defect pairs. Phys. Rev. Lett. *78*, 4059–4062.
9. Anand, S., Xia, K., Zhu, T., Wolverton, C., and Snyder, G.J. (2018). Temperature dependent n-type self doping in nominally 19-electron half-Heusler thermoelectric materials. Adv. Energy Mater. *8*, 1801409.
10. Anand, S., Xia, K., Hegde, V.I., Aydemir, U., Kocevski, V., Zhu, T., Wolverton, C., and Snyder, G.J. (2018). A valence balanced rule for discovery of 18-electron half-Heuslers with defects. Energy Environ. Sci. *11*, 1480–1488.
11. Xu, X., Randorn, C., Efstathiou, P., and Irvine, J.T.S. (2012). A red metallic oxide photocatalyst. Nat. Mater. *11*, 595–598.
12. Kitano, M., Inoue, Y., Yamazaki, Y., Inoue, Y., Yamazaki, Y., Hayashi, F., Kanbara, S., Matsuishi, S., Yokoyama, T., Kim, S.W., Hara, M., Hosono, H., et al. (2012). Ammonia synthesis using a stable electride as an electron donor and reversible hydrogen store. Nat. Chem. *4*, 934–940.
13. Hosono, H., Kim, J., Toda, Y., Kamiya, T., and Watanabe, S. (2017). Transparent amorphous oxide semiconductors for organic electronics: application to inverted OLEDs. Proc. Natl. Acad. Sci. USA *114*, 233–238.
14. Ducastelle, F. (1991). Order and Phase Stability in Alloys (North-Holland).
15. Svensson, G. (1988). $Ba_2Nb_5O_9$ — an intergrowth of $BaNbO_3$ (perovskite) and NbO. Mater. Res. Bull. *23*, 437–446.
16. Svensson, G., and Werner, P.-E. (1990). Determination of the composition of $BaNbO_3$ using profile refinement and phase analysis. Mater. Res. Bull. *25*, 9–14.
17. Hessen, B., Sunshine, S.A., Siegrist, T., and Jimenez, R. (1991). Crystallization of reduced strontium and barium niobate perovskites from borate fluxes. Mater. Res. Bull. *26*, 85–90.
18. Casais, M.T., Alonso, J.A., Rasines, I., and Hidalgo, M.A. (1995). Preparation, neutron structural study and characterization of $BaNbO_3$ - a Pauli-like metallic perovskite. Mater. Res. Bull. *30*, 201–208.
19. Hessen, B., Sunshine, S.A., Siegrist, T., Fiory, A.T., and Waszczak, J.V. (1991). Structure and properties of reduced barium niobium oxide single-crystals obtained from borate fluxes. Chem. Mater. *3*, 528–534.
20. Hwang, Y.K., and Kwon, Y.-U. (1997). Syntheses and electrical properties of tetragonal tungsten bronze type solid solution $Ba_{6-x}La_xNb_{10}O_{30+\delta}$ (x = 0, 1, 2, 3) and $Sr_6Nb_{10}O_{30}$. Mater. Res. Bull. *32*, 1495–1502.
21. D'yachenko, O.G., Istomin, S.Y., Fedotov, M.M., Antipov, E.V., Svensson, G., Nygren, M., and Holm, W. (1997). Structure and properties of $Ba_{6-x}Ln_xNb_{10}O_{30}$, Ln = La, Ce and Nd compounds. Mater. Res. Bull. *32*, 409–419.
22. Kolodiazhnyi, T., Sakurai, H., Isobe, M., Matsushita, Y., Forbes, S., Mozharivskyj, Y., Munsie, T.J.S., Luke, G.M., Gurak, M., and Clarke, D.R. (2015). Superconductivity and crystal structural origins of the metal-insulator transition in $Ba_{6-x}Sr_xNb_{10}O_{30}$ tetragonal tungsten bronzes. Phys. Rev. B *92*, 214508.
23. Kolodiazhnyi, T., Sakurai, H., Vasylkiv, O., Borodianska, H., and Mozharivskyj, Y. (2014). Abnormal thermal conductivity in tetragonal tungsten bronze $Ba_{6-x}Sr_xNb_{10}O_{30}$. Appl. Phys. Lett. *104*, 111903.
24. Chan, J.H., Bock, J.A., Guo, H., Trolier-McKinstry, S., and Randall, C.A. (2017). Filled oxygen-deficient strontium barium niobates. J. Am. Ceram. Soc. *100*, 774–782.
25. Chan, J.H., Bock, J.A., Guo, H., Trolier-McKinstry, S., and Randall, C.A. (2017). High-temperature thermoelectric characterization of filled strontium barium niobates: power factors and carrier concentrations. J. Mater. Res. *32*, 1160–1167.
26. Galasso, F., Layden, G., and Ganung, G. (1968). ANb_2O_6 and ATa_2O_6 phases. Mater. Res. Bull. *3*, 397–407.
27. Galasso, F., and Katz, L. (1961). Preparation and structure of $Ba_5Ta_4O_{15}$ and related compounds. Acta Cryst. *14*, 647–650.
28. Matsuishi, S., Toda, Y., Miyakawa, M., Hayashi, K., Kamiya, T., Hirano, M., Tanaka, I., and Hosono, H. (2003). High-density electron anions in a nanoporous single crystal: $[Ca_{24}Al_{28}O_{64}]^{4+}(4e^-)$. Science *301*, 626–629.
29. Miyakawa, M., Kim, S.W., Hirano, M., Kohama, Y., Kawaji, H., Atake, T., Ikegami, H., Kono, K., and Hosono, H. (2007). Superconductivity in an inorganic electride 12CaO center dot $7Al_2O_3{:}e^-$. J. Am. Chem. Soc. *129*, 7270–7271.
30. Christensen, A.N. (1987). Neutron powder diffraction profile refinement studies on $Ca_{11.3}Al_{14}O_{32.3}$ and $CaCiO(D_{0.88}H_{0.12})$. Acta Chem. Scand. A *41*, 110–112.
31. Sirotinkin, S., Sirotinkin, V., and Trunov, V. (1990). Structure of low-temperature modification of $BaNb_2O_6$. Zh. Neorgan. Khim. *35*, 1609–1611.
32. Vanderah, T.A., Collins, T.R., Wong-Ng, W., Roth, R.S., and Farber, L. (2002). Phase equilibria and crystal chemistry in the BaO–Al_2O_3–Nb_2O_5 and BaO–Nb_2O_5 systems. J. Alloys Compd. *346*, 116–128.
33. Cho, I.-S., Bae, S.T., Kim, D.H., and Hong, K.S. (2010). Effects of crystal and electronic structures of ANb_2O_6 (A=Ca, Sr, Ba) metaniobate compounds on their photocatalytic H_2 evolution from pure water. Int. J. Hydrogen Energy *35*, 12954–12960.
34. Miseki, Y., Kato, H., and Kudo, A. (2006). Water splitting into H_2 and O_2 over $Ba_5Nb_4O_{15}$ photocatalysts with layered perovskite structure prepared by polymerizable complex method. Chem. Lett. *35*, 1052–1053.
35. Drude, P. (1900). Zur elektronentheorie der Metalle. Ann. Phys. (Berl.) *306*, 566–613.
36. Perdew, J.P., Burke, K., and Ernzerhof, M. (1996). Generalized gradient approximation made simple. Phys. Rev. Lett. *77*, 3865–3868.
37. Dudarev, S.L., Botton, G.A., Savrasov, S.Y., Humphreys, C.J., and Sutton, A.P. (1998). Electron-energy-loss spectra and the structural stability of nickel oxide: an LSDA+U study. Phys. Rev. B *57*, 1505–1509.
38. Kresse, G., and Furthmüller, J. (1996). Efficiency of ab-initio total energy calculations for metals and semiconductors using a plane-wave basis set. Comp. Mater. Sci. *6*, 15–50.

39. Dalpian, G.M., Liu, Q., Varignon, J., Bibes, M., and Zunger, A. (2018). Bond disproportionation, charge self-regulation, and ligand holes in ABX_3 perovskites by density functional theory. Phys. Rev. B *98*, 075135.

40. Liu, Q., Dalpian, G.M., and Zunger, A. (2019). Antidoping in insulators and semiconductors having intermediate bands with trapped carriers. Phys. Rev. Lett. *122*, 106403.

41. Monkhorst, H.J., and Pack, J.D. (1976). Special points for Brillouin-zone integrations. Phys. Rev. B *13*, 5188–5192.

42. Momma, K., and Izumi, F. (2011). VESTA 3 for three-dimensional visualization of crystal, volumetric and morphology data. J. Appl. Crystallogr. *44*, 1272–1276.

43. Ong, S.P., Richards, W.D., Jain, A., Hautier, G., Kocher, M., Cholia, S., Gunter, D., Chevrier, V.L., Persson, K.A., and Ceder, G. (2013). Python Materials Genomics (pymatgen): a robust, open-source python library for materials analysis. Comp. Mater. Sci. *68*, 314–319.

44. SpringerMaterials, The Landolt–Börnstein Database. https://materials.springer.com/.

45. Jain, A., Ong, S.P., Hautier, G., Chen, W., Richards, W.D., Dacek, S., Cholia, S., Gunter, D., Skinner, D., Ceder, G., and Persson, K.A. (2013). Commentary: the Materials Project: a materials genome approach to accelerating materials innovation. APL Mat. *1*, 011002.

46. Stevanović, V., Lany, S., Zhang, X., and Zunger, A. (2012). Correcting density functional theory for accurate predictions of compound enthalpies of formation: fitted elemental-phase reference energies. Phys. Rev. B *85*, 115104.

47. Gajdoš, M., Hummer, K., Kresse, G., Furthmüller, J., and Bechstedt, F. (2006). Linear optical properties in the projector-augmented wave methodology. Phys. Rev. B *73*, 045112.

48. Blaha, P., Schwarz, K., Madsen, G.K.H., Kvasnicka, D., Luitz, J., Laskowski, R., Tran, F., and Marks, L.D. (2001). WIEN2k, an Augmented Plane Wave + Local Orbitals Program for Calculating Crystal Properties (Karlheinz Schwarz, Technische Universität Wien).

49. Naik, G.V., Kim, J., and Boltasseva, A. (2011). Oxides and nitrides as alternative plasmonic materials in the optical range [Invited]. Opt. Mater. Express *1*, 1090–1099.

50. Lany, S., and Zunger, A. (2008). Assessment of correction methods for the band-gap problem and for finite-size effects in supercell defect calculations: case studies for ZnO and GaAs. Phys. Rev. B *78*, 235104.

51. Lany, S., and Zunger, A. (2009). Accurate prediction of defect properties in density functional supercell calculations. Modell. Simul. Mater. Sci. Eng. *17*, 084002.

52. Goyal, A., Gorai, P., Peng, H., Lany, S., and Stevanović, V. (2017). A computational framework for automation of point defect calculations. Comp. Mater. Sci. *130*, 1–9.

Matter, Volume *1*

Supplemental Information

Spontaneous Non-stoichiometry and Ordering in Degenerate but Gapped Transparent Conductors

Oleksandr I. Malyi, Michael T. Yeung, Kenneth R. Poeppelmeier, Clas Persson, and Alex Zunger

Supplementary Note I: Experimental observation of Ag formation in $Ag_3Al_{22}O_{34+x}$ under reduced atmosphere

$Ag_3Al_{22}O_{34}$ was predicted to be a transparent conducting oxide with a periodic 2-dimensional electron gas.[1] This composition is unusual for β-aluminas in two ways, notably the high monovalent cation loading and the partial reduced silver species, and thus an alternative synthetic route was needed. The typical sodium (or any other cation) loading in unstabilized sodium β-aluminas has been traditionally limited to about $Na_{2-2.5}Al_{22}O_{34+\delta}$.[2] This cap is a culmination of two factors: (1) the high ionic mobility of sodium and (2) the high volatility of Na_2O at synthesis temperatures. To get around this, we sintered $Ba_{1.5}Al_{22}O_{34.5}$ at high temperatures as the precursor, as the divalent barium is far less mobile at high temperatures than sodium. The divalent barium is then ion exchanged at the relatively low temperature of 980°C in molten sodium chloride, preventing the volatilization of Na_2O seen at sintering temperatures. From there, the highly non-stoichiometric sodium β-alumina can be ion exchanged to yield the desired the highly non-stoichiometric silver β-alumina $Ag_3Al_{22}O_{34.5}$

Powder X-ray diffraction confirms the synthesis of $Ag_3Al_{22}O_{34.5}$, and the peaks can be indexed to the JCPDS reference pattern #01-084-0514 (Supplementary Fig. 1a), corresponding with the phase "$Ag_3Al_{22}O_{34}$" identified by Tofield *et.al*.[3] $Ag_3Al_{22}O_{34.5}$, $Ag_3Al_{22}O_{34}$, and $Ag_{2.5}Al_{22}O_{34.25}$ all crystallize in the same space group of $P6_3/mmc$; the primary difference between all three being occupancy. The lack of conductivity is attributed to the presence of 0.5 moles interstitial oxygen, which has been found in other non-stoichiometric β-aluminas.[4, 5] Heating the compound to 700 °C so that the compound may auto-reduce and liberate both oxygen and free carriers instead resulted in the formation of free metallic silver (Supplementary Fig. 1b) and the decomposition from $Ag_3Al_{22}O_{34.5}$ to $Ag_{2.5}Al_{22}O_{34.25}$. While the presence of free silver is clear from the powder X-ray diffraction (and the fact that the formerly white compound turns a red hue from the formation of silver particles), the formation $Ag_{2.5}Al_{22}O_{34.25}$ is subtle but can be identified by two key markers: the increase in intensity of the (101) peak, and the presence of the (104) peak. Silver β-alumina have been used as fast ion conductors at elevated temperatures at varying oxygen partial pressures.[2, 6] Furthermore, any attempts to mildly reduce the compounds and raise the carrier concentration results immediately in the compensation and cation vacancy formation/silver precipitation.

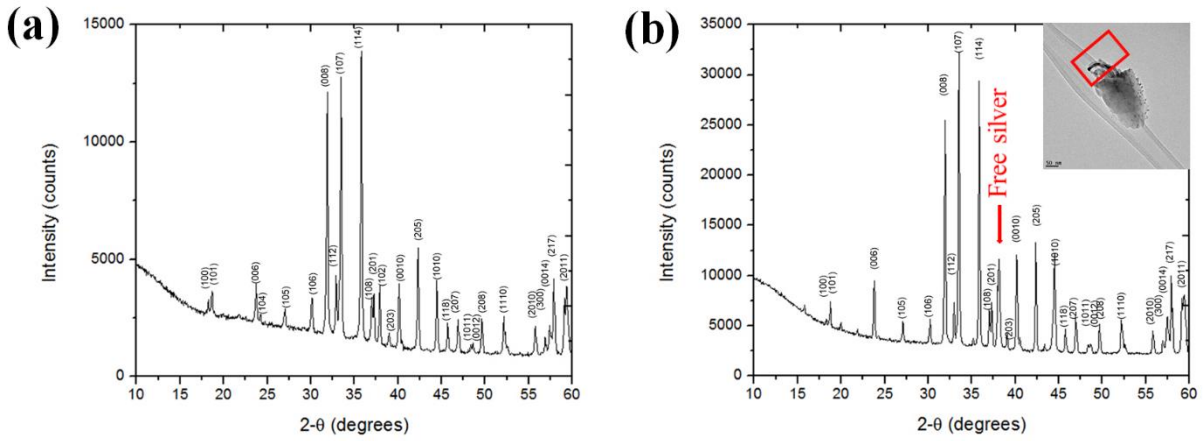

Supplementary Figure 1. Ag formation in $Ag_3Al_{22}O_{34+x}$ under reduced atmosphere. (a) The powder X-ray diffraction of $Ag_3Al_{22}O_{34.5}$ can be indexed to the JCPDS reference pattern #01-084-0514, corresponding with the phase "$Ag_3Al_{22}O_{34}$" identified by Tofield *et al.*[3] (b) Any attempts to reduce $Ag_3Al_{22}O_{34.5}$ and introduce carriers results in the precipitation of free metallic silver and the possible formation of $Ag_{2.5}Al_{22}O_{34.25}$.

Supplementary Note II: Synthesis of $Ba_3Nb_5O_{15}$

Our procedure was developed taking into consideration of all other synthetic routes, which showed that for polycrystalline compacts, long (> 40 hrs) sintering durations, multiple intermittent regrinding, and low partial oxygen pressure atmospheres were needed to prepare phase pure towards $Ba_3Nb_5O_{15}$/$Ba_6Nb_{10}O_{30}$. In our work, we have found that the targeted $Ba_3Nb_5O_{15}$ can be prepared after 72 hours of heating with intermittent grinding (Supplementary Fig. 2a). The oxygen partial pressure was kept low with a 5% H_2/balance argon atmosphere. The progress was monitored with pXRD at 24 hour intervals, and we can confirm the presence of two secondary phases (OVCs identified in our theoretical calculations, see Fig. 2a and 6a in the main text): $Ba_5Nb_4O_{15}$ and $BaNb_2O_6$. Given the tiny range of chemical potentials under which $Ba_3Nb_5O_{15}$ is stable, it is not surprising to find these more stable secondary phases on the way to $Ba_3Nb_5O_{15}$. These secondary phases react and disappear with further heating, and completely disappear by 72 hours of heating (Supplementary Fig. 2b).

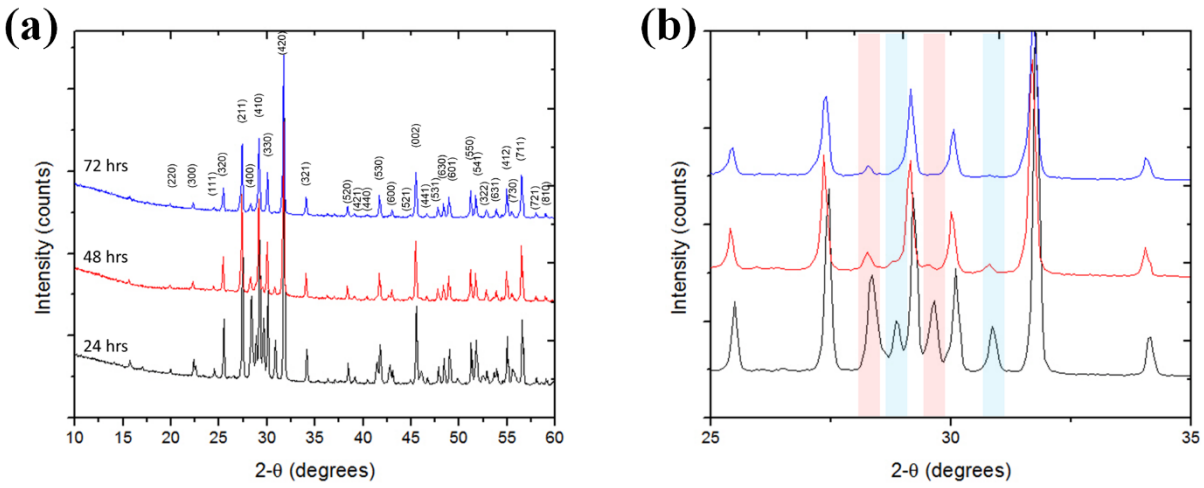

Supplementary Figure 2. Synthesis of $Ba_3Nb_5O_{15}$. (a) Monitoring the progress on the formation of $Ba_3Nb_5O_{15}$ monitored through powder X-ray diffraction of $Ba_3Nb_5O_{15}$. (b) The peak intensities for phases $Ba_5Nb_4O_{15}$ (light blue) and $BaNb_2O_6$ (light red) decrease with increasing heating duration, resulting in phase pure $Ba_3Nb_5O_{15}$ after 72 hours of heating.

Supplementary Note III: The delocalized nature of the conducting electrons in degenerate insulators

For Ba-Nb-O degenerate insulators, the conducting electrons are localized near Nb atoms. Specifically, for the 1:1:3 cubic perovskite compound, the charge density in the NbO plane is about 9 times larger than that in the BaO plane. The vacancy formation does not significantly change the nature of the charge distribution (Supplementary Figs. 3a, b). For Ca-Al-O degenerate insulators, the conduction band electrons reside within the cavity of well-defined cage-like blocks (Supplementary Figs. 3c, d). Because of this, the formation of Ca vacancy destroys the surrounding cage-like blocks and reduces the carrier concentration within the vacancy region. Despite this, both 6:7:24 and its 23:28:64 OVC have clearly defined 0-dimensional charge carrier density localization which implies that the compounds are not only degenerate insulators but also stable inorganic electrides.

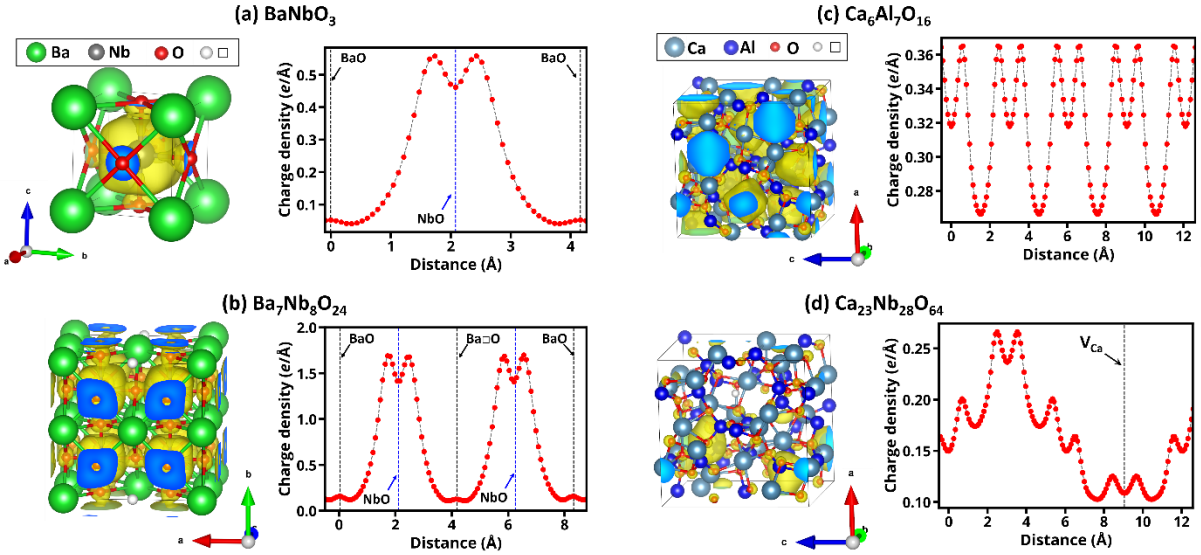

Supplementary Figure 3. Delocalization nature of conducting electrons in degenerate insulators. Real space partial electron density of conducting electrons in (a) $BaNbO_3$, (b) $Ba_7Nb_8O_{28}$, (c) $Ca_6Al_7O_{16}$, and (d) $Ca_{23}Al_{28}O_{64}$ and its projection on the direction *a*. The isosurfaces are set at 0.001 *e*/bohr^3 and 0.0005 *e*/bohr^3 for Ba-Nb-O and Ca-Al-O systems, respectively.

Supplementary Data I: Ground state compounds in Ba-Nb-O system

Ba

```
_symmetry_space_group_name_H-M   'P 1'
_cell_length_a   4.35636765
_cell_length_b   4.35636704
_cell_length_c   4.35636800
_cell_angle_alpha   109.47121581
_cell_angle_beta   109.47121298
_cell_angle_gamma   109.47122455
_symmetry_Int_Tables_number   1
_chemical_formula_structural   Ba
_chemical_formula_sum   Ba1
_cell_volume   63.64315513
_cell_formula_units_Z   1
loop_
 _symmetry_equiv_pos_site_id
 _symmetry_equiv_pos_as_xyz
  1  'x, y, z'
loop_
 _atom_site_type_symbol
 _atom_site_label
 _atom_site_symmetry_multiplicity
 _atom_site_fract_x
 _atom_site_fract_y
 _atom_site_fract_z
 _atom_site_occupancy
  Ba  Ba1  1  0.976128  0.995450  0.980601  1
```

BaO

```
_symmetry_space_group_name_H-M   'P 1'
_cell_length_a   5.61544600
_cell_length_b   5.61562200
_cell_length_c   5.61599000
_cell_angle_alpha   90.00057131
_cell_angle_beta   90.00037748
_cell_angle_gamma   90.00044893
_symmetry_Int_Tables_number   1
_chemical_formula_structural   BaO
_chemical_formula_sum   'Ba4 O4'
_cell_volume   177.09587597
_cell_formula_units_Z   4
loop_
 _symmetry_equiv_pos_site_id
 _symmetry_equiv_pos_as_xyz
  1  'x, y, z'
loop_
 _atom_site_type_symbol
 _atom_site_label
 _atom_site_symmetry_multiplicity
 _atom_site_fract_x
 _atom_site_fract_y
 _atom_site_fract_z
 _atom_site_occupancy
  Ba  Ba1  1  0.994098  0.997505  0.993681  1
  Ba  Ba2  1  0.494047  0.997522  0.493534  1
  Ba  Ba3  1  0.994260  0.497584  0.493721  1
  Ba  Ba4  1  0.494310  0.497563  0.993622  1
  O  O5  1  0.494182  0.497568  0.493218  1
  O  O6  1  0.994110  0.497705  0.993399  1
  O  O7  1  0.493929  0.997359  0.993115  1
  O  O8  1  0.993923  0.997404  0.493306  1
```

BaO_2

```
_symmetry_space_group_name_H-M   'P 1'
_cell_length_a   4.43253442
_cell_length_b   4.43253442
_cell_length_c   7.72989432
_cell_angle_alpha   64.10308353
_cell_angle_beta   64.10308353
_cell_angle_gamma   51.68671041
_symmetry_Int_Tables_number   1
_chemical_formula_structural   BaO2
_chemical_formula_sum   'Ba2 O4'
_cell_volume   104.19138075
_cell_formula_units_Z   2
loop_
 _symmetry_equiv_pos_site_id
 _symmetry_equiv_pos_as_xyz
  1  'x, y, z'
loop_
 _atom_site_type_symbol
 _atom_site_label
 _atom_site_symmetry_multiplicity
 _atom_site_fract_x
 _atom_site_fract_y
 _atom_site_fract_z
 _atom_site_occupancy
  Ba  Ba1  1  0.500535  0.499465  0.250000  1
  Ba  Ba2  1  0.499465  0.500535  0.750000  1
  O  O3  1  0.888579  0.895978  0.054472  1
  O  O4  1  0.104022  0.111421  0.445528  1
  O  O5  1  0.111421  0.104022  0.945528  1
  O  O6  1  0.895978  0.888579  0.554472  1
```

Nb

```
_symmetry_space_group_name_H-M   'P 1'
_cell_length_a   2.90286990
_cell_length_b   2.90286979
_cell_length_c   2.90286989
_cell_angle_alpha   109.47120777
_cell_angle_beta   109.47120700
_cell_angle_gamma   109.47123504
_symmetry_Int_Tables_number   1
_chemical_formula_structural   Nb
_chemical_formula_sum   Nb1
_cell_volume   18.83045752
_cell_formula_units_Z   1
loop_
 _symmetry_equiv_pos_site_id
 _symmetry_equiv_pos_as_xyz
  1  'x, y, z'
loop_
 _atom_site_type_symbol
 _atom_site_label
 _atom_site_symmetry_multiplicity
 _atom_site_fract_x
 _atom_site_fract_y
 _atom_site_fract_z
 _atom_site_occupancy
  Nb  Nb1  1  0.989315  0.011287  0.970412  1
```

Nb_8O

```
_symmetry_space_group_name_H-M   'P 1'
_cell_length_a   3.33819808
_cell_length_b   9.70864476
_cell_length_c   9.70054127
_cell_angle_alpha   89.94499925
_cell_angle_beta   89.99641670
_cell_angle_gamma   89.99435529
_symmetry_Int_Tables_number   1
_chemical_formula_structural   Nb8O
_chemical_formula_sum   'Nb16 O2'
_cell_volume   314.38837414
_cell_formula_units_Z   2
loop_
 _symmetry_equiv_pos_site_id
 _symmetry_equiv_pos_as_xyz
  1  'x, y, z'
loop_
 _atom_site_type_symbol
 _atom_site_label
 _atom_site_symmetry_multiplicity
 _atom_site_fract_x
 _atom_site_fract_y
 _atom_site_fract_z
 _atom_site_occupancy
  Nb  Nb1  1  0.502301  0.127693  0.383456  1
  Nb  Nb2  1  0.502376  0.868509  0.616799  1
  Nb  Nb3  1  0.002331  0.627667  0.116797  1
  Nb  Nb4  1  0.002086  0.368558  0.883454  1
  Nb  Nb5  1  0.502211  0.381333  0.129773  1
  Nb  Nb6  1  0.502231  0.614875  0.870486  1
  Nb  Nb7  1  0.002441  0.114851  0.629711  1
  Nb  Nb8  1  0.002202  0.881324  0.370550  1
  Nb  Nb9  1  0.501894  0.651434  0.346653  1
  Nb  Nb10  1  0.501875  0.344707  0.653627  1
  Nb  Nb11  1  0.002629  0.151361  0.153523  1
  Nb  Nb12  1  0.002765  0.844838  0.846713  1
  Nb  Nb13  1  0.502983  0.880124  0.118046  1
  Nb  Nb14  1  0.502987  0.116100  0.882237  1
  Nb  Nb15  1  0.001753  0.380053  0.382178  1
  Nb  Nb16  1  0.001461  0.616152  0.618093  1
  O  O17  1  0.501405  0.498093  0.500170  1
  O  O18  1  0.003083  0.998097  0.000129  1
```

$Nb_{12}O_{29}$

```
_symmetry_space_group_name_H-M   'P 1'
_cell_length_a   10.76552232
_cell_length_b   10.76552083
_cell_length_c   29.49183109
_cell_angle_alpha   89.99362541
_cell_angle_beta   90.00417228
_cell_angle_gamma   159.18185378
_symmetry_Int_Tables_number   1
_chemical_formula_structural   Nb12O29
_chemical_formula_sum   'Nb24 O58'
_cell_volume   1214.76701743
_cell_formula_units_Z   2
loop_
 _symmetry_equiv_pos_site_id
 _symmetry_equiv_pos_as_xyz
  1  'x, y, z'
loop_
 _atom_site_type_symbol
 _atom_site_label
 _atom_site_symmetry_multiplicity
 _atom_site_fract_x
 _atom_site_fract_y
 _atom_site_fract_z
 _atom_site_occupancy
  Nb  Nb1  1  0.461127  0.533690  0.050341  1
  Nb  Nb2  1  0.535152  0.459544  0.949864  1
  Nb  Nb3  1  0.459105  0.532570  0.449848  1
  Nb  Nb4  1  0.532916  0.458215  0.550327  1
  Nb  Nb5  1  0.829424  0.165358  0.049971  1
  Nb  Nb6  1  0.166894  0.827877  0.950202  1
  Nb  Nb7  1  0.827401  0.164254  0.450169  1
  Nb  Nb8  1  0.164644  0.826560  0.549994  1
  Nb  Nb9  1  0.646395  0.348623  0.048248  1
  Nb  Nb10  1  0.349983  0.644694  0.951915  1
  Nb  Nb11  1  0.644246  0.347387  0.451945  1
  Nb  Nb12  1  0.347761  0.643429  0.548211  1
  Nb  Nb13  1  0.462384  0.531936  0.184771  1
  Nb  Nb14  1  0.532266  0.460764  0.815420  1
  Nb  Nb15  1  0.461219  0.531000  0.315414  1
  Nb  Nb16  1  0.530247  0.458999  0.684764  1
  Nb  Nb17  1  0.829338  0.164971  0.184251  1
  Nb  Nb18  1  0.165305  0.827707  0.815912  1
  Nb  Nb19  1  0.828187  0.164044  0.315880  1
  Nb  Nb20  1  0.163295  0.825957  0.684283  1
  Nb  Nb21  1  0.646746  0.349698  0.184585  1
  Nb  Nb22  1  0.344630  0.639737  0.815577  1
```

Nb Nb23 1 0.648180 0.351357 0.315624 1
Nb Nb24 1 0.352774 0.648138 0.684530 1
O O25 1 0.454811 0.538502 0.250094 1
O O26 1 0.538262 0.452974 0.750090 1
O O27 1 0.832029 0.161325 0.250066 1
O O28 1 0.161138 0.830145 0.750093 1
O O29 1 0.649067 0.346411 0.250103 1
O O30 1 0.345526 0.646439 0.750057 1
O O31 1 0.937128 0.057686 0.043963 1
O O32 1 0.059187 0.935474 0.956237 1
O O33 1 0.935077 0.056591 0.456221 1
O O34 1 0.056959 0.934175 0.543965 1
O O35 1 0.354151 0.640619 0.036505 1
O O36 1 0.642195 0.352556 0.963687 1
O O37 1 0.352086 0.639516 0.463646 1
O O38 1 0.639959 0.351260 0.536514 1
O O39 1 0.741758 0.253260 0.042414 1
O O40 1 0.254813 0.740195 0.957717 1
O O41 1 0.739547 0.251979 0.457714 1
O O42 1 0.252502 0.738839 0.542414 1
O O43 1 0.148917 0.846045 0.027798 1
O O44 1 0.847525 0.147253 0.972370 1
O O45 1 0.146698 0.844814 0.472395 1
O O46 1 0.845307 0.146010 0.527760 1
O O47 1 0.547452 0.447421 0.030545 1
O O48 1 0.448979 0.545917 0.969689 1
O O49 1 0.545266 0.446163 0.469680 1
O O50 1 0.446744 0.544621 0.530508 1
O O51 1 0.465315 0.529249 0.111821 1
O O52 1 0.530148 0.463743 0.888397 1
O O53 1 0.463752 0.528279 0.388379 1
O O54 1 0.528258 0.462414 0.611800 1
O O55 1 0.834376 0.160080 0.111703 1
O O56 1 0.161086 0.832577 0.888471 1
O O57 1 0.832871 0.159276 0.388442 1
O O58 1 0.159223 0.831394 0.611725 1
O O59 1 0.639554 0.355726 0.108852 1
O O60 1 0.356228 0.637308 0.891300 1
O O61 1 0.637791 0.354735 0.391336 1
O O62 1 0.354464 0.636323 0.608824 1
O O63 1 0.937325 0.056926 0.180230 1
O O64 1 0.057212 0.935608 0.819977 1
O O65 1 0.936269 0.056116 0.319971 1
O O66 1 0.055519 0.934187 0.680220 1
O O67 1 0.354553 0.639694 0.179776 1
O O68 1 0.639969 0.352854 0.820381 1
O O69 1 0.353507 0.638879 0.320355 1

O	O70	1	0.638284	0.351434	0.679804	1
O	O71	1	0.742572	0.252292	0.179970	1
O	O72	1	0.252602	0.740888	0.820121	1
O	O73	1	0.741039	0.250981	0.320149	1
O	O74	1	0.249942	0.738497	0.680013	1
O	O75	1	0.146809	0.848400	0.176342	1
O	O76	1	0.847834	0.144389	0.823827	1
O	O77	1	0.145864	0.847598	0.323890	1
O	O78	1	0.847059	0.143820	0.676265	1
O	O79	1	0.550007	0.444853	0.184215	1
O	O80	1	0.445122	0.548308	0.816002	1
O	O81	1	0.548487	0.443558	0.316002	1
O	O82	1	0.442490	0.545934	0.684156	1

NbO_2

```
_symmetry_space_group_name_H-M   'P 1'
_cell_length_a   6.07119815
_cell_length_b   9.87925843
_cell_length_c   9.87701218
_cell_angle_alpha   90.00173369
_cell_angle_beta   90.00746424
_cell_angle_gamma   90.00302134
_symmetry_Int_Tables_number   1
_chemical_formula_structural   NbO2
_chemical_formula_sum   'Nb16 O32'
_cell_volume   592.41267097
_cell_formula_units_Z   16
loop_
 _symmetry_equiv_pos_site_id
 _symmetry_equiv_pos_as_xyz
  1  'x, y, z'
loop_
 _atom_site_type_symbol
 _atom_site_label
 _atom_site_symmetry_multiplicity
 _atom_site_fract_x
 _atom_site_fract_y
 _atom_site_fract_z
 _atom_site_occupancy
  Nb  Nb1  1  0.720502  0.509567  0.760391  1
  Nb  Nb2  1  0.720519  0.487464  0.243637  1
  Nb  Nb3  1  0.970489  0.740168  0.513078  1
  Nb  Nb4  1  0.970526  0.256885  0.490994  1
  Nb  Nb5  1  0.220589  0.009600  0.260422  1
  Nb  Nb6  1  0.220551  0.987414  0.743636  1
  Nb  Nb7  1  0.470541  0.240130  0.013076  1
  Nb  Nb8  1  0.470561  0.756929  0.990968  1
  Nb  Nb9  1  0.272387  0.487437  0.743672  1
  Nb  Nb10  1  0.272456  0.509582  0.260428  1
  Nb  Nb11  1  0.522316  0.756880  0.490915  1
  Nb  Nb12  1  0.522391  0.240125  0.513125  1
  Nb  Nb13  1  0.772464  0.987470  0.243659  1
  Nb  Nb14  1  0.772463  0.009579  0.760395  1
  Nb  Nb15  1  0.022443  0.256933  0.990972  1
  Nb  Nb16  1  0.022475  0.740096  0.013068  1
  O  O17  1  0.741175  0.150235  0.900689  1
  O  O18  1  0.741180  0.846734  0.103422  1
  O  O19  1  0.991149  0.599667  0.153544  1
  O  O20  1  0.991054  0.397369  0.850494  1
  O  O21  1  0.240954  0.650282  0.400679  1
  O  O22  1  0.241072  0.346716  0.603442  1
```

O	O23	1	0.491071	0.099715	0.653686	1
O	O24	1	0.491115	0.897280	0.350364	1
O	O25	1	0.756096	0.362104	0.611880	1
O	O26	1	0.756078	0.635087	0.392008	1
O	O27	1	0.006150	0.888958	0.365898	1
O	O28	1	0.006125	0.108100	0.638169	1
O	O29	1	0.256071	0.862216	0.111769	1
O	O30	1	0.255937	0.134902	0.892191	1
O	O31	1	0.506085	0.388753	0.865734	1
O	O32	1	0.505954	0.608185	0.138238	1
O	O33	1	0.236968	0.362047	0.111990	1
O	O34	1	0.236980	0.634862	0.892207	1
O	O35	1	0.487004	0.388982	0.365957	1
O	O36	1	0.486886	0.608057	0.638125	1
O	O37	1	0.736760	0.862152	0.611815	1
O	O38	1	0.736735	0.134877	0.392233	1
O	O39	1	0.986987	0.888783	0.865719	1
O	O40	1	0.986995	0.108172	0.138254	1
O	O41	1	0.501930	0.099700	0.153588	1
O	O42	1	0.501896	0.897331	0.850414	1
O	O43	1	0.751882	0.346835	0.103318	1
O	O44	1	0.751779	0.650199	0.900709	1
O	O45	1	0.001783	0.599713	0.653569	1
O	O46	1	0.001784	0.397365	0.350534	1
O	O47	1	0.251897	0.846721	0.603355	1
O	O48	1	0.251917	0.150367	0.400629	1

NbO

```
_symmetry_space_group_name_H-M   'P 1'
_cell_length_a   4.28364712
_cell_length_b   4.28323117
_cell_length_c   4.28269574
_cell_angle_alpha   90.02163794
_cell_angle_beta   90.02487418
_cell_angle_gamma   89.97714155
_symmetry_Int_Tables_number   1
_chemical_formula_structural   NbO
_chemical_formula_sum   'Nb3 O3'
_cell_volume   78.57824324
_cell_formula_units_Z   3
loop_
 _symmetry_equiv_pos_site_id
 _symmetry_equiv_pos_as_xyz
  1  'x, y, z'
loop_
 _atom_site_type_symbol
 _atom_site_label
 _atom_site_symmetry_multiplicity
 _atom_site_fract_x
 _atom_site_fract_y
 _atom_site_fract_z
 _atom_site_occupancy
  Nb  Nb1  1  0.505882  0.994045  0.500982  1
  Nb  Nb2  1  0.505847  0.494398  0.000883  1
  Nb  Nb3  1  0.005871  0.494443  0.501004  1
  O  O4  1  0.005984  0.994384  0.501149  1
  O  O5  1  0.506078  0.994360  0.001096  1
  O  O6  1  0.005938  0.493956  0.001060  1
```

Nb_2O_5

```
_symmetry_space_group_name_H-M   'P 1'
_cell_length_a   3.89190501
_cell_length_b   19.79300144
_cell_length_c   20.82946079
_cell_angle_alpha   64.37219889
_cell_angle_beta   90.00103500
_cell_angle_gamma   90.00214144
_symmetry_Int_Tables_number   1
_chemical_formula_structural   Nb2O5
_chemical_formula_sum   'Nb28 O70'
_cell_volume   1446.69434171
_cell_formula_units_Z   14
loop_
 _symmetry_equiv_pos_site_id
 _symmetry_equiv_pos_as_xyz
  1  'x, y, z'
loop_
 _atom_site_type_symbol
 _atom_site_label
 _atom_site_symmetry_multiplicity
 _atom_site_fract_x
 _atom_site_fract_y
 _atom_site_fract_z
 _atom_site_occupancy
  Nb  Nb1  1  0.989629  0.160998  0.834128  1
  Nb  Nb2  1  0.498987  0.421155  0.703005  1
  Nb  Nb3  1  0.005453  0.004647  0.763546  1
  Nb  Nb4  1  0.984459  0.156122  0.566579  1
  Nb  Nb5  1  0.001231  0.693061  0.628814  1
  Nb  Nb6  1  0.004717  0.995881  0.235761  1
  Nb  Nb7  1  0.998223  0.152055  0.302579  1
  Nb  Nb8  1  0.498459  0.734115  0.839873  1
  Nb  Nb9  1  0.999145  0.316040  0.638360  1
  Nb  Nb10  1  0.999282  0.684483  0.360997  1
  Nb  Nb11  1  0.998396  0.848526  0.696649  1
  Nb  Nb12  1  0.998945  0.531305  0.562205  1
  Nb  Nb13  1  0.509791  0.110158  0.093378  1
  Nb  Nb14  1  0.499428  0.580409  0.770062  1
  Nb  Nb15  1  0.494823  0.264543  0.898402  1
  Nb  Nb16  1  0.524979  0.424311  0.964523  1
  Nb  Nb17  1  0.498679  0.579400  0.296328  1
  Nb  Nb18  1  0.026399  0.000297  0.499620  1
  Nb  Nb19  1  0.230222  0.000228  0.999650  1
  Nb  Nb20  1  0.510444  0.890377  0.905938  1
  Nb  Nb21  1  0.998776  0.469211  0.437128  1
  Nb  Nb22  1  0.984298  0.844413  0.432737  1
```

Nb Nb23 1 0.499141 0.420155 0.229248 1
Nb Nb24 1 0.497758 0.266458 0.159396 1
Nb Nb25 1 0.989352 0.839513 0.165228 1
Nb Nb26 1 0.000436 0.307464 0.370488 1
Nb Nb27 1 0.524589 0.576263 0.034796 1
Nb Nb28 1 0.495010 0.736011 0.100934 1
O O29 1 0.500450 0.182188 0.131228 1
O O30 1 0.499135 0.339419 0.066171 1
O O31 1 0.999335 0.755514 0.812460 1
O O32 1 0.998864 0.576999 0.461025 1
O O33 1 0.992455 0.087884 0.938351 1
O O34 1 0.503197 0.014132 0.205145 1
O O35 1 0.999371 0.405337 0.258987 1
O O36 1 0.995124 0.079776 0.535933 1
O O37 1 0.998870 0.423526 0.538308 1
O O38 1 0.498638 0.165543 0.573157 1
O O39 1 0.499170 0.341437 0.200835 1
O O40 1 0.500302 0.501212 0.861213 1
O O41 1 0.998983 0.426534 0.670082 1
O O42 1 0.498768 0.834985 0.426159 1
O O43 1 0.999859 0.595180 0.740331 1
O O44 1 0.497716 0.340879 0.791309 1
O O45 1 0.500445 0.664588 0.653052 1
O O46 1 0.498947 0.503910 0.585329 1
O O47 1 0.004371 0.416485 0.962484 1
O O48 1 0.499881 0.659189 0.798373 1
O O49 1 0.005030 0.917931 0.326127 1
O O50 1 0.998360 0.247300 0.736605 1
O O51 1 0.498978 0.344085 0.645187 1
O O52 1 0.000246 0.076289 0.263778 1
O O53 1 0.493981 0.819475 0.152970 1
O O54 1 0.001779 0.238788 0.465502 1
O O55 1 0.498743 0.496613 0.414003 1
O O56 1 0.999883 0.762388 0.668414 1
O O57 1 0.999206 0.607237 0.588940 1
O O58 1 0.499278 0.826105 0.723656 1
O O59 1 0.500978 0.818335 0.868084 1
O O60 1 0.503524 0.000369 0.499557 1
O O61 1 0.506030 0.026317 0.058775 1
O O62 1 0.998797 0.574000 0.329268 1
O O63 1 0.992493 0.912587 0.060993 1
O O64 1 0.500589 0.181444 0.996455 1
O O65 1 0.005363 0.082609 0.673189 1
O O66 1 0.500503 0.499420 0.138138 1
O O67 1 0.004260 0.584135 0.036838 1
O O68 1 0.999812 0.919131 0.602532 1
O O69 1 0.497501 0.659680 0.208037 1

O O70 1 0.995534 0.914039 0.195169 1
O O71 1 0.996472 0.086485 0.804171 1
O O72 1 0.498953 0.501014 0.272165 1
O O73 1 0.999177 0.238140 0.330897 1
O O74 1 0.998709 0.245084 0.186783 1
O O75 1 0.999122 0.253805 0.596298 1
O O76 1 0.503955 0.986400 0.794168 1
O O77 1 0.498827 0.174512 0.275550 1
O O78 1 0.494059 0.181062 0.846384 1
O O79 1 0.000061 0.081447 0.396689 1
O O80 1 0.498977 0.656455 0.354170 1
O O81 1 0.999520 0.746724 0.403061 1
O O82 1 0.005407 0.916157 0.881529 1
O O83 1 0.497711 0.339438 0.926887 1
O O84 1 0.499784 0.335921 0.346243 1
O O85 1 0.500934 0.819088 0.002857 1
O O86 1 0.499654 0.499536 0.727169 1
O O87 1 0.506676 0.974165 0.940576 1
O O88 1 0.998890 0.393299 0.410366 1
O O89 1 0.995062 0.920773 0.463384 1
O O90 1 0.002748 0.761761 0.533817 1
O O91 1 0.504492 0.500237 0.999727 1
O O92 1 0.004738 0.084364 0.117765 1
O O93 1 0.000968 0.924281 0.735478 1
O O94 1 0.499509 0.661092 0.933077 1
O O95 1 0.995599 0.247686 0.884518 1
O O96 1 0.497806 0.661120 0.072462 1
O O97 1 0.995697 0.752869 0.114818 1
O O98 1 0.998332 0.753214 0.262756 1

$BaNbO_3$

```
_symmetry_space_group_name_H-M   'P 1'
_cell_length_a   4.16511600
_cell_length_b   4.16511600
_cell_length_c   4.16511600
_cell_angle_alpha   90.00000000
_cell_angle_beta   90.00000000
_cell_angle_gamma   90.00000000
_symmetry_Int_Tables_number   1
_chemical_formula_structural   BaNbO3
_chemical_formula_sum   'Ba1 Nb1 O3'
_cell_volume   72.25722913
_cell_formula_units_Z   1
loop_
 _symmetry_equiv_pos_site_id
 _symmetry_equiv_pos_as_xyz
  1  'x, y, z'
loop_
 _atom_site_type_symbol
 _atom_site_label
 _atom_site_symmetry_multiplicity
 _atom_site_fract_x
 _atom_site_fract_y
 _atom_site_fract_z
 _atom_site_occupancy
  Ba  Ba1  1  0.000000  0.996563  0.996223  1
  Nb  Nb2  1  0.500000  0.496597  0.495748  1
  O  O3  1  0.500000  0.996596  0.495700  1
  O  O4  1  0.000000  0.496811  0.495554  1
  O  O5  1  0.500000  0.496409  0.995686  1
```

$Ba_7Nb_8O_{24}$

```
_symmetry_space_group_name_H-M   'P 1'
_cell_length_a   8.27994302
_cell_length_b   8.27994900
_cell_length_c   8.27998003
_cell_angle_alpha   90.00119026
_cell_angle_beta   90.00157769
_cell_angle_gamma   89.99963327
_symmetry_Int_Tables_number   1
_chemical_formula_structural   Ba7Nb8O24
_chemical_formula_sum   'Ba7 Nb8 O24'
_cell_volume   567.65477975
_cell_formula_units_Z   1
loop_
 _symmetry_equiv_pos_site_id
 _symmetry_equiv_pos_as_xyz
  1  'x, y, z'
loop_
 _atom_site_type_symbol
 _atom_site_label
 _atom_site_symmetry_multiplicity
 _atom_site_fract_x
 _atom_site_fract_y
 _atom_site_fract_z
 _atom_site_occupancy
  Ba  Ba1  1  0.502159  0.999855  0.505525  1
  Ba  Ba2  1  0.502174  0.499821  0.005554  1
  Ba  Ba3  1  0.502175  0.499874  0.505554  1
  Ba  Ba4  1  0.002197  0.999847  0.005519  1
  Ba  Ba5  1  0.002158  0.999846  0.505526  1
  Ba  Ba6  1  0.002163  0.499840  0.005521  1
  Ba  Ba7  1  0.002178  0.499857  0.505530  1
  Nb  Nb8  1  0.255044  0.246978  0.252681  1
  Nb  Nb9  1  0.255037  0.246976  0.758411  1
  Nb  Nb10  1  0.255055  0.752701  0.252653  1
  Nb  Nb11  1  0.255044  0.752699  0.758392  1
  Nb  Nb12  1  0.749323  0.246985  0.252662  1
  Nb  Nb13  1  0.749309  0.246996  0.758398  1
  Nb  Nb14  1  0.749317  0.752718  0.252643  1
  Nb  Nb15  1  0.749306  0.752730  0.758385  1
  O  O16  1  0.502186  0.253681  0.259354  1
  O  O17  1  0.502169  0.253512  0.751698  1
  O  O18  1  0.502183  0.746027  0.259201  1
  O  O19  1  0.502174  0.746178  0.751855  1
  O  O20  1  0.002184  0.249551  0.255182  1
  O  O21  1  0.002181  0.249704  0.755858  1
  O  O22  1  0.002177  0.750131  0.255341  1
```

O	O23	1	0.002169	0.749996	0.755711	1
O	O24	1	0.248539	0.253625	0.005544	1
O	O25	1	0.252281	0.249588	0.505538	1
O	O26	1	0.248412	0.746074	0.005525	1
O	O27	1	0.252495	0.750109	0.505533	1
O	O28	1	0.755781	0.253719	0.005523	1
O	O29	1	0.752092	0.249495	0.505519	1
O	O30	1	0.755963	0.745978	0.005511	1
O	O31	1	0.751916	0.750231	0.505515	1
O	O32	1	0.248574	0.999833	0.259258	1
O	O33	1	0.248346	0.999841	0.751818	1
O	O34	1	0.252332	0.499831	0.255349	1
O	O35	1	0.252496	0.499844	0.755727	1
O	O36	1	0.755836	0.999850	0.259113	1
O	O37	1	0.756002	0.999863	0.751929	1
O	O38	1	0.752092	0.499853	0.255439	1
O	O39	1	0.751881	0.499858	0.755621	1

$Ba_{26}Nb_{27}O_{81}$

```
_symmetry_space_group_name_H-M   'P 1'
_cell_length_a   12.47207171
_cell_length_b   12.47135761
_cell_length_c   12.47190954
_cell_angle_alpha   90.00037313
_cell_angle_beta   90.00111581
_cell_angle_gamma   89.99996577
_symmetry_Int_Tables_number   1
_chemical_formula_structural   Ba26Nb27O81
_chemical_formula_sum   'Ba26 Nb27 O81'
_cell_volume   1939.92653677
_cell_formula_units_Z   1
loop_
 _symmetry_equiv_pos_site_id
 _symmetry_equiv_pos_as_xyz
  1  'x, y, z'
loop_
 _atom_site_type_symbol
 _atom_site_label
 _atom_site_symmetry_multiplicity
 _atom_site_fract_x
 _atom_site_fract_y
 _atom_site_fract_z
 _atom_site_occupancy
  Ba  Ba1  1  0.332447  0.000890  0.331109  1
  Ba  Ba2  1  0.332425  0.000930  0.675241  1
  Ba  Ba3  1  0.332409  0.328832  0.003214  1
  Ba  Ba4  1  0.332438  0.333550  0.335849  1
  Ba  Ba5  1  0.332417  0.333592  0.670576  1
  Ba  Ba6  1  0.332436  0.672975  0.003174  1
  Ba  Ba7  1  0.332458  0.668256  0.335827  1
  Ba  Ba8  1  0.332438  0.668289  0.670551  1
  Ba  Ba9  1  0.660345  0.000894  0.003124  1
  Ba  Ba10  1  0.665071  0.000894  0.335761  1
  Ba  Ba11  1  0.665073  0.000924  0.670505  1
  Ba  Ba12  1  0.665028  0.333537  0.003172  1
  Ba  Ba13  1  0.664992  0.333471  0.335733  1
  Ba  Ba14  1  0.664990  0.333511  0.670606  1
  Ba  Ba15  1  0.665066  0.668262  0.003139  1
  Ba  Ba16  1  0.665027  0.668316  0.335710  1
  Ba  Ba17  1  0.665022  0.668341  0.670576  1
  Ba  Ba18  1  0.004493  0.000904  0.003189  1
  Ba  Ba19  1  0.999792  0.000900  0.335823  1
  Ba  Ba20  1  0.999795  0.000929  0.670566  1
  Ba  Ba21  1  0.999773  0.333554  0.003220  1
  Ba  Ba22  1  0.999849  0.333488  0.335792  1
```

Ba Ba23 1 0.999850 0.333520 0.670661 1
Ba Ba24 1 0.999809 0.668282 0.003186 1
Ba Ba25 1 0.999880 0.668330 0.335765 1
Ba Ba26 1 0.999880 0.668363 0.670635 1
Nb Nb27 1 0.167677 0.165627 0.167949 1
Nb Nb28 1 0.166087 0.167244 0.503226 1
Nb Nb29 1 0.167672 0.165660 0.838491 1
Nb Nb30 1 0.166090 0.500900 0.169551 1
Nb Nb31 1 0.165949 0.500925 0.503229 1
Nb Nb32 1 0.166084 0.500933 0.836905 1
Nb Nb33 1 0.167710 0.836185 0.167920 1
Nb Nb34 1 0.166112 0.834610 0.503203 1
Nb Nb35 1 0.167709 0.836220 0.838470 1
Nb Nb36 1 0.497141 0.165603 0.167886 1
Nb Nb37 1 0.498761 0.167232 0.503166 1
Nb Nb38 1 0.497137 0.165642 0.838435 1
Nb Nb39 1 0.498761 0.500888 0.169494 1
Nb Nb40 1 0.498928 0.500916 0.503183 1
Nb Nb41 1 0.498755 0.500920 0.836848 1
Nb Nb42 1 0.497179 0.836163 0.167866 1
Nb Nb43 1 0.498794 0.834594 0.503143 1
Nb Nb44 1 0.497173 0.836195 0.838406 1
Nb Nb45 1 0.832413 0.167207 0.169495 1
Nb Nb46 1 0.832438 0.167374 0.503181 1
Nb Nb47 1 0.832419 0.167242 0.836846 1
Nb Nb48 1 0.832441 0.500892 0.169663 1
Nb Nb49 1 0.832454 0.500915 0.503190 1
Nb Nb50 1 0.832431 0.500921 0.836700 1
Nb Nb51 1 0.832443 0.834574 0.169471 1
Nb Nb52 1 0.832462 0.834457 0.503155 1
Nb Nb53 1 0.832447 0.834604 0.836816 1
O O54 1 0.332411 0.170454 0.172770 1
O O55 1 0.332431 0.167715 0.503213 1
O O56 1 0.332418 0.170494 0.833630 1
O O57 1 0.332427 0.500891 0.170006 1
O O58 1 0.332443 0.500933 0.503215 1
O O59 1 0.332426 0.500938 0.836408 1
O O60 1 0.332437 0.831326 0.172752 1
O O61 1 0.332454 0.834122 0.503171 1
O O62 1 0.332446 0.831379 0.833609 1
O O63 1 0.665620 0.167466 0.169743 1
O O64 1 0.665708 0.167632 0.503181 1
O O65 1 0.665616 0.167525 0.836558 1
O O66 1 0.665709 0.500881 0.169903 1
O O67 1 0.665830 0.500911 0.503185 1
O O68 1 0.665697 0.500914 0.836442 1
O O69 1 0.665657 0.834294 0.169723 1

O O70 1 0.665737 0.834202 0.503150 1
O O71 1 0.665645 0.834331 0.836520 1
O O72 1 0.999205 0.167476 0.169792 1
O O73 1 0.999147 0.167628 0.503202 1
O O74 1 0.999197 0.167518 0.836605 1
O O75 1 0.999156 0.500886 0.169947 1
O O76 1 0.999060 0.500919 0.503225 1
O O77 1 0.999145 0.500927 0.836482 1
O O78 1 0.999234 0.834314 0.169763 1
O O79 1 0.999178 0.834220 0.503176 1
O O80 1 0.999233 0.834359 0.836572 1
O O81 1 0.162900 0.170448 0.003227 1
O O82 1 0.165800 0.167502 0.336443 1
O O83 1 0.165781 0.167530 0.669993 1
O O84 1 0.165603 0.500915 0.003232 1
O O85 1 0.165706 0.500913 0.336516 1
O O86 1 0.165700 0.500931 0.669938 1
O O87 1 0.162936 0.831406 0.003203 1
O O88 1 0.165816 0.834326 0.336422 1
O O89 1 0.165824 0.834349 0.669969 1
O O90 1 0.501921 0.170414 0.003155 1
O O91 1 0.499036 0.167481 0.336393 1
O O92 1 0.499026 0.167529 0.669939 1
O O93 1 0.499234 0.500910 0.003171 1
O O94 1 0.499164 0.500892 0.336465 1
O O95 1 0.499145 0.500909 0.669891 1
O O96 1 0.501970 0.831379 0.003130 1
O O97 1 0.499086 0.834314 0.336370 1
O O98 1 0.499053 0.834323 0.669919 1
O O99 1 0.832419 0.167713 0.003173 1
O O100 1 0.832429 0.167597 0.336459 1
O O101 1 0.832430 0.167627 0.669890 1
O O102 1 0.832440 0.500913 0.003183 1
O O103 1 0.832454 0.500890 0.336578 1
O O104 1 0.832453 0.500926 0.669791 1
O O105 1 0.832451 0.834090 0.003144 1
O O106 1 0.832469 0.834205 0.336432 1
O O107 1 0.832467 0.834220 0.669865 1
O O108 1 0.162908 0.000898 0.172755 1
O O109 1 0.165632 0.000922 0.503229 1
O O110 1 0.162913 0.000932 0.833693 1
O O111 1 0.165800 0.334134 0.169839 1
O O112 1 0.165707 0.334223 0.503242 1
O O113 1 0.165792 0.334165 0.836643 1
O O114 1 0.165811 0.667673 0.169804 1
O O115 1 0.165723 0.667633 0.503229 1
O O116 1 0.165816 0.667711 0.836620 1

O O117 1 0.501951 0.000884 0.172673 1
O O118 1 0.499254 0.000913 0.503163 1
O O119 1 0.501973 0.000920 0.833592 1
O O120 1 0.499018 0.334114 0.169756 1
O O121 1 0.499150 0.334211 0.503169 1
O O122 1 0.499014 0.334154 0.836580 1
O O123 1 0.499046 0.667658 0.169738 1
O O124 1 0.499176 0.667616 0.503157 1
O O125 1 0.499038 0.667688 0.836537 1
O O126 1 0.832440 0.000891 0.169942 1
O O127 1 0.832453 0.000918 0.503168 1
O O128 1 0.832429 0.000919 0.836349 1
O O129 1 0.832423 0.334181 0.169897 1
O O130 1 0.832452 0.334320 0.503190 1
O O131 1 0.832426 0.334217 0.836461 1
O O132 1 0.832459 0.667600 0.169876 1
O O133 1 0.832474 0.667510 0.503171 1
O O134 1 0.832454 0.667630 0.836433 1

$Ba_9Nb_{10}O_{30}$

```
_symmetry_space_group_name_H-M   'P 1'
_cell_length_a   9.26754274
_cell_length_b   9.27228384
_cell_length_c   9.26830481
_cell_angle_alpha   113.60161535
_cell_angle_beta   101.52578376
_cell_angle_gamma   89.98263001
_symmetry_Int_Tables_number   1
_chemical_formula_structural   Ba9Nb10O30
_chemical_formula_sum   'Ba9 Nb10 O30'
_cell_volume   712.27721602
_cell_formula_units_Z   1
loop_
 _symmetry_equiv_pos_site_id
 _symmetry_equiv_pos_as_xyz
  1  'x, y, z'
loop_
 _atom_site_type_symbol
 _atom_site_label
 _atom_site_symmetry_multiplicity
 _atom_site_fract_x
 _atom_site_fract_y
 _atom_site_fract_z
 _atom_site_occupancy
  Ba  Ba1  1  0.802277  0.605618  0.000570  1
  Ba  Ba2  1  0.605397  0.197384  0.999818  1
  Ba  Ba3  1  0.393799  0.802596  0.999722  1
  Ba  Ba4  1  0.901395  0.802192  0.506365  1
  Ba  Ba5  1  0.196897  0.394382  0.998966  1
  Ba  Ba6  1  0.699577  0.399063  0.499898  1
  Ba  Ba7  1  0.499583  0.999961  0.499781  1
  Ba  Ba8  1  0.299590  0.600892  0.499695  1
  Ba  Ba9  1  0.097836  0.197827  0.493342  1
  Nb  Nb10  1  0.950641  0.396241  0.247232  1
  Nb  Nb11  1  0.752018  0.000306  0.247542  1
  Nb  Nb12  1  0.851909  0.198030  0.752319  1
  Nb  Nb13  1  0.653416  0.802889  0.753474  1
  Nb  Nb14  1  0.549860  0.599991  0.249887  1
  Nb  Nb15  1  0.345717  0.197067  0.246070  1
  Nb  Nb16  1  0.449344  0.399991  0.749689  1
  Nb  Nb17  1  0.147265  0.801941  0.247221  1
  Nb  Nb18  1  0.247186  0.999672  0.752042  1
  Nb  Nb19  1  0.048544  0.603733  0.752343  1
  O  O20  1  0.898397  0.305855  0.999813  1
  O  O21  1  0.846800  0.695112  0.745935  1
  O  O22  1  0.847103  0.203609  0.253876  1
```

O O23 1 0.949491 0.399829 0.749274 1
O O24 1 0.694372 0.898841 0.000152 1
O O25 1 0.799430 0.100308 0.499949 1
O O26 1 0.649550 0.300400 0.749846 1
O O27 1 0.948548 0.898497 0.254504 1
O O28 1 0.649241 0.800126 0.250010 1
O O29 1 0.745803 0.000444 0.746212 1
O O30 1 0.599521 0.700225 0.499974 1
O O31 1 0.499722 0.499932 0.999784 1
O O32 1 0.449792 0.900031 0.749829 1
O O33 1 0.749549 0.500426 0.250001 1
O O34 1 0.449866 0.399685 0.249370 1
O O35 1 0.549318 0.600288 0.750191 1
O O36 1 0.304851 0.101130 0.999421 1
O O37 1 0.399448 0.299779 0.499587 1
O O38 1 0.249713 0.499679 0.749848 1
O O39 1 0.549381 0.099951 0.249834 1
O O40 1 0.253346 0.999511 0.253291 1
O O41 1 0.349983 0.199847 0.749609 1
O O42 1 0.100611 0.694219 0.999745 1
O O43 1 0.199869 0.899685 0.499649 1
O O44 1 0.050663 0.101495 0.745160 1
O O45 1 0.349615 0.699505 0.249469 1
O O46 1 0.049753 0.600130 0.250316 1
O O47 1 0.152045 0.796380 0.745679 1
O O48 1 0.999696 0.499919 0.499805 1
O49 1 0.152319 0.304752 0.253419 1

$Ba_2Nb_5O_9$

```
_symmetry_space_group_name_H-M   'P 1'
_cell_length_a   4.24427900
_cell_length_b   4.24430501
_cell_length_c   12.43007201
_cell_angle_alpha   89.99971548
_cell_angle_beta   89.99578851
_cell_angle_gamma   89.99671969
_symmetry_Int_Tables_number   1
_chemical_formula_structural   Ba2Nb5O9
_chemical_formula_sum   'Ba2 Nb5 O9'
_cell_volume   223.91549800
_cell_formula_units_Z   1
loop_
 _symmetry_equiv_pos_site_id
 _symmetry_equiv_pos_as_xyz
  1  'x, y, z'
loop_
 _atom_site_type_symbol
 _atom_site_label
 _atom_site_symmetry_multiplicity
 _atom_site_fract_x
 _atom_site_fract_y
 _atom_site_fract_z
 _atom_site_occupancy
  Ba  Ba1  1  0.004334  0.002399  0.168067  1
  Ba  Ba2  1  0.004678  0.002242  0.831704  1
  Nb  Nb3  1  0.504344  0.501894  0.999908  1
  Nb  Nb4  1  0.504755  0.502639  0.337074  1
  Nb  Nb5  1  0.504807  0.502589  0.662686  1
  Nb  Nb6  1  0.004850  0.502827  0.499878  1
  Nb  Nb7  1  0.504851  0.002833  0.499875  1
  O  O8  1  0.504249  0.001869  0.999907  1
  O  O9  1  0.004391  0.501759  0.999903  1
  O  O10  1  0.504577  0.502014  0.161129  1
  O  O11  1  0.504494  0.501964  0.838659  1
  O  O12  1  0.504779  0.002651  0.326954  1
  O  O13  1  0.004755  0.502790  0.326954  1
  O  O14  1  0.504853  0.002597  0.672798  1
  O  O15  1  0.004837  0.002821  0.499865  1
  O  O16  1  0.004803  0.502740  0.672806  1
```

$BaNb_7O_9$

```
_symmetry_space_group_name_H-M   'P 1'
_cell_length_a   4.26656500
_cell_length_b   4.26679901
_cell_length_c   12.63075502
_cell_angle_alpha   89.99797195
_cell_angle_beta   90.00247263
_cell_angle_gamma   90.00029533
_symmetry_Int_Tables_number   1
_chemical_formula_structural   BaNb7O9
_chemical_formula_sum   'Ba1 Nb7 O9'
_cell_volume   229.93753073
_cell_formula_units_Z   1
loop_
 _symmetry_equiv_pos_site_id
 _symmetry_equiv_pos_as_xyz
  1  'x, y, z'
loop_
 _atom_site_type_symbol
 _atom_site_label
 _atom_site_symmetry_multiplicity
 _atom_site_fract_x
 _atom_site_fract_y
 _atom_site_fract_z
 _atom_site_occupancy
  Ba  Ba1  1  0.989408  0.005548  0.000030  1
  Nb  Nb2  1  0.489417  0.505643  0.500013  1
  Nb  Nb3  1  0.989587  0.505637  0.671313  1
  Nb  Nb4  1  0.489668  0.005550  0.671329  1
  Nb  Nb5  1  0.989328  0.505660  0.328693  1
  Nb  Nb6  1  0.489326  0.005622  0.328683  1
  Nb  Nb7  1  0.489561  0.505670  0.831492  1
  Nb  Nb8  1  0.489303  0.505740  0.168512  1
  O  O9  1  0.489273  0.005634  0.500007  1
  O  O10  1  0.989400  0.505594  0.500004  1
  O  O11  1  0.989658  0.005622  0.665531  1
  O  O12  1  0.989318  0.005649  0.334457  1
  O  O13  1  0.489613  0.005669  0.839399  1
  O  O14  1  0.989555  0.505590  0.839377  1
  O  O15  1  0.489198  0.005745  0.160607  1
  O  O16  1  0.989278  0.505772  0.160623  1
  O  O17  1  0.489587  0.506039  -0.000000  1
```

$Ba_6Nb_2O_{11}$

```
_symmetry_space_group_name_H-M   'P 1'
_cell_length_a   6.29863509
_cell_length_b   6.31021801
_cell_length_c   20.62786560
_cell_angle_alpha   91.04383036
_cell_angle_beta   97.47155254
_cell_angle_gamma   119.74476774
_symmetry_Int_Tables_number   1
_chemical_formula_structural   Ba6Nb2O11
_chemical_formula_sum   'Ba12 Nb4 O22'
_cell_volume   702.53673442
_cell_formula_units_Z   2
loop_
 _symmetry_equiv_pos_site_id
 _symmetry_equiv_pos_as_xyz
  1  'x, y, z'
loop_
 _atom_site_type_symbol
 _atom_site_label
 _atom_site_symmetry_multiplicity
 _atom_site_fract_x
 _atom_site_fract_y
 _atom_site_fract_z
 _atom_site_occupancy
  Ba  Ba1  1  0.485520  0.800779  0.076577  1
  Ba  Ba2  1  0.833261  0.459959  0.108996  1
  Ba  Ba3  1  0.941051  0.531908  0.292260  1
  Ba  Ba4  1  0.324932  0.243323  0.386399  1
  Ba  Ba5  1  0.214523  0.166590  0.202972  1
  Ba  Ba6  1  0.395691  0.201110  0.576365  1
  Ba  Ba7  1  0.740282  0.886950  0.609426  1
  Ba  Ba8  1  0.873319  0.975637  0.792767  1
  Ba  Ba9  1  0.695159  0.929612  0.419484  1
  Ba  Ba10  1  0.252273  0.660334  0.886713  1
  Ba  Ba11  1  0.152067  0.603829  0.703660  1
  Ba  Ba12  1  0.599856  0.350647  0.919174  1
  Nb  Nb13  1  0.043004  0.000757  0.997934  1
  Nb  Nb14  1  0.580021  0.848090  0.247925  1
  Nb  Nb15  1  0.969069  0.564611  0.497962  1
  Nb  Nb16  1  0.508122  0.282790  0.747910  1
  O  O17  1  0.742330  0.728315  0.187558  1
  O  O18  1  0.243420  0.617801  0.191607  1
  O  O19  1  0.413534  0.159796  0.028977  1
  O  O20  1  0.983710  0.126453  0.075162  1
  O  O21  1  0.626412  0.123729  0.189699  1
  O  O22  1  0.921292  0.075478  0.301670  1
```

O	O23	1	0.021143	0.430605	0.420975	1
O	O24	1	0.537447	0.577929	0.307767	1
O	O25	1	0.412345	0.960587	0.308971	1
O	O26	1	0.099975	0.904387	0.466504	1
O	O27	1	0.220200	0.697095	0.574978	1
O	O28	1	0.172015	0.168371	0.688279	1
O	O29	1	0.785709	0.224964	0.529316	1
O	O30	1	0.042949	0.685067	0.998012	1
O	O31	1	0.653252	0.565702	0.497929	1
O	O32	1	0.683010	0.550955	0.688012	1
O	O33	1	0.573548	0.056087	0.692778	1
O	O34	1	0.836076	0.394744	0.808381	1
O	O35	1	0.672264	0.787503	0.966668	1
O	O36	1	0.332429	0.003237	0.805878	1
O	O37	1	0.452528	0.516742	0.804606	1
O	O38	1	0.101950	0.177385	0.920937	1

$BaNb_5O_8$

```
_symmetry_space_group_name_H-M   'P 1'
_cell_length_a   4.18373802
_cell_length_b   6.72819011
_cell_length_c   6.72311020
_cell_angle_alpha   89.97578764
_cell_angle_beta   90.00797859
_cell_angle_gamma   90.00314405
_symmetry_Int_Tables_number   1
_chemical_formula_structural   BaNb5O8
_chemical_formula_sum   'Ba1 Nb5 O8'
_cell_volume   189.24870779
_cell_formula_units_Z   1
loop_
 _symmetry_equiv_pos_site_id
 _symmetry_equiv_pos_as_xyz
  1  'x, y, z'
loop_
 _atom_site_type_symbol
 _atom_site_label
 _atom_site_symmetry_multiplicity
 _atom_site_fract_x
 _atom_site_fract_y
 _atom_site_fract_z
 _atom_site_occupancy
  Ba  Ba1  1  0.999130  0.000273  0.003188  1
  Nb  Nb2  1  0.499136  0.211862  0.601927  1
  Nb  Nb3  1  0.499091  0.401540  0.214950  1
  Nb  Nb4  1  0.999178  0.500264  0.503196  1
  Nb  Nb5  1  0.499251  0.598962  0.791449  1
  Nb  Nb6  1  0.499174  0.788648  0.404460  1
  O  O7  1  0.499052  0.098914  0.304240  1
  O  O8  1  0.999140  0.204599  0.617098  1
  O  O9  1  0.499132  0.301272  0.904555  1
  O  O10  1  0.999098  0.386461  0.207484  1
  O  O11  1  0.999274  0.614012  0.798938  1
  O  O12  1  0.499287  0.699209  0.101839  1
  O  O13  1  0.999187  0.795912  0.389246  1
  O  O14  1  0.499223  0.901598  0.702172  1
```

$Ba_4Nb_2O_9$

```
_symmetry_space_group_name_H-M   'P 1'
_cell_length_a   6.10372112
_cell_length_b   10.42767657
_cell_length_c   17.19094999
_cell_angle_alpha   90.42508018
_cell_angle_beta   89.99308306
_cell_angle_gamma   89.99778826
_symmetry_Int_Tables_number   1
_chemical_formula_structural   Ba4Nb2O9
_chemical_formula_sum   'Ba16 Nb8 O36'
_cell_volume   1094.13309695
_cell_formula_units_Z   4
loop_
 _symmetry_equiv_pos_site_id
 _symmetry_equiv_pos_as_xyz
  1  'x, y, z'
loop_
 _atom_site_type_symbol
 _atom_site_label
 _atom_site_symmetry_multiplicity
 _atom_site_fract_x
 _atom_site_fract_y
 _atom_site_fract_z
 _atom_site_occupancy
  Ba  Ba1  1  0.991086  0.350495  0.804487  1
  Ba  Ba2  1  0.993966  0.682311  0.697795  1
  Ba  Ba3  1  0.009439  0.660322  0.432081  1
  Ba  Ba4  1  0.998764  0.322059  0.065788  1
  Ba  Ba5  1  0.501599  0.174946  0.436569  1
  Ba  Ba6  1  0.491337  0.836661  0.070255  1
  Ba  Ba7  1  0.494887  0.814647  0.304569  1
  Ba  Ba8  1  0.492024  0.146423  0.197969  1
  Ba  Ba9  1  0.505004  0.814494  0.804603  1
  Ba  Ba10  1  0.507919  0.146186  0.697976  1
  Ba  Ba11  1  0.498242  0.174883  0.936618  1
  Ba  Ba12  1  0.509157  0.836694  0.570302  1
  Ba  Ba13  1  0.001146  0.321905  0.565790  1
  Ba  Ba14  1  0.990705  0.660250  0.932121  1
  Ba  Ba15  1  0.006052  0.682333  0.197732  1
  Ba  Ba16  1  0.008635  0.350663  0.304431  1
  Nb  Nb17  1  0.012061  0.002918  0.782011  1
  Nb  Nb18  1  0.008113  0.994062  0.603459  1
  Nb  Nb19  1  0.508493  0.502840  0.398879  1
  Nb  Nb20  1  0.513000  0.493991  0.220320  1
  Nb  Nb21  1  0.486880  0.493778  0.720285  1
  Nb  Nb22  1  0.491514  0.502708  0.898854  1
```

Nb Nb23 1 0.987895 0.003063 0.281950 1
Nb Nb24 1 0.992307 0.994147 0.103379 1
O O25 1 0.957744 0.142552 0.192973 1
O O26 1 0.780111 0.908023 0.189062 1
O O27 1 0.979195 0.823745 0.555222 1
O O28 1 0.803515 0.109781 0.833571 1
O O29 1 0.694895 0.386719 0.668590 1
O O30 1 0.728087 0.407702 0.946538 1
O O31 1 0.771443 0.088994 0.555807 1
O O32 1 0.963039 0.835764 0.828335 1
O O33 1 0.720775 0.589062 0.313231 1
O O34 1 0.777096 0.935673 0.693441 1
O O35 1 0.788116 0.450342 0.172240 1
O O36 1 0.479839 0.673146 0.447160 1
O O37 1 0.712853 0.046808 0.330067 1
O O38 1 0.744083 0.070152 0.051471 1
O O39 1 0.756876 0.426625 0.450627 1
O O40 1 0.463749 0.661146 0.174059 1
O O41 1 0.456714 0.354413 0.809301 1
O O42 1 0.722195 0.560824 0.808782 1
O O43 1 0.277637 0.561008 0.308900 1
O O44 1 0.543118 0.354530 0.309232 1
O O45 1 0.536107 0.660873 0.673982 1
O O46 1 0.243209 0.426653 0.950759 1
O O47 1 0.256336 0.070180 0.551561 1
O O48 1 0.286952 0.046669 0.830163 1
O O49 1 0.211609 0.450049 0.672373 1
O O50 1 0.520457 0.673074 0.947114 1
O O51 1 0.223084 0.936033 0.193419 1
O O52 1 0.279182 0.588994 0.813295 1
O O53 1 0.228961 0.088999 0.055657 1
O O54 1 0.037243 0.835986 0.328309 1
O O55 1 0.304752 0.387079 0.168644 1
O O56 1 0.272020 0.407944 0.446673 1
O O57 1 0.196177 0.110071 0.333563 1
O O58 1 0.021339 0.823755 0.055206 1
O O59 1 0.042307 0.142375 0.693106 1
O O60 1 0.220284 0.907922 0.689057 1

$Ba_5Nb_4O_{15}$

```
_symmetry_space_group_name_H-M   'P 1'
_cell_length_a   5.89549505
_cell_length_b   5.89549505
_cell_length_c   12.02127367
_cell_angle_alpha   90.00000000
_cell_angle_beta   90.00000000
_cell_angle_gamma   120.00000000
_symmetry_Int_Tables_number   1
_chemical_formula_structural   Ba5Nb4O15
_chemical_formula_sum   'Ba5 Nb4 O15'
_cell_volume   361.84424839
_cell_formula_units_Z   1
loop_
 _symmetry_equiv_pos_site_id
 _symmetry_equiv_pos_as_xyz
  1  'x, y, z'
loop_
 _atom_site_type_symbol
 _atom_site_label
 _atom_site_symmetry_multiplicity
 _atom_site_fract_x
 _atom_site_fract_y
 _atom_site_fract_z
 _atom_site_occupancy
  Ba  Ba1  1  0.666667  0.333333  0.569945  1
  Ba  Ba2  1  0.333333  0.666667  0.430055  1
  Ba  Ba3  1  0.666667  0.333333  0.209847  1
  Ba  Ba4  1  0.333333  0.666667  0.790153  1
  Ba  Ba5  1  0.000000  0.000000  0.000000  1
  Nb  Nb6  1  0.666667  0.333333  0.895592  1
  Nb  Nb7  1  0.333333  0.666667  0.104408  1
  Nb  Nb8  1  0.000000  0.000000  0.315808  1
  Nb  Nb9  1  0.000000  0.000000  0.684192  1
  O  O10  1  0.835892  0.164108  0.387245  1
  O  O11  1  0.835892  0.671784  0.387245  1
  O  O12  1  0.328216  0.164108  0.387245  1
  O  O13  1  0.671784  0.835892  0.612755  1
  O  O14  1  0.164108  0.328216  0.612755  1
  O  O15  1  0.164108  0.835892  0.612755  1
  O  O16  1  0.831130  0.168870  0.808300  1
  O  O17  1  0.831130  0.662260  0.808300  1
  O  O18  1  0.337740  0.168870  0.808300  1
  O  O19  1  0.500000  0.000000  0.000000  1
  O  O20  1  1.000000  0.500000  0.000000  1
  O  O21  1  0.500000  0.500000  0.000000  1
  O  O22  1  0.168870  0.831130  0.191700  1
```

O O23 1 0.168870 0.337740 0.191700 1
O O24 1 0.662260 0.831130 0.191700 1

$BaNb_4O_6$

```
_symmetry_space_group_name_H-M   'P 1'
_cell_length_a   4.25714701
_cell_length_b   4.25663504
_cell_length_c   8.34068503
_cell_angle_alpha   89.99554072
_cell_angle_beta   90.00262671
_cell_angle_gamma   90.00480550
_symmetry_Int_Tables_number   1
_chemical_formula_structural   BaNb4O6
_chemical_formula_sum   'Ba1 Nb4 O6'
_cell_volume   151.14256274
_cell_formula_units_Z   1
loop_
 _symmetry_equiv_pos_site_id
 _symmetry_equiv_pos_as_xyz
  1  'x, y, z'
loop_
 _atom_site_type_symbol
 _atom_site_label
 _atom_site_symmetry_multiplicity
 _atom_site_fract_x
 _atom_site_fract_y
 _atom_site_fract_z
 _atom_site_occupancy
  Ba  Ba1  1  0.991840  0.001874  0.999936  1
  Nb  Nb2  1  0.491972  0.001707  0.499924  1
  Nb  Nb3  1  0.991914  0.501690  0.499878  1
  Nb  Nb4  1  0.491783  0.501724  0.253829  1
  Nb  Nb5  1  0.492007  0.501632  0.745978  1
  O  O6  1  0.491985  0.501516  0.999908  1
  O  O7  1  0.491612  0.001715  0.242629  1
  O  O8  1  0.991754  0.501785  0.242568  1
  O  O9  1  0.491863  0.001594  0.757212  1
  O  O10  1  0.992039  0.501648  0.757176  1
  O  O11  1  0.991961  0.001685  0.499875  1
```

$Ba_7Nb_6O_{21}$

```
_symmetry_space_group_name_H-M   'P 1'
_cell_length_a   17.17666038
_cell_length_b   17.17666038
_cell_length_c   17.17666048
_cell_angle_alpha   19.75304374
_cell_angle_beta   19.75304374
_cell_angle_gamma   19.75304487
_symmetry_Int_Tables_number   1
_chemical_formula_structural   Ba7Nb6O21
_chemical_formula_sum   'Ba7 Nb6 O21'
_cell_volume   506.26041811
_cell_formula_units_Z   1
loop_
 _symmetry_equiv_pos_site_id
 _symmetry_equiv_pos_as_xyz
  1  'x, y, z'
loop_
 _atom_site_type_symbol
 _atom_site_label
 _atom_site_symmetry_multiplicity
 _atom_site_fract_x
 _atom_site_fract_y
 _atom_site_fract_z
 _atom_site_occupancy
  Ba  Ba1  1  0.000000  0.000000  0.000000  1
  Ba  Ba2  1  0.849975  0.849975  0.849975  1
  Ba  Ba3  1  0.150025  0.150025  0.150025  1
  Ba  Ba4  1  0.764830  0.764830  0.764830  1
  Ba  Ba5  1  0.235170  0.235170  0.235170  1
  Ba  Ba6  1  0.617918  0.617918  0.617918  1
  Ba  Ba7  1  0.382082  0.382082  0.382082  1
  Nb  Nb8  1  0.927947  0.927947  0.927947  1
  Nb  Nb9  1  0.072053  0.072053  0.072053  1
  Nb  Nb10  1  0.690249  0.690249  0.690249  1
  Nb  Nb11  1  0.309751  0.309751  0.309751  1
  Nb  Nb12  1  0.544082  0.544082  0.544082  1
  Nb  Nb13  1  0.455918  0.455918  0.455918  1
  O  O14  1  0.500000  0.500000  0.000000  1
  O  O15  1  0.000000  0.500000  0.500000  1
  O  O16  1  0.500000  0.000000  0.500000  1
  O  O17  1  0.118760  0.118760  0.622206  1
  O  O18  1  0.622206  0.118760  0.118760  1
  O  O19  1  0.118760  0.622206  0.118760  1
  O  O20  1  0.881240  0.881240  0.377794  1
  O  O21  1  0.377794  0.881240  0.881240  1
  O  O22  1  0.881240  0.377794  0.881240  1
```

O	O23	1	0.237946	0.741484	0.741484	1
O	O24	1	0.741484	0.237946	0.741484	1
O	O25	1	0.741484	0.741484	0.237946	1
O	O26	1	0.762054	0.258516	0.258516	1
O	O27	1	0.258516	0.762054	0.258516	1
O	O28	1	0.258516	0.258516	0.762054	1
O	O29	1	0.362798	0.855068	0.362798	1
O	O30	1	0.362798	0.362798	0.855068	1
O	O31	1	0.855068	0.362798	0.362798	1
O	O32	1	0.637202	0.144932	0.637202	1
O	O33	1	0.637202	0.637202	0.144932	1
O	O34	1	0.144932	0.637202	0.637202	1

$Ba_2Nb_{15}O_{32}$

```
_symmetry_space_group_name_H-M   'P 1'
_cell_length_a   7.92360186
_cell_length_b   7.92024685
_cell_length_c   36.45514839
_cell_angle_alpha   90.48688439
_cell_angle_beta   89.86379007
_cell_angle_gamma   119.87761907
_symmetry_Int_Tables_number   1
_chemical_formula_structural   Ba2Nb15O32
_chemical_formula_sum   'Ba6 Nb45 O96'
_cell_volume   1983.66548680
_cell_formula_units_Z   3
loop_
 _symmetry_equiv_pos_site_id
 _symmetry_equiv_pos_as_xyz
  1  'x, y, z'
loop_
 _atom_site_type_symbol
 _atom_site_label
 _atom_site_symmetry_multiplicity
 _atom_site_fract_x
 _atom_site_fract_y
 _atom_site_fract_z
 _atom_site_occupancy
  Ba  Ba1  1  0.006969  0.003960  0.639409  1
  Ba  Ba2  1  0.993057  0.995908  0.360595  1
  Ba  Ba3  1  0.673598  0.337301  0.972750  1
  Ba  Ba4  1  0.659814  0.329503  0.693910  1
  Ba  Ba5  1  0.340231  0.670687  0.306082  1
  Ba  Ba6  1  0.326336  0.662636  0.027251  1
  Nb  Nb7  1  0.999973  0.999975  0.999997  1
  Nb  Nb8  1  0.666662  0.333298  0.333343  1
  Nb  Nb9  1  0.333362  0.666733  0.666659  1
  Nb  Nb10  1  0.070507  0.262322  0.733675  1
  Nb  Nb11  1  0.187155  0.923302  0.734462  1
  Nb  Nb12  1  0.734449  0.804640  0.733796  1
  Nb  Nb13  1  0.929495  0.737724  0.266318  1
  Nb  Nb14  1  0.812859  0.076754  0.265540  1
  Nb  Nb15  1  0.265562  0.195406  0.266208  1
  Nb  Nb16  1  0.737089  0.595495  0.067022  1
  Nb  Nb17  1  0.853737  0.256472  0.067810  1
  Nb  Nb18  1  0.401045  0.137800  0.067142  1
  Nb  Nb19  1  0.596244  0.071131  0.599643  1
  Nb  Nb20  1  0.479570  0.410134  0.598863  1
  Nb  Nb21  1  0.932257  0.528782  0.599528  1
  Nb  Nb22  1  0.403810  0.928866  0.400365  1
```

Nb Nb23 1 0.520451 0.589845 0.401142 1
Nb Nb24 1 0.067776 0.471195 0.400472 1
Nb Nb25 1 0.262861 0.404462 0.932976 1
Nb Nb26 1 0.146227 0.743499 0.932184 1
Nb Nb27 1 0.598914 0.862175 0.932854 1
Nb Nb28 1 0.023545 0.218597 0.532753 1
Nb Nb29 1 0.194961 0.978537 0.532653 1
Nb Nb30 1 0.783814 0.807006 0.532678 1
Nb Nb31 1 0.976506 0.781398 0.467252 1
Nb Nb32 1 0.805096 0.021453 0.467353 1
Nb Nb33 1 0.216244 0.193002 0.467325 1
Nb Nb34 1 0.690192 0.551994 0.866074 1
Nb Nb35 1 0.861612 0.311950 0.865974 1
Nb Nb36 1 0.450445 0.140397 0.866000 1
Nb Nb37 1 0.643180 0.114820 0.800570 1
Nb Nb38 1 0.471746 0.354881 0.800668 1
Nb Nb39 1 0.882905 0.526416 0.800646 1
Nb Nb40 1 0.356800 0.885195 0.199429 1
Nb Nb41 1 0.528234 0.645137 0.199328 1
Nb Nb42 1 0.117072 0.473586 0.199354 1
Nb Nb43 1 0.309779 0.447996 0.133922 1
Nb Nb44 1 0.138350 0.688042 0.134023 1
Nb Nb45 1 0.549525 0.859593 0.133998 1
Nb Nb46 1 0.000246 0.002256 0.861668 1
Nb Nb47 1 0.999725 0.997731 0.138328 1
Nb Nb48 1 0.666833 0.335431 0.195018 1
Nb Nb49 1 0.666481 0.331161 0.471665 1
Nb Nb50 1 0.333595 0.668869 0.528340 1
Nb Nb51 1 0.333115 0.664547 0.804981 1
O O52 1 0.028510 0.228622 0.432157 1
O O53 1 0.201209 0.967289 0.432201 1
O O54 1 0.767213 0.795114 0.432030 1
O O55 1 0.971533 0.771384 0.567851 1
O O56 1 0.798841 0.032715 0.567802 1
O O57 1 0.232838 0.204882 0.567975 1
O O58 1 0.695205 0.562062 0.765478 1
O O59 1 0.867893 0.300716 0.765522 1
O O60 1 0.433888 0.128541 0.765344 1
O O61 1 0.638166 0.104752 0.901171 1
O O62 1 0.465471 0.366098 0.901127 1
O O63 1 0.899492 0.538291 0.901299 1
O O64 1 0.361794 0.895231 0.098824 1
O O65 1 0.534490 0.633888 0.098869 1
O O66 1 0.100466 0.461694 0.098698 1
O O67 1 0.304793 0.437952 0.234519 1
O O68 1 0.132100 0.699294 0.234479 1
O O69 1 0.566103 0.871475 0.234655 1

O O70 1 0.071327 0.239260 0.166520 1
O O71 1 0.168059 0.929067 0.166834 1
O O72 1 0.760670 0.832111 0.166621 1
O O73 1 0.928644 0.760736 0.833478 1
O O74 1 0.831914 0.070925 0.833164 1
O O75 1 0.239311 0.167900 0.833375 1
O O76 1 0.738086 0.572671 0.499849 1
O O77 1 0.834792 0.262474 0.500167 1
O O78 1 0.427386 0.165513 0.499951 1
O O79 1 0.595237 0.093931 0.166832 1
O O80 1 0.498511 0.404110 0.166519 1
O O81 1 0.905925 0.501085 0.166727 1
O O82 1 0.404726 0.906082 0.833165 1
O O83 1 0.501457 0.595891 0.833479 1
O O84 1 0.094055 0.498922 0.833272 1
O O85 1 0.261982 0.427322 0.500159 1
O O86 1 0.165266 0.737531 0.499837 1
O O87 1 0.572653 0.834470 0.500055 1
O O88 1 0.001447 0.996437 0.762000 1
O O89 1 0.998551 0.003596 0.238000 1
O O90 1 0.668049 0.329619 0.095351 1
O O91 1 0.665298 0.337010 0.571322 1
O O92 1 0.334752 0.662994 0.428684 1
O O93 1 0.331902 0.670345 0.904644 1
O O94 1 0.063117 0.239251 0.895291 1
O O95 1 0.175253 0.940246 0.895587 1
O O96 1 0.764962 0.828531 0.895692 1
O O97 1 0.936844 0.760735 0.104707 1
O O98 1 0.824714 0.059731 0.104409 1
O O99 1 0.235000 0.171454 0.104302 1
O O100 1 0.729758 0.572477 0.228629 1
O O101 1 0.841857 0.273419 0.228931 1
O O102 1 0.431572 0.161747 0.229043 1
O O103 1 0.603555 0.094111 0.438058 1
O O104 1 0.491464 0.393174 0.437751 1
O O105 1 0.901738 0.504838 0.437638 1
O O106 1 0.396489 0.905869 0.561948 1
O O107 1 0.508591 0.606843 0.562257 1
O O108 1 0.098311 0.495163 0.562365 1
O O109 1 0.270235 0.427554 0.771367 1
O O110 1 0.158121 0.726588 0.771065 1
O O111 1 0.568420 0.838268 0.770959 1
O O112 1 0.060130 0.242509 0.292667 1
O O113 1 0.177236 0.944359 0.292820 1
O O114 1 0.766566 0.828452 0.293092 1
O O115 1 0.939867 0.757557 0.707327 1
O O116 1 0.822732 0.055665 0.707182 1

O O117 1 0.233433 0.171594 0.706908 1
O O118 1 0.726861 0.575878 0.625997 1
O O119 1 0.843991 0.277787 0.626142 1
O O120 1 0.433288 0.161850 0.626412 1
O O121 1 0.606430 0.090667 0.040688 1
O O122 1 0.489330 0.388817 0.040537 1
O O123 1 0.900029 0.504749 0.040260 1
O O124 1 0.393521 0.909300 0.959305 1
O O125 1 0.510623 0.611143 0.959459 1
O O126 1 0.099917 0.495205 0.959733 1
O O127 1 0.273186 0.424085 0.374015 1
O O128 1 0.156088 0.722230 0.373860 1
O O129 1 0.566764 0.838152 0.373594 1
O O130 1 0.214944 0.207057 0.966867 1
O O131 1 0.987722 0.783072 0.968124 1
O O132 1 0.791047 0.014473 0.968242 1
O O133 1 0.785030 0.792895 0.033127 1
O O134 1 0.012231 0.216890 0.031872 1
O O135 1 0.208919 0.985491 0.031752 1
O O136 1 0.881503 0.540250 0.300198 1
O O137 1 0.654363 0.116303 0.301484 1
O O138 1 0.457626 0.347666 0.301611 1
O O139 1 0.451823 0.126387 0.366499 1
O O140 1 0.678976 0.550298 0.365209 1
O O141 1 0.875686 0.318916 0.365078 1
O O142 1 0.548263 0.873642 0.633511 1
O O143 1 0.321085 0.449733 0.634795 1
O O144 1 0.124360 0.681122 0.634914 1
O O145 1 0.118435 0.459768 0.699798 1
O O146 1 0.345621 0.883706 0.698515 1
O O147 1 0.542357 0.652331 0.698401 1

$BaNb_8O_{14}$

```
_symmetry_space_group_name_H-M   'P 1'
_cell_length_a   9.62927600
_cell_length_b   10.54124300
_cell_length_c   24.14779400
_cell_angle_alpha   90.00000000
_cell_angle_beta   90.00000000
_cell_angle_gamma   90.00000000
_symmetry_Int_Tables_number   1
_chemical_formula_structural   BaNb8O14
_chemical_formula_sum   'Ba8 Nb64 O112'
_cell_volume   2451.11067924
_cell_formula_units_Z   8
loop_
 _symmetry_equiv_pos_site_id
 _symmetry_equiv_pos_as_xyz
  1  'x, y, z'
loop_
 _atom_site_type_symbol
 _atom_site_label
 _atom_site_symmetry_multiplicity
 _atom_site_fract_x
 _atom_site_fract_y
 _atom_site_fract_z
 _atom_site_occupancy
  Ba  Ba1  1  0.008574  0.015113  0.136455  1
  Ba  Ba2  1  0.508574  0.984887  0.363545  1
  Ba  Ba3  1  0.991426  0.484887  0.636455  1
  Ba  Ba4  1  0.491426  0.515113  0.863545  1
  Ba  Ba5  1  0.991426  0.984887  0.863545  1
  Ba  Ba6  1  0.491426  0.015113  0.636455  1
  Ba  Ba7  1  0.008574  0.515113  0.363545  1
  Ba  Ba8  1  0.508574  0.484887  0.136455  1
  Nb  Nb9  1  0.624951  0.075761  0.067087  1
  Nb  Nb10  1  0.124951  0.924239  0.432913  1
  Nb  Nb11  1  0.375049  0.424239  0.567087  1
  Nb  Nb12  1  0.875049  0.575761  0.932913  1
  Nb  Nb13  1  0.375049  0.924239  0.932913  1
  Nb  Nb14  1  0.875049  0.075761  0.567087  1
  Nb  Nb15  1  0.624951  0.575761  0.432913  1
  Nb  Nb16  1  0.124951  0.424239  0.067087  1
  Nb  Nb17  1  0.375709  0.921362  0.066409  1
  Nb  Nb18  1  0.875709  0.078638  0.433591  1
  Nb  Nb19  1  0.624291  0.578638  0.566409  1
  Nb  Nb20  1  0.124291  0.421362  0.933591  1
  Nb  Nb21  1  0.624291  0.078638  0.933591  1
  Nb  Nb22  1  0.124291  0.921362  0.566409  1
```

Nb Nb23 1 0.375709 0.421362 0.433591 1
Nb Nb24 1 0.875709 0.578638 0.066409 1
Nb Nb25 1 0.377054 0.927082 0.182378 1
Nb Nb26 1 0.877054 0.072918 0.317622 1
Nb Nb27 1 0.622946 0.572918 0.682378 1
Nb Nb28 1 0.122946 0.427082 0.817622 1
Nb Nb29 1 0.622946 0.072918 0.817622 1
Nb Nb30 1 0.122946 0.927082 0.682378 1
Nb Nb31 1 0.377054 0.427082 0.317622 1
Nb Nb32 1 0.877054 0.572918 0.182378 1
Nb Nb33 1 0.381809 0.161385 0.120165 1
Nb Nb34 1 0.881809 0.838615 0.379835 1
Nb Nb35 1 0.618191 0.338615 0.620165 1
Nb Nb36 1 0.118191 0.661385 0.879835 1
Nb Nb37 1 0.618191 0.838615 0.879835 1
Nb Nb38 1 0.118191 0.161385 0.620165 1
Nb Nb39 1 0.381809 0.661385 0.379835 1
Nb Nb40 1 0.881809 0.338615 0.120165 1
Nb Nb41 1 0.361827 0.185140 0.253526 1
Nb Nb42 1 0.861827 0.814860 0.246474 1
Nb Nb43 1 0.638173 0.314860 0.753526 1
Nb Nb44 1 0.138173 0.685140 0.746474 1
Nb Nb45 1 0.638173 0.814860 0.746474 1
Nb Nb46 1 0.138173 0.185140 0.753526 1
Nb Nb47 1 0.361827 0.685140 0.246474 1
Nb Nb48 1 0.861827 0.314860 0.253526 1
Nb Nb49 1 0.117159 0.159820 0.998594 1
Nb Nb50 1 0.617159 0.840180 0.501406 1
Nb Nb51 1 0.882841 0.340180 0.498594 1
Nb Nb52 1 0.382841 0.659820 0.001406 1
Nb Nb53 1 0.882841 0.840180 0.001406 1
Nb Nb54 1 0.382841 0.159820 0.498594 1
Nb Nb55 1 0.117159 0.659820 0.501406 1
Nb Nb56 1 0.617159 0.340180 0.998594 1
Nb Nb57 1 0.617001 0.834936 0.124067 1
Nb Nb58 1 0.117001 0.165064 0.375933 1
Nb Nb59 1 0.382999 0.665064 0.624067 1
Nb Nb60 1 0.882999 0.334936 0.875933 1
Nb Nb61 1 0.382999 0.165064 0.875933 1
Nb Nb62 1 0.882999 0.834936 0.624067 1
Nb Nb63 1 0.617001 0.334936 0.375933 1
Nb Nb64 1 0.117001 0.665064 0.124067 1
Nb Nb65 1 0.624232 0.076048 0.182918 1
Nb Nb66 1 0.124232 0.923952 0.317082 1
Nb Nb67 1 0.375768 0.423952 0.682918 1
Nb Nb68 1 0.875768 0.576048 0.817082 1
Nb Nb69 1 0.375768 0.923952 0.817082 1

Nb Nb70 1 0.875768 0.076048 0.682918 1
Nb Nb71 1 0.624232 0.576048 0.317082 1
Nb Nb72 1 0.124232 0.423952 0.182918 1
O O73 1 0.492806 0.746499 0.063384 1
O O74 1 0.992806 0.253501 0.436616 1
O O75 1 0.507194 0.753501 0.563384 1
O O76 1 0.007194 0.246499 0.936616 1
O O77 1 0.507194 0.253501 0.936616 1
O O78 1 0.007194 0.746499 0.563384 1
O O79 1 0.492806 0.246499 0.436616 1
O O80 1 0.992806 0.753501 0.063384 1
O O81 1 0.750463 0.910352 0.188317 1
O O82 1 0.250463 0.089648 0.311683 1
O O83 1 0.249537 0.589648 0.688317 1
O O84 1 0.749537 0.410352 0.811683 1
O O85 1 0.249537 0.089648 0.811683 1
O O86 1 0.749537 0.910352 0.688317 1
O O87 1 0.750463 0.410352 0.311683 1
O O88 1 0.250463 0.589648 0.188317 1
O O89 1 0.489415 0.751247 0.186705 1
O O90 1 0.989415 0.248753 0.313295 1
O O91 1 0.510585 0.748753 0.686705 1
O O92 1 0.010585 0.251247 0.813295 1
O O93 1 0.510585 0.248753 0.813295 1
O O94 1 0.010585 0.751247 0.686705 1
O O95 1 0.489415 0.251247 0.313295 1
O O96 1 0.989415 0.748753 0.186705 1
O O97 1 0.755704 0.912306 0.062871 1
O O98 1 0.255704 0.087694 0.437129 1
O O99 1 0.244296 0.587694 0.562871 1
O O100 1 0.744296 0.412306 0.937129 1
O O101 1 0.244296 0.087694 0.937129 1
O O102 1 0.744296 0.912306 0.562871 1
O O103 1 0.755704 0.412306 0.437129 1
O O104 1 0.255704 0.587694 0.062871 1
O O105 1 0.239808 0.846775 0.125087 1
O O106 1 0.739808 0.153225 0.374913 1
O O107 1 0.760192 0.653225 0.625087 1
O O108 1 0.260192 0.346775 0.874913 1
O O109 1 0.760192 0.153225 0.874913 1
O O110 1 0.260192 0.846775 0.625087 1
O O111 1 0.239808 0.346775 0.374913 1
O O112 1 0.739808 0.653225 0.125087 1
O O113 1 0.757252 0.157628 0.124763 1
O O114 1 0.257252 0.842372 0.375237 1
O O115 1 0.242748 0.342372 0.624763 1
O O116 1 0.742748 0.657628 0.875237 1

O O117 1 0.242748 0.842372 0.875237 1
O O118 1 0.742748 0.157628 0.624763 1
O O119 1 0.757252 0.657628 0.375237 1
O O120 1 0.257252 0.342372 0.124763 1
O O121 1 0.487412 0.018593 0.247209 1
O O122 1 0.987412 0.981407 0.252791 1
O O123 1 0.512588 0.481407 0.747209 1
O O124 1 0.012588 0.518593 0.752791 1
O O125 1 0.512588 0.981407 0.752791 1
O O126 1 0.012588 0.018593 0.747209 1
O O127 1 0.487412 0.518593 0.252791 1
O O128 1 0.987412 0.481407 0.247209 1
O O129 1 0.493081 0.238861 0.189072 1
O O130 1 0.993081 0.761139 0.310928 1
O O131 1 0.506919 0.261139 0.689072 1
O O132 1 0.006919 0.738861 0.810928 1
O O133 1 0.506919 0.761139 0.810928 1
O O134 1 0.006919 0.238861 0.689072 1
O O135 1 0.493081 0.738861 0.310928 1
O O136 1 0.993081 0.261139 0.189072 1
O O137 1 0.755456 0.161658 0.248569 1
O O138 1 0.255456 0.838342 0.251431 1
O O139 1 0.244544 0.338342 0.748569 1
O O140 1 0.744544 0.661658 0.751431 1
O O141 1 0.244544 0.838342 0.751431 1
O O142 1 0.744544 0.161658 0.748569 1
O O143 1 0.755456 0.661658 0.251431 1
O O144 1 0.255456 0.338342 0.248569 1
O O145 1 0.500000 0.000000 0.000000 1
O O146 1 0.000000 0.000000 0.500000 1
O O147 1 0.500000 0.500000 0.500000 1
O O148 1 0.000000 0.500000 0.000000 1
O O149 1 0.509289 0.253900 0.062752 1
O O150 1 0.009289 0.746100 0.437248 1
O O151 1 0.490711 0.246100 0.562752 1
O O152 1 0.990711 0.753900 0.937248 1
O O153 1 0.490711 0.746100 0.937248 1
O O154 1 0.990711 0.253900 0.562752 1
O O155 1 0.509289 0.753900 0.437248 1
O O156 1 0.009289 0.246100 0.062752 1
O O157 1 0.728666 0.181070 0.000347 1
O O158 1 0.228666 0.818930 0.499653 1
O O159 1 0.271334 0.318930 0.500347 1
O O160 1 0.771334 0.681070 0.999653 1
O O161 1 0.271334 0.818930 0.999653 1
O O162 1 0.771334 0.181070 0.500347 1
O O163 1 0.728666 0.681070 0.499653 1

O O164 1 0.228666 0.318930 0.000347 1
O O165 1 0.241464 0.083710 0.061080 1
O O166 1 0.741464 0.916290 0.438920 1
O O167 1 0.758536 0.416290 0.561080 1
O O168 1 0.258536 0.583710 0.938920 1
O O169 1 0.758536 0.916290 0.938920 1
O O170 1 0.258536 0.083710 0.561080 1
O O171 1 0.241464 0.583710 0.438920 1
O O172 1 0.741464 0.416290 0.061080 1
O O173 1 0.258178 0.095366 0.188295 1
O O174 1 0.758178 0.904634 0.311705 1
O O175 1 0.741822 0.404634 0.688295 1
O O176 1 0.241822 0.595366 0.811705 1
O O177 1 0.741822 0.904634 0.811705 1
O O178 1 0.241822 0.095366 0.688295 1
O O179 1 0.258178 0.595366 0.311705 1
O O180 1 0.758178 0.404634 0.188295 1
O O181 1 0.000000 0.000000 0.000000 1
O O182 1 0.500000 0.000000 0.500000 1
O O183 1 0.000000 0.500000 0.500000 1
O O184 1 0.500000 0.500000 0.000000 1

$Ba_4Nb_{14}O_{23}$

```
_symmetry_space_group_name_H-M   'P 1'
_cell_length_a   4.21901700
_cell_length_b   12.66576800
_cell_length_c   21.13886408
_cell_angle_alpha   89.65959083
_cell_angle_beta   90.00121860
_cell_angle_gamma   90.00008583
_symmetry_Int_Tables_number   1
_chemical_formula_structural   Ba4Nb14O23
_chemical_formula_sum   'Ba8 Nb28 O46'
_cell_volume   1129.57945662
_cell_formula_units_Z   2
loop_
 _symmetry_equiv_pos_site_id
 _symmetry_equiv_pos_as_xyz
  1  'x, y, z'
loop_
 _atom_site_type_symbol
 _atom_site_label
 _atom_site_symmetry_multiplicity
 _atom_site_fract_x
 _atom_site_fract_y
 _atom_site_fract_z
 _atom_site_occupancy
  Ba  Ba1  1  0.998320  0.669201  0.898036  1
  Ba  Ba2  1  0.998220  0.328842  0.102196  1
  Ba  Ba3  1  0.998320  0.330384  0.898400  1
  Ba  Ba4  1  0.998250  0.667636  0.101798  1
  Ba  Ba5  1  0.998199  0.169279  0.398043  1
  Ba  Ba6  1  0.998248  0.828997  0.602159  1
  Ba  Ba7  1  0.998207  0.830466  0.398408  1
  Ba  Ba8  1  0.998225  0.167833  0.601826  1
  Nb  Nb9  1  0.998372  0.998999  0.000097  1
  Nb  Nb10  1  0.998119  0.499139  0.500107  1
  Nb  Nb11  1  0.498369  0.000011  0.900658  1
  Nb  Nb12  1  0.498364  0.997980  0.099544  1
  Nb  Nb13  1  0.498097  0.500060  0.400654  1
  Nb  Nb14  1  0.498154  0.498229  0.599547  1
  Nb  Nb15  1  0.998394  0.000180  0.796596  1
  Nb  Nb16  1  0.998370  0.997881  0.203598  1
  Nb  Nb17  1  0.998065  0.500189  0.296608  1
  Nb  Nb18  1  0.998166  0.498081  0.703607  1
  Nb  Nb19  1  0.498395  0.998013  0.702325  1
  Nb  Nb20  1  0.498377  0.000241  0.297873  1
  Nb  Nb21  1  0.498058  0.497869  0.202341  1
  Nb  Nb22  1  0.498166  0.500222  0.797875  1
```

Nb Nb23 1 0.498306 0.836120 0.000161 1
Nb Nb24 1 0.498305 0.161875 0.000035 1
Nb Nb25 1 0.498181 0.336272 0.500191 1
Nb Nb26 1 0.498193 0.662014 0.500018 1
Nb Nb27 1 0.498370 0.840869 0.798970 1
Nb Nb28 1 0.498340 0.157168 0.201214 1
Nb Nb29 1 0.498367 0.161043 0.798903 1
Nb Nb30 1 0.498324 0.836965 0.201300 1
Nb Nb31 1 0.498104 0.340893 0.298989 1
Nb Nb32 1 0.498190 0.657389 0.701221 1
Nb Nb33 1 0.498087 0.661119 0.298899 1
Nb Nb34 1 0.498198 0.337203 0.701317 1
Nb Nb35 1 0.498068 0.999157 0.500104 1
Nb Nb36 1 0.498328 0.498996 0.000099 1
O O37 1 0.998384 0.000062 0.899719 1
O O38 1 0.998370 0.997911 0.100475 1
O O39 1 0.998114 0.500128 0.399728 1
O O40 1 0.998165 0.498156 0.600484 1
O O41 1 0.998409 0.999542 0.695866 1
O O42 1 0.998384 0.998629 0.304327 1
O O43 1 0.998069 0.499441 0.195879 1
O O44 1 0.998176 0.498715 0.804334 1
O O45 1 0.998337 0.828349 0.000119 1
O O46 1 0.998323 0.169641 0.000071 1
O O47 1 0.998185 0.328494 0.500166 1
O O48 1 0.998183 0.669781 0.500038 1
O O49 1 0.498398 0.829911 0.900558 1
O O50 1 0.498379 0.168096 0.099621 1
O O51 1 0.498388 0.169986 0.900234 1
O O52 1 0.498387 0.828007 0.099969 1
O O53 1 0.498129 0.329950 0.400593 1
O O54 1 0.498167 0.668330 0.599620 1
O O55 1 0.498113 0.670034 0.400218 1
O O56 1 0.498183 0.328248 0.599990 1
O O57 1 0.998382 0.833241 0.804191 1
O O58 1 0.998359 0.164825 0.195961 1
O O59 1 0.998378 0.167073 0.803478 1
O O60 1 0.998336 0.830975 0.196750 1
O O61 1 0.998115 0.333245 0.304229 1
O O62 1 0.998201 0.665025 0.695994 1
O O63 1 0.998095 0.667094 0.303457 1
O O64 1 0.998206 0.331183 0.696737 1
O O65 1 0.498379 0.831775 0.698563 1
O O66 1 0.498346 0.166470 0.301597 1
O O67 1 0.498405 0.164545 0.698074 1
O O68 1 0.498334 0.833730 0.302152 1
O O69 1 0.498133 0.331616 0.198601 1

O	O70	1	0.498218	0.666480	0.801629	1
O	O71	1	0.498105	0.664369	0.198059	1
O	O72	1	0.498238	0.333700	0.802139	1
O	O73	1	0.498468	0.997286	0.595980	1
O	O74	1	0.498475	0.001069	0.404219	1
O	O75	1	0.498016	0.497162	0.095988	1
O	O76	1	0.498049	0.500795	0.904221	1
O	O77	1	0.998470	0.999134	0.500099	1
O	O78	1	0.998051	0.498995	0.000107	1
O	O79	1	0.498341	0.837641	0.499571	1
O	O80	1	0.498329	0.160664	0.500632	1
O	O81	1	0.498151	0.337487	0.999636	1
O	O82	1	0.498159	0.660504	0.000563	1

$Ba_3Nb_{16}O_{23}$

```
_symmetry_space_group_name_H-M   'P 1'
_cell_length_a   4.23317500
_cell_length_b   12.66309700
_cell_length_c   21.30748300
_cell_angle_alpha   90.00022649
_cell_angle_beta   89.99923621
_cell_angle_gamma   89.99911484
_symmetry_Int_Tables_number   1
_chemical_formula_structural   Ba3Nb16O23
_chemical_formula_sum   'Ba6 Nb32 O46'
_cell_volume   1142.18987747
_cell_formula_units_Z   2
loop_
 _symmetry_equiv_pos_site_id
 _symmetry_equiv_pos_as_xyz
  1  'x, y, z'
loop_
 _atom_site_type_symbol
 _atom_site_label
 _atom_site_symmetry_multiplicity
 _atom_site_fract_x
 _atom_site_fract_y
 _atom_site_fract_z
 _atom_site_occupancy
  Ba  Ba1  1  0.996455  0.000016  0.999922  1
  Ba  Ba2  1  0.998217  0.500675  0.499959  1
  Ba  Ba3  1  0.997041  0.000301  0.201349  1
  Ba  Ba4  1  0.997601  0.000231  0.798534  1
  Ba  Ba5  1  0.997651  0.500464  0.701363  1
  Ba  Ba6  1  0.997053  0.500554  0.298517  1
  Nb  Nb7  1  0.496530  0.327557  0.999963  1
  Nb  Nb8  1  0.496431  0.672401  0.999930  1
  Nb  Nb9  1  0.498117  0.828310  0.499937  1
  Nb  Nb10  1  0.498101  0.173153  0.499946  1
  Nb  Nb11  1  0.996413  0.329049  0.101486  1
  Nb  Nb12  1  0.996678  0.671085  0.898411  1
  Nb  Nb13  1  0.996320  0.671150  0.101449  1
  Nb  Nb14  1  0.996719  0.328996  0.898416  1
  Nb  Nb15  1  0.998249  0.829577  0.601462  1
  Nb  Nb16  1  0.997913  0.171739  0.398416  1
  Nb  Nb17  1  0.998224  0.171674  0.601488  1
  Nb  Nb18  1  0.997933  0.829638  0.398422  1
  Nb  Nb19  1  0.496339  0.500063  0.100993  1
  Nb  Nb20  1  0.496685  0.500000  0.898893  1
  Nb  Nb21  1  0.498275  0.000672  0.601001  1
  Nb  Nb22  1  0.497889  0.000720  0.398895  1
```

Nb Nb23 1 0.496437 0.168853 0.101008 1
Nb Nb24 1 0.496710 0.831285 0.898868 1
Nb Nb25 1 0.496358 0.831349 0.100976 1
Nb Nb26 1 0.496754 0.168813 0.898884 1
Nb Nb27 1 0.498231 0.669383 0.600995 1
Nb Nb28 1 0.497885 0.331937 0.398895 1
Nb Nb29 1 0.498239 0.331871 0.601020 1
Nb Nb30 1 0.497859 0.669433 0.398892 1
Nb Nb31 1 0.496523 0.333144 0.195068 1
Nb Nb32 1 0.496950 0.667309 0.804871 1
Nb Nb33 1 0.496462 0.667417 0.195000 1
Nb Nb34 1 0.496925 0.333058 0.804840 1
Nb Nb35 1 0.498105 0.833343 0.695003 1
Nb Nb36 1 0.497702 0.167694 0.304832 1
Nb Nb37 1 0.498172 0.167602 0.695061 1
Nb Nb38 1 0.497642 0.833421 0.304867 1
O O39 1 0.496433 0.499956 0.999942 1
O O40 1 0.498196 0.000749 0.499950 1
O O41 1 0.996507 0.333567 0.999954 1
O O42 1 0.996446 0.666368 0.999930 1
O O43 1 0.998130 0.834333 0.499944 1
O O44 1 0.998141 0.167154 0.499951 1
O O45 1 0.996358 0.500087 0.096401 1
O O46 1 0.996677 0.500027 0.903489 1
O O47 1 0.998288 0.000644 0.596403 1
O O48 1 0.997926 0.000701 0.403492 1
O O49 1 0.496567 0.159192 0.999953 1
O O50 1 0.496442 0.840765 0.999920 1
O O51 1 0.498169 0.659947 0.499941 1
O O52 1 0.498161 0.341515 0.499959 1
O O53 1 0.996449 0.161059 0.099220 1
O O54 1 0.996720 0.839060 0.900733 1
O O55 1 0.996365 0.839123 0.099095 1
O O56 1 0.996770 0.161009 0.900711 1
O O57 1 0.998246 0.661604 0.599125 1
O O58 1 0.997907 0.339730 0.400707 1
O O59 1 0.998251 0.339663 0.599212 1
O O60 1 0.997879 0.661663 0.400743 1
O O61 1 0.496739 0.165962 0.199695 1
O O62 1 0.497209 0.834420 0.800171 1
O O63 1 0.496673 0.834538 0.199679 1
O O64 1 0.497274 0.165880 0.800204 1
O O65 1 0.497952 0.666216 0.699692 1
O O66 1 0.497599 0.334881 0.300211 1
O O67 1 0.497942 0.334778 0.699700 1
O O68 1 0.497480 0.666300 0.300186 1
O O69 1 0.997713 0.160509 0.300507 1

O	O70	1	0.998147	0.840694	0.699380	1
O	O71	1	0.997678	0.840783	0.300499	1
O	O72	1	0.998186	0.160411	0.699397	1
O	O73	1	0.996954	0.659935	0.800494	1
O	O74	1	0.996544	0.340343	0.199395	1
O	O75	1	0.996955	0.340244	0.800508	1
O	O76	1	0.996453	0.660057	0.199370	1
O	O77	1	0.496338	0.500259	0.201067	1
O	O78	1	0.496845	0.500159	0.798815	1
O	O79	1	0.498326	0.000494	0.701073	1
O	O80	1	0.497860	0.000585	0.298822	1
O	O81	1	0.496263	0.000122	0.103115	1
O	O82	1	0.496696	0.000053	0.896717	1
O	O83	1	0.498494	0.500621	0.603133	1
O	O84	1	0.497931	0.500669	0.396786	1

$BaNb_2O_6$

```
_symmetry_space_group_name_H-M   'P 1'
_cell_length_a   5.96810002
_cell_length_b   8.06862644
_cell_length_c   11.10818714
_cell_angle_alpha   90.42081796
_cell_angle_beta   89.99370218
_cell_angle_gamma   90.00010577
_symmetry_Int_Tables_number   1
_chemical_formula_structural   BaNb2O6
_chemical_formula_sum   'Ba4 Nb8 O24'
_cell_volume   534.89331878
_cell_formula_units_Z   4
loop_
 _symmetry_equiv_pos_site_id
 _symmetry_equiv_pos_as_xyz
  1  'x, y, z'
loop_
 _atom_site_type_symbol
 _atom_site_label
 _atom_site_symmetry_multiplicity
 _atom_site_fract_x
 _atom_site_fract_y
 _atom_site_fract_z
 _atom_site_occupancy
  Ba  Ba1  1  0.033853  0.248643  0.534089  1
  Ba  Ba2  1  0.533805  0.749133  0.965257  1
  Ba  Ba3  1  0.973419  0.749155  0.465078  1
  Ba  Ba4  1  0.473271  0.248626  0.034166  1
  Nb  Nb5  1  0.533523  0.017008  0.644508  1
  Nb  Nb6  1  0.033516  0.980702  0.854702  1
  Nb  Nb7  1  0.473628  0.980832  0.354751  1
  Nb  Nb8  1  0.973661  0.017014  0.144484  1
  Nb  Nb9  1  0.967262  0.522466  0.143142  1
  Nb  Nb10  1  0.467309  0.475314  0.356209  1
  Nb  Nb11  1  0.039928  0.475216  0.856186  1
  Nb  Nb12  1  0.539983  0.522518  0.643117  1
  O  O13  1  0.711816  0.024002  0.474798  1
  O  O14  1  0.211825  0.973767  0.024403  1
  O  O15  1  0.295359  0.973753  0.524442  1
  O  O16  1  0.795392  0.023980  0.974806  1
  O  O17  1  0.794666  0.473139  0.975992  1
  O  O18  1  0.294721  0.524599  0.523320  1
  O  O19  1  0.212590  0.524548  0.023314  1
  O  O20  1  0.712626  0.473097  0.475942  1
  O  O21  1  0.856013  0.030343  0.712136  1
  O  O22  1  0.356053  0.967184  0.787091  1
```

O	O23	1	0.151045	0.967329	0.287092	1
O	O24	1	0.651083	0.030475	0.212108	1
O	O25	1	0.654909	0.464715	0.213837	1
O	O26	1	0.154757	0.532969	0.285507	1
O	O27	1	0.352448	0.533061	0.785473	1
O	O28	1	0.852428	0.464696	0.713819	1
O	O29	1	0.494506	0.249297	0.647454	1
O	O30	1	0.994630	0.748378	0.851843	1
O	O31	1	0.512485	0.748482	0.351825	1
O	O32	1	0.012747	0.249300	0.147375	1
O	O33	1	0.613995	0.749793	0.637868	1
O	O34	1	0.113981	0.247912	0.861271	1
O	O35	1	0.393155	0.247999	0.361240	1
O	O36	1	0.893360	0.749807	0.138018	1

$Ba_3Nb_5O_{15}$

```
_symmetry_space_group_name_H-M   'P 1'
_cell_length_a   4.05161200
_cell_length_b   12.85274900
_cell_length_c   12.85647601
_cell_angle_alpha   90.00058404
_cell_angle_beta   89.99766312
_cell_angle_gamma   90.00188315
_symmetry_Int_Tables_number   1
_chemical_formula_structural   Ba3Nb5O15
_chemical_formula_sum   'Ba6 Nb10 O30'
_cell_volume   669.49265749
_cell_formula_units_Z   2
loop_
 _symmetry_equiv_pos_site_id
 _symmetry_equiv_pos_as_xyz
  1  'x, y, z'
loop_
 _atom_site_type_symbol
 _atom_site_label
 _atom_site_symmetry_multiplicity
 _atom_site_fract_x
 _atom_site_fract_y
 _atom_site_fract_z
 _atom_site_occupancy
  Ba  Ba1  1  0.997266  0.498912  0.499286  1
  Ba  Ba2  1  0.997152  0.998922  0.999326  1
  Ba  Ba3  1  0.998406  0.326327  0.836083  1
  Ba  Ba4  1  0.998052  0.671701  0.162551  1
  Ba  Ba5  1  0.996608  0.826648  0.662972  1
  Ba  Ba6  1  0.997047  0.171843  0.336332  1
  Nb  Nb7  1  0.499996  0.498922  0.999267  1
  Nb  Nb8  1  0.496011  0.998864  0.499275  1
  Nb  Nb9  1  0.497430  0.422084  0.286386  1
  Nb  Nb10  1  0.496941  0.575868  0.712192  1
  Nb  Nb11  1  0.497211  0.922169  0.212254  1
  Nb  Nb12  1  0.497340  0.075769  0.786397  1
  Nb  Nb13  1  0.497348  0.711127  0.421121  1
  Nb  Nb14  1  0.497435  0.286755  0.577561  1
  Nb  Nb15  1  0.496923  0.786721  0.921193  1
  Nb  Nb16  1  0.497330  0.211144  0.077479  1
  O  O17  1  0.997869  0.498929  0.999258  1
  O  O18  1  0.996904  0.998808  0.499258  1
  O  O19  1  0.497348  0.219703  0.719867  1
  O  O20  1  0.497282  0.778203  0.278806  1
  O  O21  1  0.496997  0.719749  0.778781  1
  O  O22  1  0.497418  0.278112  0.219785  1
```

O	O23	1	0.997501	0.419816	0.291393	1
O	O24	1	0.997132	0.578012	0.707260	1
O	O25	1	0.997154	0.919949	0.207318	1
O	O26	1	0.997166	0.077862	0.791314	1
O	O27	1	0.997238	0.706926	0.421387	1
O	O28	1	0.997263	0.290879	0.577142	1
O	O29	1	0.997104	0.790851	0.921522	1
O	O30	1	0.997414	0.207053	0.077013	1
O	O31	1	0.497021	0.155502	0.493289	1
O	O32	1	0.497140	0.842203	0.505577	1
O	O33	1	0.497591	0.655573	0.005535	1
O	O34	1	0.497728	0.342296	0.993048	1
O	O35	1	0.497858	0.506942	0.156183	1
O	O36	1	0.497501	0.490870	0.842358	1
O	O37	1	0.496845	0.990820	0.656203	1
O	O38	1	0.496997	0.007153	0.342385	1
O	O39	1	0.497493	0.357962	0.430800	1
O	O40	1	0.497321	0.639601	0.567695	1
O	O41	1	0.496963	0.858115	0.067794	1
O	O42	1	0.497166	0.139711	0.930815	1
O	O43	1	0.497235	0.565948	0.360726	1
O	O44	1	0.497034	0.431857	0.637847	1
O	O45	1	0.497229	0.931814	0.860726	1
O	O46	1	0.497357	0.065997	0.137775	1

Supplementary Data II: Ground state compounds in Ca-Al-O system

Ca_8Al_3

```
_symmetry_space_group_name_H-M   'P 1'
_cell_length_a   9.45444800
_cell_length_b   9.52417724
_cell_length_c   9.61302941
_cell_angle_alpha   98.99568942
_cell_angle_beta   101.05673721
_cell_angle_gamma   119.71752218
_symmetry_Int_Tables_number   1
_chemical_formula_structural   Ca8Al3
_chemical_formula_sum   'Ca16 Al6'
_cell_volume   704.98265563
_cell_formula_units_Z   2
loop_
 _symmetry_equiv_pos_site_id
 _symmetry_equiv_pos_as_xyz
  1  'x, y, z'
loop_
 _atom_site_type_symbol
 _atom_site_label
 _atom_site_symmetry_multiplicity
 _atom_site_fract_x
 _atom_site_fract_y
 _atom_site_fract_z
 _atom_site_occupancy
  Ca  Ca1  1  0.531993  0.701328  0.649456  1
  Ca  Ca2  1  0.468007  0.298672  0.350544  1
  Ca  Ca3  1  0.079721  0.230386  0.106950  1
  Ca  Ca4  1  0.920279  0.769614  0.893050  1
  Ca  Ca5  1  0.878513  0.400728  0.648007  1
  Ca  Ca6  1  0.121487  0.599272  0.351993  1
  Ca  Ca7  1  0.332551  0.878966  0.110265  1
  Ca  Ca8  1  0.667449  0.121034  0.889735  1
  Ca  Ca9  1  0.960279  0.060756  0.669722  1
  Ca  Ca10  1  0.039721  0.939244  0.330278  1
  Ca  Ca11  1  0.701537  0.497909  0.110530  1
  Ca  Ca12  1  0.298463  0.502091  0.889470  1
  Ca  Ca13  1  0.774152  0.152828  0.298912  1
  Ca  Ca14  1  0.225848  0.847172  0.701088  1
  Ca  Ca15  1  0.544172  0.710658  0.296785  1
  Ca  Ca16  1  0.455828  0.289342  0.703215  1
  Al  Al17  1  -0.000000  0.500000  0.000000  1
  Al  Al18  1  0.500000  -0.000000  0.500000  1
  Al  Al19  1  0.172695  0.337461  0.500337  1
  Al  Al20  1  0.827305  0.662539  0.499663  1
```

Al Al21 1 0.676291 0.839839 0.025977 1
Al Al22 1 0.323709 0.160161 0.974023 1

CaO_2

```
_symmetry_space_group_name_H-M   'P 1'
_cell_length_a   3.87428343
_cell_length_b   3.87428343
_cell_length_c   7.03166330
_cell_angle_alpha   65.78303287
_cell_angle_beta   65.78303287
_cell_angle_gamma   56.73067843
_symmetry_Int_Tables_number   1
_chemical_formula_structural   CaO2
_chemical_formula_sum   'Ca2 O4'
_cell_volume   78.07200303
_cell_formula_units_Z   2
loop_
 _symmetry_equiv_pos_site_id
 _symmetry_equiv_pos_as_xyz
  1  'x, y, z'
loop_
 _atom_site_type_symbol
 _atom_site_label
 _atom_site_symmetry_multiplicity
 _atom_site_fract_x
 _atom_site_fract_y
 _atom_site_fract_z
 _atom_site_occupancy
  Ca  Ca1  1  0.640785  0.359215  0.750000  1
  Ca  Ca2  1  0.359215  0.640785  0.250000  1
  O  O3  1  0.885628  0.604588  0.911486  1
  O  O4  1  0.395412  0.114372  0.588514  1
  O  O5  1  0.114372  0.395412  0.088514  1
  O  O6  1  0.604588  0.885628  0.411486  1
```

Al_2O_3

```
_symmetry_space_group_name_H-M   'P 1'
_cell_length_a   5.17748333
_cell_length_b   5.17748333
_cell_length_c   5.17748380
_cell_angle_alpha   55.30162853
_cell_angle_beta   55.30162853
_cell_angle_gamma   55.30163320
_symmetry_Int_Tables_number   1
_chemical_formula_structural   Al2O3
_chemical_formula_sum   'Al4 O6'
_cell_volume   87.42409448
_cell_formula_units_Z   2
loop_
 _symmetry_equiv_pos_site_id
 _symmetry_equiv_pos_as_xyz
  1  'x, y, z'
loop_
 _atom_site_type_symbol
 _atom_site_label
 _atom_site_symmetry_multiplicity
 _atom_site_fract_x
 _atom_site_fract_y
 _atom_site_fract_z
 _atom_site_occupancy
  Al  Al1  1  0.352148  0.352148  0.352148  1
  Al  Al2  1  0.147852  0.147852  0.147852  1
  Al  Al3  1  0.852148  0.852148  0.852148  1
  Al  Al4  1  0.647852  0.647852  0.647852  1
  O  O5  1  0.943816  0.250000  0.556184  1
  O  O6  1  0.750000  0.443816  0.056184  1
  O  O7  1  0.250000  0.556184  0.943816  1
  O  O8  1  0.556184  0.943816  0.250000  1
  O  O9  1  0.443816  0.056184  0.750000  1
  O  O10  1  0.056184  0.750000  0.443816  1
```

Al

```
_symmetry_space_group_name_H-M   'P 1'
_cell_length_a   2.85042097
_cell_length_b   2.85042097
_cell_length_c   2.85042097
_cell_angle_alpha   60.00000000
_cell_angle_beta   60.00000000
_cell_angle_gamma   60.00000000
_symmetry_Int_Tables_number   1
_chemical_formula_structural   Al
_chemical_formula_sum   Al1
_cell_volume   16.37615790
_cell_formula_units_Z   1
loop_
 _symmetry_equiv_pos_site_id
 _symmetry_equiv_pos_as_xyz
  1  'x, y, z'
loop_
 _atom_site_type_symbol
 _atom_site_label
 _atom_site_symmetry_multiplicity
 _atom_site_fract_x
 _atom_site_fract_y
 _atom_site_fract_z
 _atom_site_occupancy
  Al  Al1  1  0.000000  0.000000  0.000000  1
```

$CaAl_4$

```
_symmetry_space_group_name_H-M   'P 1'
_cell_length_a   6.39847767
_cell_length_b   6.39847767
_cell_length_c   6.39847767
_cell_angle_alpha   140.30519444
_cell_angle_beta   140.30519444
_cell_angle_gamma   57.39019638
_symmetry_Int_Tables_number   1
_chemical_formula_structural   CaAl4
_chemical_formula_sum   'Ca1 Al4'
_cell_volume   105.95058245
_cell_formula_units_Z   1
loop_
 _symmetry_equiv_pos_site_id
 _symmetry_equiv_pos_as_xyz
  1  'x, y, z'
loop_
 _atom_site_type_symbol
 _atom_site_label
 _atom_site_symmetry_multiplicity
 _atom_site_fract_x
 _atom_site_fract_y
 _atom_site_fract_z
 _atom_site_occupancy
  Ca  Ca1  1  -0.000000  -0.000000  -0.000000  1
  Al  Al2  1  0.750000  0.250000  0.500000  1
  Al  Al3  1  0.386251  0.386251  -0.000000  1
  Al  Al4  1  0.613749  0.613749  0.000000  1
  Al  Al5  1  0.250000  0.750000  0.500000  1
```

$CaAl_2$

```
_symmetry_space_group_name_H-M   'P 1'
_cell_length_a   5.66432978
_cell_length_b   5.66432978
_cell_length_c   5.66432978
_cell_angle_alpha   60.00000000
_cell_angle_beta   60.00000000
_cell_angle_gamma   60.00000000
_symmetry_Int_Tables_number   1
_chemical_formula_structural   CaAl2
_chemical_formula_sum   'Ca2 Al4'
_cell_volume   128.50812690
_cell_formula_units_Z   2
loop_
 _symmetry_equiv_pos_site_id
 _symmetry_equiv_pos_as_xyz
  1  'x, y, z'
loop_
 _atom_site_type_symbol
 _atom_site_label
 _atom_site_symmetry_multiplicity
 _atom_site_fract_x
 _atom_site_fract_y
 _atom_site_fract_z
 _atom_site_occupancy
  Ca  Ca1  1  0.250000  0.250000  0.250000  1
  Ca  Ca2  1  0.000000  0.000000  0.000000  1
  Al  Al3  1  0.625000  0.125000  0.625000  1
  Al  Al4  1  0.625000  0.625000  0.625000  1
  Al  Al5  1  0.625000  0.625000  0.125000  1
  Al  Al6  1  0.125000  0.625000  0.625000  1
```

CaO

```
_symmetry_space_group_name_H-M   'P 1'
_cell_length_a   3.41543748
_cell_length_b   3.41543748
_cell_length_c   3.41543748
_cell_angle_alpha   60.00000000
_cell_angle_beta   60.00000000
_cell_angle_gamma   60.00000000
_symmetry_Int_Tables_number   1
_chemical_formula_structural   CaO
_chemical_formula_sum   'Ca1 O1'
_cell_volume   28.17241132
_cell_formula_units_Z   1
loop_
 _symmetry_equiv_pos_site_id
 _symmetry_equiv_pos_as_xyz
  1  'x, y, z'
loop_
 _atom_site_type_symbol
 _atom_site_label
 _atom_site_symmetry_multiplicity
 _atom_site_fract_x
 _atom_site_fract_y
 _atom_site_fract_z
 _atom_site_occupancy
  Ca  Ca1  1  0.000000  0.000000  0.000000  1
  O  O2  1  0.500000  0.500000  0.500000  1
```

Ca

```
_symmetry_space_group_name_H-M   'P 1'
_cell_length_a   3.89902498
_cell_length_b   3.89902498
_cell_length_c   3.89902498
_cell_angle_alpha   60.00000000
_cell_angle_beta   60.00000000
_cell_angle_gamma   60.00000000
_symmetry_Int_Tables_number   1
_chemical_formula_structural   Ca
_chemical_formula_sum   Ca1
_cell_volume   41.91341557
_cell_formula_units_Z   1
loop_
 _symmetry_equiv_pos_site_id
 _symmetry_equiv_pos_as_xyz
  1  'x, y, z'
loop_
 _atom_site_type_symbol
 _atom_site_label
 _atom_site_symmetry_multiplicity
 _atom_site_fract_x
 _atom_site_fract_y
 _atom_site_fract_z
 _atom_site_occupancy
  Ca  Ca1  1  0.000000  0.000000  0.000000  1
```

$CaAl_4O_7$

```
_symmetry_space_group_name_H-M   'P 1'
_cell_length_a   7.87908043
_cell_length_b   7.87908043
_cell_length_c   5.49135228
_cell_angle_alpha   76.63155928
_cell_angle_beta   76.63155928
_cell_angle_gamma   69.28149864
_symmetry_Int_Tables_number   1
_chemical_formula_structural   CaAl4O7
_chemical_formula_sum   'Ca2 Al8 O14'
_cell_volume   306.00622724
_cell_formula_units_Z   2
loop_
 _symmetry_equiv_pos_site_id
 _symmetry_equiv_pos_as_xyz
  1  'x, y, z'
loop_
 _atom_site_type_symbol
 _atom_site_label
 _atom_site_symmetry_multiplicity
 _atom_site_fract_x
 _atom_site_fract_y
 _atom_site_fract_z
 _atom_site_occupancy
  Ca  Ca1  1  0.804883  0.195117  0.250000  1
  Ca  Ca2  1  0.195117  0.804883  0.750000  1
  Al  Al3  1  0.319417  0.439886  0.243609  1
  Al  Al4  1  0.560114  0.680583  0.256391  1
  Al  Al5  1  0.680583  0.560114  0.756391  1
  Al  Al6  1  0.439886  0.319417  0.743609  1
  Al  Al7  1  0.922581  0.751201  0.305795  1
  Al  Al8  1  0.248799  0.077419  0.194205  1
  Al  Al9  1  0.077419  0.248799  0.694205  1
  Al  Al10  1  0.751201  0.922581  0.805795  1
  O  O11  1  0.251362  0.362711  0.579734  1
  O  O12  1  0.637289  0.748638  0.920266  1
  O  O13  1  0.748638  0.637289  0.420266  1
  O  O14  1  0.362711  0.251362  0.079734  1
  O  O15  1  0.135780  0.627911  0.149387  1
  O  O16  1  0.372089  0.864220  0.350613  1
  O  O17  1  0.864220  0.372089  0.850613  1
  O  O18  1  0.627911  0.135780  0.649387  1
  O  O19  1  0.939148  0.829950  0.572687  1
  O  O20  1  0.170050  0.060852  0.927313  1
  O  O21  1  0.468228  0.531772  0.750000  1
  O  O22  1  0.531772  0.468228  0.250000  1
```

O O23 1 0.829950 0.939148 0.072687 1
O O24 1 0.060852 0.170050 0.427313 1

$Ca_6Al_7O_{16}$

```
_symmetry_space_group_name_H-M   'P 1'
_cell_length_a   10.47574813
_cell_length_b   10.47574813
_cell_length_c   10.47574813
_cell_angle_alpha   109.47122063
_cell_angle_beta   109.47122063
_cell_angle_gamma   109.47122063
_symmetry_Int_Tables_number   1
_chemical_formula_structural   Ca6Al7O16
_chemical_formula_sum   'Ca12 Al14 O32'
_cell_volume   884.97958599
_cell_formula_units_Z   2
loop_
 _symmetry_equiv_pos_site_id
 _symmetry_equiv_pos_as_xyz
  1  'x, y, z'
loop_
 _atom_site_type_symbol
 _atom_site_label
 _atom_site_symmetry_multiplicity
 _atom_site_fract_x
 _atom_site_fract_y
 _atom_site_fract_z
 _atom_site_occupancy
  Ca  Ca1  1  0.637845  0.250000  0.887845  1
  Ca  Ca2  1  0.862155  0.750000  0.612155  1
  Ca  Ca3  1  0.387845  0.750000  0.137845  1
  Ca  Ca4  1  0.112155  0.250000  0.362155  1
  Ca  Ca5  1  0.887845  0.637845  0.250000  1
  Ca  Ca6  1  0.612155  0.862155  0.750000  1
  Ca  Ca7  1  0.137845  0.387845  0.750000  1
  Ca  Ca8  1  0.362155  0.112155  0.250000  1
  Ca  Ca9  1  0.250000  0.887845  0.637845  1
  Ca  Ca10  1  0.750000  0.612155  0.862155  1
  Ca  Ca11  1  0.750000  0.137845  0.387845  1
  Ca  Ca12  1  0.250000  0.362155  0.112155  1
  Al  Al13  1  0.375000  0.250000  0.625000  1
  Al  Al14  1  0.125000  0.750000  0.875000  1
  Al  Al15  1  0.625000  0.375000  0.250000  1
  Al  Al16  1  0.875000  0.125000  0.750000  1
  Al  Al17  1  0.250000  0.625000  0.375000  1
  Al  Al18  1  0.750000  0.875000  0.125000  1
  Al  Al19  1  0.500000  0.000000  0.034143  1
  Al  Al20  1  0.034143  0.500000  0.000000  1
  Al  Al21  1  0.000000  0.034143  0.500000  1
  Al  Al22  1  0.465857  0.465857  0.465857  1
```

Al Al23 1 0.534143 0.500000 0.000000 1
Al Al24 1 0.500000 0.000000 0.534143 1
Al Al25 1 0.000000 0.534143 0.500000 1
Al Al26 1 0.965857 0.965857 0.965857 1
O O27 1 0.500000 0.000000 0.867850 1
O O28 1 0.867850 0.500000 0.000000 1
O O29 1 0.000000 0.867850 0.500000 1
O O30 1 0.632150 0.632150 0.632150 1
O O31 1 0.367850 0.500000 0.000000 1
O O32 1 0.500000 0.000000 0.367850 1
O O33 1 0.000000 0.367850 0.500000 1
O O34 1 0.132150 0.132150 0.132150 1
O O35 1 0.408850 0.094214 0.615227 1
O O36 1 0.521013 0.405786 0.814635 1
O O37 1 0.091150 0.706377 0.685365 1
O O38 1 0.978987 0.793623 0.884773 1
O O39 1 0.115227 0.594214 0.908850 1
O O40 1 0.314635 0.905786 0.021013 1
O O41 1 0.185365 0.206377 0.591150 1
O O42 1 0.384773 0.293623 0.478987 1
O O43 1 0.615227 0.408850 0.094214 1
O O44 1 0.814635 0.521013 0.405786 1
O O45 1 0.685365 0.091150 0.706377 1
O O46 1 0.884773 0.978987 0.793623 1
O O47 1 0.908850 0.115227 0.594214 1
O O48 1 0.021013 0.314635 0.905786 1
O O49 1 0.591150 0.185365 0.206377 1
O O50 1 0.478987 0.384773 0.293623 1
O O51 1 0.094214 0.615227 0.408850 1
O O52 1 0.405786 0.814635 0.521013 1
O O53 1 0.706377 0.685365 0.091150 1
O O54 1 0.793623 0.884773 0.978987 1
O O55 1 0.594214 0.908850 0.115227 1
O O56 1 0.905786 0.021013 0.314635 1
O O57 1 0.206377 0.591150 0.185365 1
O O58 1 0.293623 0.478987 0.384773 1

$Ca_{11}Al_{14}O_{32}$

```
_symmetry_space_group_name_H-M   'P 1'
_cell_length_a   12.04438581
_cell_length_b   12.08491300
_cell_length_c   12.15689086
_cell_angle_alpha   90.00000000
_cell_angle_beta   89.95748726
_cell_angle_gamma   90.00000000
_symmetry_Int_Tables_number   1
_chemical_formula_structural   Ca11Al14O32
_chemical_formula_sum   'Ca22 Al28 O64'
_cell_volume   1769.50007290
_cell_formula_units_Z   2
loop_
 _symmetry_equiv_pos_site_id
 _symmetry_equiv_pos_as_xyz
  1  'x, y, z'
loop_
 _atom_site_type_symbol
 _atom_site_label
 _atom_site_symmetry_multiplicity
 _atom_site_fract_x
 _atom_site_fract_y
 _atom_site_fract_z
 _atom_site_occupancy
  Ca  Ca1  1  0.250000  0.364371  0.500000  1
  Ca  Ca2  1  0.250000  0.889391  0.500000  1
  Ca  Ca3  1  0.250000  0.117723  0.000000  1
  Ca  Ca4  1  0.995769  0.245354  0.634206  1
  Ca  Ca5  1  0.504231  0.245354  0.365794  1
  Ca  Ca6  1  0.498647  0.253206  0.886992  1
  Ca  Ca7  1  0.001353  0.253206  0.113008  1
  Ca  Ca8  1  0.633859  0.001359  0.252286  1
  Ca  Ca9  1  0.365879  0.501316  0.247622  1
  Ca  Ca10  1  0.886815  0.499388  0.250223  1
  Ca  Ca11  1  0.112942  0.999411  0.249930  1
  Ca  Ca12  1  0.750000  0.864381  0.000000  1
  Ca  Ca13  1  0.750000  0.389460  0.000000  1
  Ca  Ca14  1  0.750000  0.617908  0.500000  1
  Ca  Ca15  1  0.495267  0.745331  0.133979  1
  Ca  Ca16  1  0.004733  0.745331  0.866021  1
  Ca  Ca17  1  0.998448  0.753300  0.387150  1
  Ca  Ca18  1  0.501552  0.753300  0.612850  1
  Ca  Ca19  1  0.134121  0.501316  0.752378  1
  Ca  Ca20  1  0.866141  0.001359  0.747714  1
  Ca  Ca21  1  0.387058  0.999411  0.750070  1
  Ca  Ca22  1  0.613185  0.499388  0.749777  1
```

Al	Al23	1	0.250000	0.378655	0.000000	1
Al	Al24	1	0.750000	0.125653	0.000000	1
Al	Al25	1	0.997795	0.249086	0.374848	1
Al	Al26	1	0.001875	0.748966	0.125332	1
Al	Al27	1	0.373889	0.999505	0.248917	1
Al	Al28	1	0.126111	0.999505	0.751083	1
Al	Al29	1	0.763486	0.266993	0.226260	1
Al	Al30	1	0.236071	0.766877	0.273715	1
Al	Al31	1	0.267560	0.233312	0.767443	1
Al	Al32	1	0.232440	0.233312	0.232557	1
Al	Al33	1	0.980823	0.016757	0.517770	1
Al	Al34	1	0.019321	0.516697	0.982398	1
Al	Al35	1	0.517159	0.983390	0.016809	1
Al	Al36	1	0.482791	0.483489	0.483029	1
Al	Al37	1	0.750000	0.878898	0.500000	1
Al	Al38	1	0.250000	0.625649	0.500000	1
Al	Al39	1	0.498125	0.748966	0.874668	1
Al	Al40	1	0.502205	0.249086	0.625152	1
Al	Al41	1	0.874182	0.499652	0.749039	1
Al	Al42	1	0.625818	0.499652	0.250961	1
Al	Al43	1	0.263929	0.766877	0.726285	1
Al	Al44	1	0.736514	0.266993	0.773740	1
Al	Al45	1	0.767168	0.733328	0.267470	1
Al	Al46	1	0.732832	0.733328	0.732530	1
Al	Al47	1	0.480679	0.516697	0.017602	1
Al	Al48	1	0.519177	0.016757	0.482230	1
Al	Al49	1	0.017209	0.483489	0.516971	1
Al	Al50	1	0.982841	0.983390	0.983191	1
O	O51	1	0.161130	0.685366	0.780854	1
O	O52	1	0.839571	0.185518	0.719564	1
O	O53	1	0.685089	0.813243	0.180451	1
O	O54	1	0.314534	0.313191	0.319593	1
O	O55	1	0.065747	0.935567	0.431598	1
O	O56	1	0.934323	0.435492	0.068557	1
O	O57	1	0.433580	0.068541	0.935599	1
O	O58	1	0.066420	0.068541	0.064401	1
O	O59	1	0.140786	0.448587	0.937383	1
O	O60	1	0.359214	0.448587	0.062617	1
O	O61	1	0.650831	0.034504	0.055681	1
O	O62	1	0.349081	0.534514	0.444171	1
O	O63	1	0.689069	0.217509	0.905388	1
O	O64	1	0.311099	0.717400	0.594556	1
O	O65	1	0.305280	0.286557	0.899479	1
O	O66	1	0.194720	0.286557	0.100521	1
O	O67	1	0.956156	0.150633	0.468739	1
O	O68	1	0.056183	0.355291	0.456224	1
O	O69	1	0.044061	0.650548	0.031595	1

O O70 1 0.443817 0.355291 0.543776 1
O O71 1 0.901791 0.694557 0.217727 1
O O72 1 0.604745 0.302382 0.714341 1
O O73 1 0.895255 0.302382 0.285659 1
O O74 1 0.097750 0.194680 0.282262 1
O O75 1 0.461331 0.942838 0.147324 1
O O76 1 0.461670 0.052852 0.349762 1
O O77 1 0.038330 0.052852 0.650238 1
O O78 1 0.538325 0.442816 0.352428 1
O O79 1 0.219001 0.904505 0.691711 1
O O80 1 0.714650 0.600334 0.307833 1
O O81 1 0.280999 0.904505 0.308289 1
O O82 1 0.285008 0.100289 0.192327 1
O O83 1 0.660429 0.185518 0.280436 1
O O84 1 0.338870 0.685366 0.219146 1
O O85 1 0.185466 0.313191 0.680407 1
O O86 1 0.814911 0.813243 0.819549 1
O O87 1 0.565677 0.435492 0.931443 1
O O88 1 0.434253 0.935567 0.568402 1
O O89 1 0.933501 0.568601 0.435802 1
O O90 1 0.566499 0.568601 0.564198 1
O O91 1 0.640758 0.948780 0.437366 1
O O92 1 0.859242 0.948780 0.562634 1
O O93 1 0.150919 0.534514 0.555829 1
O O94 1 0.849169 0.034504 0.944319 1
O O95 1 0.188901 0.717400 0.405444 1
O O96 1 0.810931 0.217509 0.094612 1
O O97 1 0.805105 0.786734 0.399415 1
O O98 1 0.694895 0.786734 0.600585 1
O O99 1 0.455939 0.650548 0.968405 1
O O100 1 0.556279 0.855165 0.956202 1
O O101 1 0.543844 0.150633 0.531261 1
O O102 1 0.943721 0.855165 0.043798 1
O O103 1 0.402250 0.194680 0.717738 1
O O104 1 0.104152 0.802417 0.214723 1
O O105 1 0.395848 0.802417 0.785277 1
O O106 1 0.598209 0.694557 0.782273 1
O O107 1 0.961675 0.442816 0.647572 1
O O108 1 0.961924 0.553038 0.849915 1
O O109 1 0.538076 0.553038 0.150085 1
O O110 1 0.038669 0.942838 0.852676 1
O O111 1 0.718762 0.404700 0.191564 1
O O112 1 0.214992 0.100289 0.807673 1
O O113 1 0.781238 0.404700 0.808436 1
O O114 1 0.785350 0.600334 0.692167 1

$Ca_{23}Al_{28}O_{64}$

```
_symmetry_space_group_name_H-M   'P 1'
_cell_length_a   12.07214259
_cell_length_b   12.09020809
_cell_length_c   12.12961665
_cell_angle_alpha   90.00000000
_cell_angle_beta   89.99195483
_cell_angle_gamma   90.00000000
_symmetry_Int_Tables_number   1
_chemical_formula_structural   Ca23Al28O64
_chemical_formula_sum   'Ca23 Al28 O64'
_cell_volume   1770.37473638
_cell_formula_units_Z   1
loop_
 _symmetry_equiv_pos_site_id
 _symmetry_equiv_pos_as_xyz
  1  'x, y, z'
loop_
 _atom_site_type_symbol
 _atom_site_label
 _atom_site_symmetry_multiplicity
 _atom_site_fract_x
 _atom_site_fract_y
 _atom_site_fract_z
 _atom_site_occupancy
  Ca  Ca1  1  0.250000  0.639453  -0.000000  1
  Ca  Ca2  1  0.250000  0.363106  0.500000  1
  Ca  Ca3  1  0.250000  0.887496  0.500000  1
  Ca  Ca4  1  0.250000  0.111280  -0.000000  1
  Ca  Ca5  1  0.995768  0.244617  0.633740  1
  Ca  Ca6  1  0.504232  0.244617  0.366260  1
  Ca  Ca7  1  0.500027  0.250835  0.885660  1
  Ca  Ca8  1  0.999973  0.250835  0.114340  1
  Ca  Ca9  1  0.634996  0.002980  0.253318  1
  Ca  Ca10  1  0.362710  0.498329  0.250523  1
  Ca  Ca11  1  0.887005  0.498802  0.251662  1
  Ca  Ca12  1  0.112268  0.000654  0.251396  1
  Ca  Ca13  1  0.750000  0.864140  -0.000000  1
  Ca  Ca14  1  0.750000  0.389214  -0.000000  1
  Ca  Ca15  1  0.750000  0.617536  0.500000  1
  Ca  Ca16  1  0.499919  0.750962  0.136514  1
  Ca  Ca17  1  0.000081  0.750962  0.863486  1
  Ca  Ca18  1  0.998442  0.752778  0.388771  1
  Ca  Ca19  1  0.501558  0.752778  0.611229  1
  Ca  Ca20  1  0.137290  0.498329  0.749477  1
  Ca  Ca21  1  0.865004  0.002980  0.746682  1
  Ca  Ca22  1  0.387732  0.000654  0.748604  1
```

Ca Ca23 1 0.612995 0.498802 0.748338 1
Al Al24 1 0.250000 0.375569 -0.000000 1
Al Al25 1 0.750000 0.125760 -0.000000 1
Al Al26 1 0.997463 0.249276 0.375104 1
Al Al27 1 0.999287 0.749649 0.125512 1
Al Al28 1 0.373887 0.999023 0.249105 1
Al Al29 1 0.126113 0.999023 0.750895 1
Al Al30 1 0.762658 0.267615 0.226974 1
Al Al31 1 0.231473 0.766349 0.267462 1
Al Al32 1 0.267937 0.233360 0.767333 1
Al Al33 1 0.232063 0.233360 0.232667 1
Al Al34 1 0.981651 0.015543 0.517447 1
Al Al35 1 0.017437 0.517947 0.982714 1
Al Al36 1 0.517600 0.983093 0.016927 1
Al Al37 1 0.483312 0.483359 0.482861 1
Al Al38 1 0.750000 0.878259 0.500000 1
Al Al39 1 0.250000 0.625058 0.500000 1
Al Al40 1 0.500713 0.749649 0.874488 1
Al Al41 1 0.502537 0.249276 0.624896 1
Al Al42 1 0.875208 0.500453 0.749703 1
Al Al43 1 0.624792 0.500453 0.250297 1
Al Al44 1 0.268527 0.766349 0.732538 1
Al Al45 1 0.737342 0.267615 0.773026 1
Al Al46 1 0.766293 0.732929 0.267205 1
Al Al47 1 0.733707 0.732929 0.732795 1
Al Al48 1 0.482563 0.517947 0.017286 1
Al Al49 1 0.518349 0.015543 0.482553 1
Al Al50 1 0.016688 0.483359 0.517139 1
Al Al51 1 0.982400 0.983093 0.983073 1
O O52 1 0.184421 0.682892 0.814577 1
O O53 1 0.839876 0.186404 0.718262 1
O O54 1 0.683709 0.813567 0.181243 1
O O55 1 0.314826 0.315506 0.317185 1
O O56 1 0.067761 0.933628 0.432924 1
O O57 1 0.934965 0.435348 0.066735 1
O O58 1 0.435288 0.067291 0.933772 1
O O59 1 0.064712 0.067291 0.066228 1
O O60 1 0.150062 0.464718 0.943245 1
O O61 1 0.349938 0.464718 0.056755 1
O O62 1 0.651084 0.034128 0.054984 1
O O63 1 0.349917 0.535848 0.442919 1
O O64 1 0.689885 0.217970 0.904873 1
O O65 1 0.306976 0.714526 0.599193 1
O O66 1 0.305432 0.285687 0.900514 1
O O67 1 0.194568 0.285687 0.099486 1
O O68 1 0.956591 0.149074 0.467466 1
O O69 1 0.055973 0.354197 0.458588 1

O O70 1 0.056162 0.651326 0.034493 1
O O71 1 0.444027 0.354197 0.541412 1
O O72 1 0.899168 0.692227 0.214141 1
O O73 1 0.605362 0.302827 0.713907 1
O O74 1 0.894638 0.302827 0.286093 1
O O75 1 0.097627 0.195947 0.282170 1
O O76 1 0.463199 0.943609 0.148553 1
O O77 1 0.461067 0.052988 0.350196 1
O O78 1 0.038933 0.052988 0.649804 1
O O79 1 0.536002 0.443321 0.350402 1
O O80 1 0.216042 0.899422 0.694462 1
O O81 1 0.713245 0.600501 0.308000 1
O O82 1 0.283958 0.899422 0.305538 1
O O83 1 0.284011 0.099760 0.193848 1
O O84 1 0.660124 0.186404 0.281738 1
O O85 1 0.315579 0.682892 0.185423 1
O O86 1 0.185174 0.315506 0.682815 1
O O87 1 0.816291 0.813567 0.818757 1
O O88 1 0.565035 0.435348 0.933265 1
O O89 1 0.432239 0.933628 0.567076 1
O O90 1 0.932788 0.568003 0.435920 1
O O91 1 0.567212 0.568003 0.564080 1
O O92 1 0.640250 0.947987 0.437957 1
O O93 1 0.859750 0.947987 0.562043 1
O O94 1 0.150083 0.535848 0.557081 1
O O95 1 0.848916 0.034128 0.945016 1
O O96 1 0.193024 0.714526 0.400807 1
O O97 1 0.810115 0.217970 0.095127 1
O O98 1 0.805779 0.786067 0.399093 1
O O99 1 0.694221 0.786067 0.600907 1
O O100 1 0.443838 0.651326 0.965507 1
O O101 1 0.556554 0.850464 0.962978 1
O O102 1 0.543409 0.149074 0.532534 1
O O103 1 0.943446 0.850464 0.037022 1
O O104 1 0.402373 0.195947 0.717830 1
O O105 1 0.097879 0.805891 0.216208 1
O O106 1 0.402121 0.805891 0.783792 1
O O107 1 0.600832 0.692227 0.785859 1
O O108 1 0.963998 0.443321 0.649598 1
O O109 1 0.965193 0.556292 0.849533 1
O O110 1 0.534807 0.556292 0.150467 1
O O111 1 0.036801 0.943609 0.851447 1
O O112 1 0.717556 0.405348 0.191132 1
O O113 1 0.215989 0.099760 0.806152 1
O O114 1 0.782444 0.405348 0.808868 1
O O115 1 0.786755 0.600501 0.692000 1

Supplementary Data III: Ground state compounds in Ag-Al-O system

$AlAgO_2$

```
_symmetry_space_group_name_H-M   'P 1'
_cell_length_a   5.49885510
_cell_length_b   7.07696514
_cell_length_c   5.43662305
_cell_angle_alpha   90.00366335
_cell_angle_beta   89.98376019
_cell_angle_gamma   90.01752150
_symmetry_Int_Tables_number   1
_chemical_formula_structural   AlAgO2
_chemical_formula_sum   'Al4 Ag4 O8'
_cell_volume   211.56728619
_cell_formula_units_Z   4
loop_
 _symmetry_equiv_pos_site_id
 _symmetry_equiv_pos_as_xyz
  1  'x, y, z'
loop_
 _atom_site_type_symbol
 _atom_site_label
 _atom_site_symmetry_multiplicity
 _atom_site_fract_x
 _atom_site_fract_y
 _atom_site_fract_z
 _atom_site_occupancy
  Al  Al1  1  0.563781  0.375162  0.998725  1
  Al  Al2  1  0.442996  0.624743  0.498830  1
  Al  Al3  1  0.943050  0.874995  0.498485  1
  Al  Al4  1  0.063706  0.124931  0.998444  1
  Ag  Ag5  1  0.562203  0.873148  0.994550  1
  Ag  Ag6  1  0.444586  0.126781  0.494266  1
  Ag  Ag7  1  0.943984  0.372572  0.494657  1
  Ag  Ag8  1  0.062508  0.627496  0.994559  1
  O  O9  1  0.533517  0.429617  0.316149  1
  O  O10  1  0.473323  0.570297  0.816200  1
  O  O11  1  0.973130  0.929940  0.815681  1
  O  O12  1  0.033627  0.070013  0.315740  1
  O  O13  1  0.633421  0.821861  0.432252  1
  O  O14  1  0.373344  0.178036  0.932017  1
  O  O15  1  0.873444  0.322175  0.932448  1
  O  O16  1  0.133357  0.677736  0.432519  1
```

Al_2O_3

```
_symmetry_space_group_name_H-M   'P 1'
_cell_length_a   5.17726765
_cell_length_b   5.17706401
_cell_length_c   5.17689501
_cell_angle_alpha   55.30669557
_cell_angle_beta   55.30751733
_cell_angle_gamma   55.30817578
_symmetry_Int_Tables_number   1
_chemical_formula_structural   Al2O3
_chemical_formula_sum   'Al4 O6'
_cell_volume   87.41699389
_cell_formula_units_Z   2
loop_
 _symmetry_equiv_pos_site_id
 _symmetry_equiv_pos_as_xyz
  1  'x, y, z'
loop_
 _atom_site_type_symbol
 _atom_site_label
 _atom_site_symmetry_multiplicity
 _atom_site_fract_x
 _atom_site_fract_y
 _atom_site_fract_z
 _atom_site_occupancy
  Al  Al1  1  0.651255  0.641948  0.650058  1
  Al  Al2  1  0.855542  0.846282  0.854423  1
  Al  Al3  1  0.151165  0.142048  0.150085  1
  Al  Al4  1  0.355617  0.346310  0.354366  1
  O  O5  1  0.447266  0.050306  0.752237  1
  O  O6  1  0.947289  0.244061  0.558481  1
  O  O7  1  0.059569  0.744168  0.445995  1
  O  O8  1  0.753406  0.437975  0.058469  1
  O  O9  1  0.253415  0.550235  0.946081  1
  O  O10  1  0.559536  0.937976  0.252284  1
```

Ag

```
_symmetry_space_group_name_H-M   'P 1'
_cell_length_a   2.95853434
_cell_length_b   2.95853403
_cell_length_c   2.95853400
_cell_angle_alpha   60.00000031
_cell_angle_beta   60.00000385
_cell_angle_gamma   60.00000548
_symmetry_Int_Tables_number   1
_chemical_formula_structural   Ag
_chemical_formula_sum   Ag1
_cell_volume   18.31111467
_cell_formula_units_Z   1
loop_
 _symmetry_equiv_pos_site_id
 _symmetry_equiv_pos_as_xyz
  1  'x, y, z'
loop_
 _atom_site_type_symbol
 _atom_site_label
 _atom_site_symmetry_multiplicity
 _atom_site_fract_x
 _atom_site_fract_y
 _atom_site_fract_z
 _atom_site_occupancy
  Ag  Ag1  1  0.002326  0.036350  0.991529  1
```

Al

```
_symmetry_space_group_name_H-M   'P 1'
_cell_length_a   2.85041989
_cell_length_b   2.85041974
_cell_length_c   2.85042000
_cell_angle_alpha   59.99999699
_cell_angle_beta   59.99999868
_cell_angle_gamma   60.00000413
_symmetry_Int_Tables_number   1
_chemical_formula_structural   Al
_chemical_formula_sum   Al1
_cell_volume   16.37613894
_cell_formula_units_Z   1
loop_
 _symmetry_equiv_pos_site_id
 _symmetry_equiv_pos_as_xyz
  1  'x, y, z'
loop_
 _atom_site_type_symbol
 _atom_site_label
 _atom_site_symmetry_multiplicity
 _atom_site_fract_x
 _atom_site_fract_y
 _atom_site_fract_z
 _atom_site_occupancy
  Al  Al1  1  0.983300  0.969832  0.014358  1
```

Ag_2O

```
_symmetry_space_group_name_H-M   'P 1'
_cell_length_a   4.87074867
_cell_length_b   4.87219122
_cell_length_c   4.87737072
_cell_angle_alpha   89.58493007
_cell_angle_beta   89.60775610
_cell_angle_gamma   89.91504569
_symmetry_Int_Tables_number   1
_chemical_formula_structural   Ag2O
_chemical_formula_sum   'Ag4 O2'
_cell_volume   115.74008401
_cell_formula_units_Z   2
loop_
 _symmetry_equiv_pos_site_id
 _symmetry_equiv_pos_as_xyz
  1  'x, y, z'
loop_
 _atom_site_type_symbol
 _atom_site_label
 _atom_site_symmetry_multiplicity
 _atom_site_fract_x
 _atom_site_fract_y
 _atom_site_fract_z
 _atom_site_occupancy
  Ag  Ag1  1  0.497228  0.502274  0.995678  1
  Ag  Ag2  1  0.997265  0.503471  0.495889  1
  Ag  Ag3  1  0.497635  0.003499  0.496859  1
  Ag  Ag4  1  0.996944  0.002850  0.997152  1
  O  O5  1  0.245733  0.251328  0.246194  1
  O  O6  1  0.749157  0.754665  0.746897  1
```

AlAg

```
_symmetry_space_group_name_H-M   'P 1'
_cell_length_a   5.13133469
_cell_length_b   2.94549779
_cell_length_c   4.52704701
_cell_angle_alpha   89.98839865
_cell_angle_beta   89.99772683
_cell_angle_gamma   89.70203224
_symmetry_Int_Tables_number   1
_chemical_formula_structural   AlAg
_chemical_formula_sum   'Al2 Ag2'
_cell_volume   68.42237845
_cell_formula_units_Z   2
loop_
 _symmetry_equiv_pos_site_id
 _symmetry_equiv_pos_as_xyz
  1  'x, y, z'
loop_
 _atom_site_type_symbol
 _atom_site_label
 _atom_site_symmetry_multiplicity
 _atom_site_fract_x
 _atom_site_fract_y
 _atom_site_fract_z
 _atom_site_occupancy
  Al  Al1  1  0.663007  0.999407  0.497725  1
  Al  Al2  1  0.162749  0.497003  0.497855  1
  Ag  Ag3  1  0.329868  0.997400  0.997848  1
  Ag  Ag4  1  0.829783  0.498826  0.997624  1
```

References

1. Zhang, X., Zhang, L., Perkins, J. D., and Zunger, A., (2015), Intrinsic transparent conductors without doping. Phys. Rev. Lett., 115, 176602.
2. Kummer, J. T., (1972), β-Alumina electrolytes. Prog. Solid State Chem., 7, 141-175.
3. England, W. A., Jacobson, A. J., and Tofield, B. C., (1982), Structural studies of highly non-stoichiometric polycrystalline sodium and silver beta-aluminas. Solid State Ion., 6, 21-27.
4. Iyi, N., Inoue, Z., and Kimura, S., (1986), The crystal structure of highly nonstoichiometric potassium β-alumina, $K_{1.50}Al_{11.0}O_{17.25}$. J. Solid State Chem., 61, 81-89.
5. van Berkel, F. P. F., Zandbergen, H. W., Verschoor, G. C., and IJdo, D. J. W., (1984), The structure of barium aluminate, $Ba_{0.75}Al_{11}O_{17.25}$. Acta Crystallogr. Sect. C: Cryst. Struct. Commun., 40, 1124-1127.
6. Whittingham, M. S., and Huggins, R. A., (1971), Transport properties of silver beta alumina. J. Electrochem. Soc., 118, 1-6.